TA7
W34
no. 3-599
rept 4
cop. 3

US-CE-C Property of the United States Government

#1512

AD-467081

TECHNICAL REPORT NO. 3-599

DYNAMIC BEARING CAPACITY OF SOILS

Report 4

INVESTIGATION OF A DIMENSIONLESS LOAD-DISPLACEMENT RELATION FOR FOOTINGS ON CLAY

by

P. F. Hadala

June 1965

Sponsored by

Defense Atomic Support Agency

and

Office, Chief of Engineers
U. S. Army

Conducted by

U. S. Army Engineer Waterways Experiment Station
CORPS OF ENGINEERS
Vicksburg, Mississippi

LIBRARY
US ARMY ENGINEER WATERWAYS EXPERIMENT STATION
VICKSBURG, MISSISSIPPI

Qualified requesters may obtain copies of this report from DDC.

Destroy this report when it is no longer needed. Do not return it to the originator.

The findings in this report are not to be construed as an official Department of the Army position, unless so designated by other authorized documents.

TECHNICAL REPORT NO. 3-599

DYNAMIC BEARING CAPACITY OF SOILS

Report 4

INVESTIGATION OF A DIMENSIONLESS LOAD-DISPLACEMENT RELATION FOR FOOTINGS ON CLAY

by

P. F. Hadala

June 1965

Sponsored by

Defense Atomic Support Agency
NWER Subtask 13.010

and

Office, Chief of Engineers
U. S. Army
Project No. 1-T-0-22601-A-091-02

Conducted by

U. S. Army Engineer Waterways Experiment Station
CORPS OF ENGINEERS
Vicksburg, Mississippi

ARMY-MRC VICKSBURG, MISS.

1/2

TA7
W34
no. 3-599
rept. 4
Cop. 3

THE CONTENTS OF THIS REPORT ARE NOT TO BE USED FOR ADVERTISING, PUBLICATION, OR PROMOTIONAL PURPOSES. CITATION OF TRADE NAMES DOES NOT CONSTITUTE AN OFFICIAL INDORSEMENT OR APPROVAL OF THE USE OF SUCH COMMERCIAL PRODUCTS.

FOREWORD

The investigation reported herein was conducted by the Soils Division of the U. S. Army Engineer Waterways Experiment Station (WES) under the joint sponsorship of the Defense Atomic Support Agency (Nuclear Weapons Effects Research Subtask 13.010, Response of Buried Structures to Ground Shock) and the Office, Chief of Engineers, U. S. Army (Effects of Nuclear Weapons Project No. 1-T-0-22601-A-091-02, Development of Design Criteria for Foundations of Army Protective Structures). The testing was conducted during the period September-November 1962. The tests were conducted and the report prepared under the supervision of Mr. R. W. Cunny and the general direction of Messrs. W. J. Turnbull, W. G. Shockley, A.A. Maxwell, and J. R. Compton.

The test program was planned by Mr. J. G. Jackson, Jr., and executed by Mr. R. C. Sloan. Messrs. P. F. Hadala, Laszlo Devay, and R. E. Manning, SP-4 W. R. Buehring, and SP-4 T. M. Forden assisted in the conduct of the tests and data reduction. Instrumentation work was supervised by Mr. G. C. Downing. This report was prepared by Mr. Hadala. The report was reviewed prior to publication by Professors W. J. Hall and R. V. Whitman. Their comments are appreciated.

Col. Alex G. Sutton, Jr., CE, and Col. John R. Oswalt, Jr., CE, were Directors of the WES during the conduct of this investigation and preparation of this report. Mr. J. B. Tiffany was Technical Director.

CONTENTS

LIST OF ILLUSTRATIONS

Page

16

19

20

21

25

31

32

33

34

35

36

37

38

39

39

39

87

88

SUMMARY

Three nondimensional relations developed to predict the maximum displacement and the time of its occurrence for dynamically loaded square footings on clay were presented in Dynamic Bearing Capacity of Soils, Report 3. Additional tests were conducted to determine if these prediction relations were dependent on the model scaling rules used to design the footing tests in which the relations were first observed.

The first of these relations is that of resistance parameter to displacement parameter where the resistance parameter is the ratio of average stress on the footing at maximum footing reaction to static unconfined compression shear strength, and the displacement parameter is the ratio of maximum footing displacement to footing width. The second relation is that of strength parameter to displacement parameter where the strength parameter is the ratio of maximum dynamic column load to the product of unconfined compression shear strength and the square of the footing width. The third relation is that of strength parameter to inertia parameter where the inertia parameter is the ratio of the product of maximum dynamic column load and the square of the time to maximum displacement to the product of footing width and column mass.

Dynamic footing tests in which the independent parameters were not related by any scaling rules were conducted on large soil specimens utilizing the specimen preparation and test procedures developed in Report 3 of this series. The results of these tests essentially confirmed the original nondimensional relations. These verification tests included footing loads ranging from 1.4 to 18.3 kips, footing widths from 5 to 16 in., and soil shear strengths from 0.60 to 1.85 kips per sq ft. The weight of the loading machine piston was 160 lb in all tests. Load-pulse shape and duration as well as wet unit weight of the soil were nearly constant. By using the original and new data it was shown that each of the nondimensional relations can be expressed as a power function. Caution is suggested for the extension of the test results to conditions other than those which have been tested in the laboratory.

It was determined that the dynamic resistance parameter-displacement parameter relation can be approximated by converting static footing test data to the same nondimensional quantities and increasing the static resistance parameter by a factor of from 1.5 to 1.9; a similar procedure could be used to approximate dynamic load-displacement curves from static plate-bearing test data.

DYNAMIC BEARING CAPACITY OF SOILS

INVESTIGATION OF A DIMENSIONLESS LOAD-DISPLACEMENT RELATION FOR FOOTINGS ON CLAY

PART I: INTRODUCTION

Background

1. The development of nuclear weapons has totally revised the concept of passive defense, both civil and military, and brought about a need for protective structures capable of withstanding intense blast loadings. To design such structures, a method of estimating the behavior of the structural foundations under high-intensity transient loads is needed. Design criteria for the foundations of surface and shallow-buried protective structures which will permit economy and yet ensure adequacy of design must be developed.

2. To assist in the development of these criteria, a study of the dynamic bearing capacity of soils was initiated at the U. S. Army Engineer Waterways Experiment Station (WES). The overall purpose of this study is to determine the relations between dynamic blast-type loads and the resulting displacement and acceleration of soil-supported footings. Both analytical studies and small-scale footing tests have been conducted. Two theoretical studies of the motion of dynamically loaded long footings employing limit-state failure theories have been carried out.[1,2*] Because the theories employed assumed failure surfaces similar to those found in static bearing capacity theory, a number of small-scale footing tests employing a dynamic loading machine[3] to deliver a pulse load to the footing were conducted to investigate the mode of failure and the subsurface motion occurring during the displacement of a dynamically loaded footing.[4] Results of these tests indicated behavior patterns quite different from those assumed for the theoretical studies.

3. Because of the difficulties encountered with a theoretical

---

* Raised numbers refer to similarly numbered items in Literature Cited at end of text..

approach, a small-scale model study was initiated. Using a postulated structure-footing-soil system subjected to blast loads and a set of scale factors derived for conditions of dynamic similitude, models of the postulated prototype were developed and tested. Analysis of the results of these tests using nondimensional parameters revealed a nondimensional maximum footing reaction-maximum displacement relation for square footings on clay. This relation is reported in Report 3[5] in this series. Also reported are two other useful dimensionless relations defining maximum displacement and time to maximum displacement as nondimensional functions of the dynamic load applied to the load column of the dynamic loading machine. Because the independent variables examined in Report 3 were studied over a limited range and because they were interrelated by the requirements for model scaling, the usefulness of the newly developed nondimensional relations was considered limited. It is intended in this report to try to extend the usefulness of these relations.

Purpose

4. The purposes of the tests reported herein were to determine if the three nondimensional relations developed in Report 3 are independent of the model scaling relations used and to extend the range of soil strengths, footing loads, and footing sizes investigated. As recommended in that report, the tests were specifically designed to check the validity of the nondimensional maximum footing load-maximum displacement relation. Since the independent parameters are not related by any scaling relation, the data will also be used to check the validity of the two other nondimensional relations developed in Report 3 and described in paragraph 3.

Scope

5. The investigation was limited to a study of the response of square footings to initially peaked dynamic axial loads of 400-msec duration. Twenty-four dynamic and three static footing tests were conducted on a clay of high plasticity. Footing size ranged from 5 to 16 in.

Maximum footing reaction ranged from 1.4 to 18.3 kips. Clays with static shear strengths approximating 0.60, 1.20, and 1.75 kips per sq ft were tested in an 86-in.-wide soil cart. Subsurface soil motions were not investigated.

PART II: NONDIMENSIONAL RELATIONS

Development of the Nondimensional Equation

6. The data reported in Report 3 showed the feasibility of using nondimensional parameters (π terms) for the analyses of the results of small-scale footing tests on clay. Reviewing the principles of dimensional analysis,[6] one finds that a problem affected by n variables defined in units that are the products of powers of three fundamental units (force, length, and time) can be stated in terms of $(n - 3)$ nondimensional quantities, or π terms. However, one of the most difficult steps in the analysis of a practical problem is the identification of those variables which significantly affect the problem.

7. Since an attempt is made in this report to verify nondimensional relations developed in Report 3, the systems tested and variables examined had to be similar. In Report 3, the load column of the dynamic loading machine used to load the footings was idealized as a lumped mass m subjected to an applied dynamic column load P of duration t_o as shown in fig. 1a. The mass was supported by a square footing of width b supported in turn by a soil specimen of mass density ρ and static unconsolidated-undrained shear strength τ_f which provided the resistance to footing motion. The objective of the investigation was to determine the resulting displacement z of the footing as a function of time. Test system parameters described above were believed to be the significant variables in the test system shown in fig. 1a and are presented as follows in tabular form along with their units.

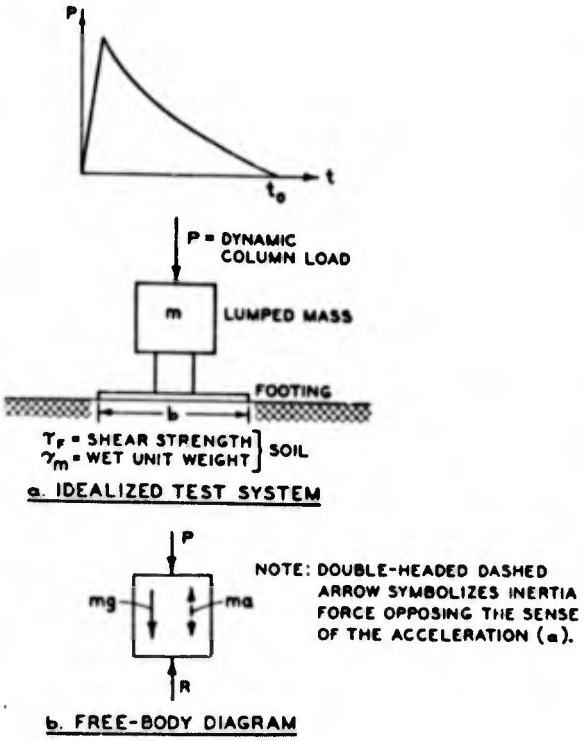

Fig. 1. Idealized test system and free-body diagram

Symbol	Quantity	Units
m	Mass of the load column of the dynamic loading machine	FT^2L^{-1}
P	Applied dynamic column load	F
t	Any time variable	T
t_o	Total pulse time	T
b	Footing width	L
ρ	Mass density of soil	FT^2L^{-4}
τ_f	Soil shear strength in unconfined compression	FL^{-2}
z	Displacement of the footing	L

8. The nondimensional equation developed for this system, given as equation 10 in Report 3, is

$$\frac{z}{b} = \zeta\left(\frac{t}{t_o}, \frac{P}{b^2\tau_f}, \frac{m}{b^3\rho}, \frac{Pt^2}{bm}\right) \qquad (1)$$

where

$\frac{z}{b}$ = displacement parameter

$\frac{t}{t_o}$ = time parameter

$\frac{P}{b^2\tau_f}$ = ratio of applied column live-load force to soil-resistance force, or strength parameter

$\frac{m}{b^3\rho}$ = ratio of "structure mass" to "soil mass," or mass parameter

$\frac{Pt^2}{bm}$ = ratio of applied column live-load force to interia force, or inertia parameter

9. The relation of the load R(t) delivered through the load column to the footing to the dynamic driving force P(t) applied to the column is evident from the free-body diagram in fig. 1b, and is as follows:

$$P(t) - R(t) = m(a - g) \qquad (2)$$

where

$P(t)$ = applied dynamic column load

$R(t)$ = footing reaction

m = load column mass

$a = \frac{d^2z}{dt^2}$ = acceleration of the system

g = gravitational acceleration

$R(t)$ is measured directly in all tests, and since the masses of the plate footings tested were small, it essentially represents the soil-resistance force opposing the footing penetration. This footing load is useful in the analysis, particularly in its dimensionless form

$\frac{R}{b^2\tau_f}$ = ratio of average stress on base of footing to soil shearing resistance, or resistance parameter

Significant Relations from Report 3

10. Fifteen dynamic and three static footing tests conducted in a model study of a postulated prototype soil-structure system and reported in Report 3 provided initial data for the three nondimensional relations under investigation. The results of the Report 3 investigation will be reviewed in this section as they provide the background for the investigation covered in this report. Five dynamic footing tests and one static test were conducted on each of the three soil specimens whose UC* shear strengths were 1.0, 1.4, and 1.7 kips per sq ft. Wet unit weight was approximately 115 lb per cu ft for all specimens. Sizes of the square footings used on each of the three specimens were 4.5, 6, and 8 in., respectively. The dynamic tests were interrelated by the force, length, time, piston mass, and soil strength scales used to design the tests as models of a common prototype subjected to several load levels.

11. Analysis of the results of these tests yielded the dimensionless footing load-displacement relations presented in fig. 2. The narrowness of the bands of data suggests the usefulness of the relation for displacement predictions provided the dynamic footing load pulses are of the type shown in the figure. However, this relation was obtained from data taken in tests

* Unconfined compression.

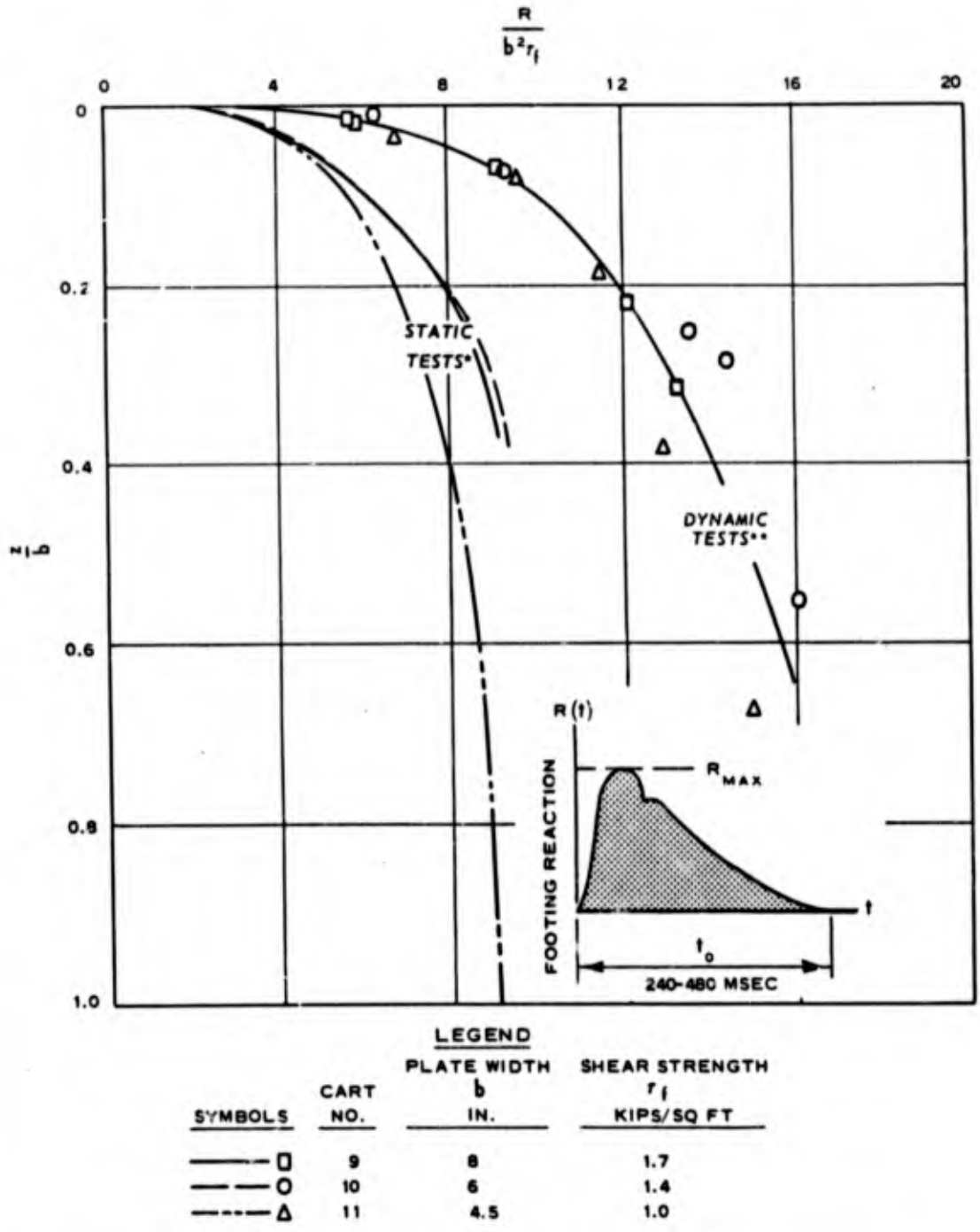

* CONTINUOUS REACTION-DISPLACEMENT CURVE FROM ONE STATIC TEST.

** CONSTRUCTED REACTION-DISPLACEMENT CURVE USING R_{MAX} AND t_{MAX} FROM FIVE DYNAMIC TESTS.

Fig. 2. Dimensionless footing reaction-displacement relation from Report 3

in which the independent variables had set relations to one another because all of these tests were conducted on distorted models of a single postulated prototype. As stated in paragraph 4, one of the objectives of this investigation is to determine if this relation still exists when the independent variables are not interrelated.

12. The second nondimensional load-displacement relation of interest obtained from the model tests in Report 3 is shown in fig. 3. It involves the maximum dynamic column load for the case where the load-column mass was approximately 160 lb and the time duration of P(t) varied as shown in fig. 3. As in the case of fig. 2, if the relation is shown to be independent

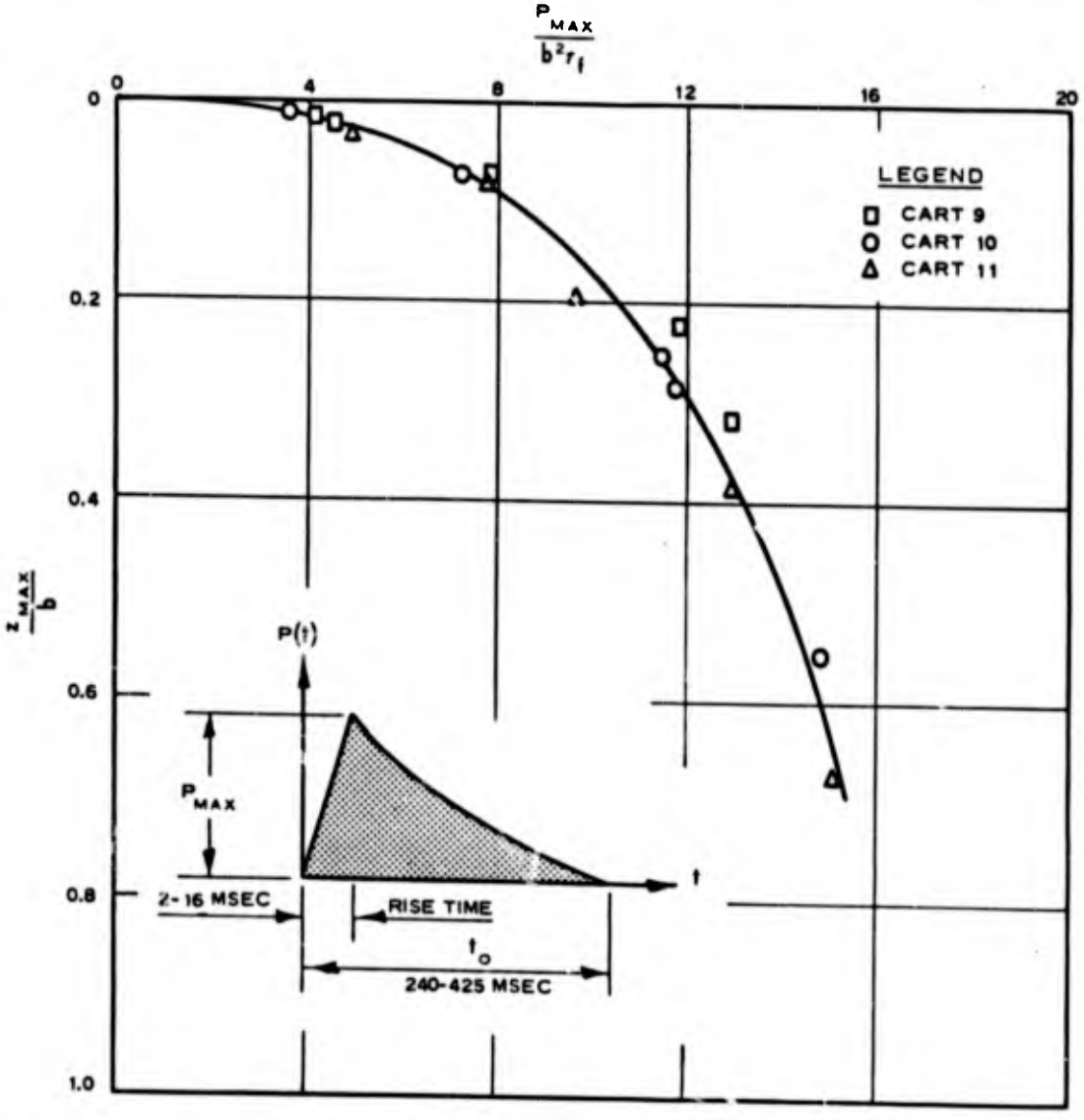

Fig. 3. Dimensionless relation of maximum applied dynamic column load versus maximum footing displacement (from Report 3)

of the scaling rules for the postulated prototype, it will be useful in predicting maximum displacement for the mass and load-pulse shape for which it was developed.

13. In addition to prediction of the maximum footing displacement, prediction of the time at which it occurs is of interest to the designer. A nondimensional relation, $\frac{P_{max}}{b^2 \tau_f}$ versus $\frac{P_{max}\, t(z_{max})^2}{bm}$, which supplies this needed information as a function of maximum dynamic column load, was also developed from the model test data in Report 3 and is shown in fig. 4.

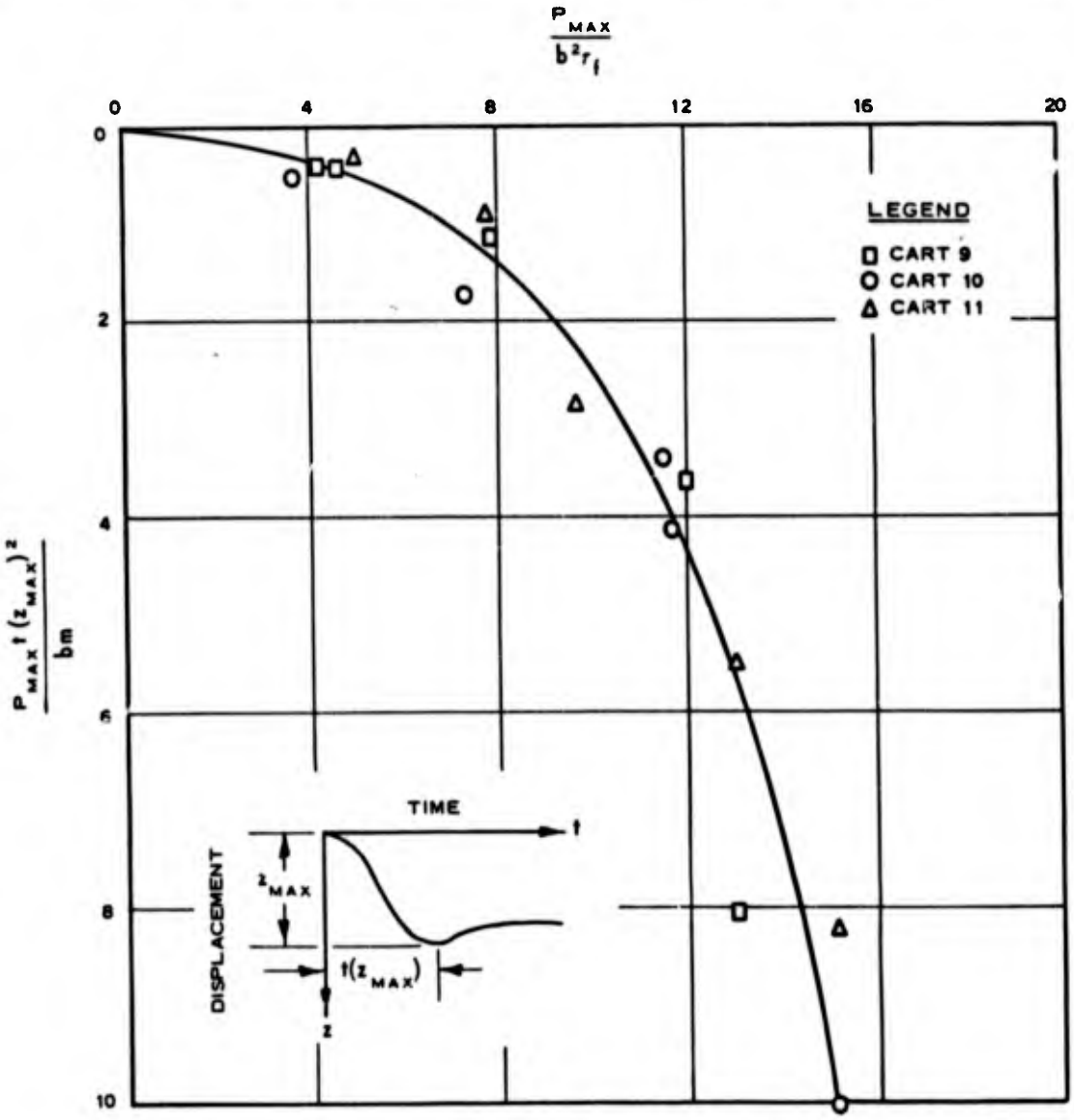

Fig. 4. Dimensionless relation between maximum applied dynamic column load and time to maximum displacement (from Report 3)

A displacement-time relation, typical of those observed in the Report 3 model tests, is shown at the base of fig. 4.

14. Based on the data presented in Report 3, confident prediction of maximum displacement and time to maximum displacement from figs. 2-4 is limited to those cases where masses and load-pulse shapes and durations are similar to those used in the investigation. It is also possible that the Report 3 relations are dependent on the interrelation of the independent variables dictated by the scaling requirements.

PART III: TESTS AND RESULTS

Plan of Test

15. A series of 24 dynamic footing tests was planned to determine if the three nondimensional relations are independent of model scaling rules and, if possible, to extend useful ranges of these relations. The tests were designed to vary maximum footing reaction R_{max}, footing width b, and soil shear strength τ_f over as wide a range as possible while maintaining their dimensionless combination, the resistance parameter $\frac{R_{max}}{b^2\tau_f}$, at a constant value. Further check on the stability of this parameter was planned by designing a few tests with constant values of R_{max} and τ_f and variable b, and others with constant values of R_{max} and b and variable τ_f. Initially peaked column-load pulses with rise times of approximately 5 msec and decay times of 400 msec were programed for all dynamic tests.

16. The plan of test is presented in the following tabulation.

Test No.	Test Location	Test* Objective	Programed Parameters: Maximum Reaction R_{max}, kips	Plate Width b, in.	Shear Strength τ_f kips/sq ft	$\frac{R_{max}}{b^2\tau_f}$
18-1	2+00	2	1.16	5.5**	0.50	11.0
2	3+50	2	1.38	6	↓	11.0
3	5+00	1	1.78	8		8.0
4	7+00	2	3.82	10		11.0
5	9+50	1	4.00	12		8.0
6	12+00	2	7.48	14		11.0
7	15+00	1	7.11	16		8.0
8	19+00	Static Test		10		--

(Continued)

* Test objectives were as follows:

(1) stability of z_{max}/b, $R_{max}/b^2\tau_f = 8$

(2) stability of z_{max}/b, $R_{max}/b^2\tau_f = 11$

(3) effect of b when R_{max} and τ_f are constant

(4) effect of τ_f when R_{max} and b are constant

** 5.5-in. plate used instead of 5-in. plate because the dynamic loading machine does not operate satisfactorily at peak dynamic reactions of less than 1.0 kip.

Test No.	Test Location	Test Objective	Programed Parameters: Maximum Reaction R_{max} Kips	Plate Width b in.	Shear Strength τ_f kips/sq ft	$\frac{R_{max}}{b^2 \tau_f}$
19-1	2+00	1	1.74	5	1.25	8.0
2	3+50	2	3.44	6		11.0
3	5+00	1,4	4.45	8		8.0
4	7+00	2	9.55	10		11.0
5	9+50	1,3	10.00	12		8.0
6	12+00	2	18.70	14		11.0
7	14+50	3	10.00	14		5.9
8	16+50	3	10.00	10		11.5
9	19+00	Static Test		10		--
20-1	2+00	1	2.78	5	2.00	8.0
2	3+50	2	5.50	6		11.0
3	5+00	1	7.11	8		8.0
4	7+00	2	15.30	10		11.0
5	9+50	1	16.00	12		8.0
6	12+00	2	9.78	8		11.0
7	13+50	3,4	4.45	8		5.0
8	15+00	3	4.45	6		8.9
9	16+50	3	4.45	5		12.8
10	19+00	Static Test		10		--

The tests were programed for three large soil-cart specimens with shear strengths of 0.50, 1.25, and 2.00 kips per sq ft and wet unit weights of approximately 115 lb per cu ft. The cart numbers (the first part of the test number) given are continuous with those in Report 3. Examination of the preceding tabulation indicates that programed maximum footing loads ranged from 1.16 to 18.70 kips and plate widths varied from 5 to 16 in. Fig. 5 shows the square aluminum plate footings used in this investigation and illustrates the range of widths investigated. The soil type, specimen construction methods, and test procedures were essentially the same as those used in the model tests described in Report 3. Details regarding these methods and procedures are given in Appendix A.

17. Static tests on 10-in.-wide square plates were programed for each soil-cart specimen to permit comparison of dynamic and static load-carrying capabilities at equal displacements in a manner similar to the comparison presented in Report 3 and shown in fig. 2, page 19.

18. The test locations given in the tabulation in paragraph 16 generally space the tests at equal or greater center-line distance to

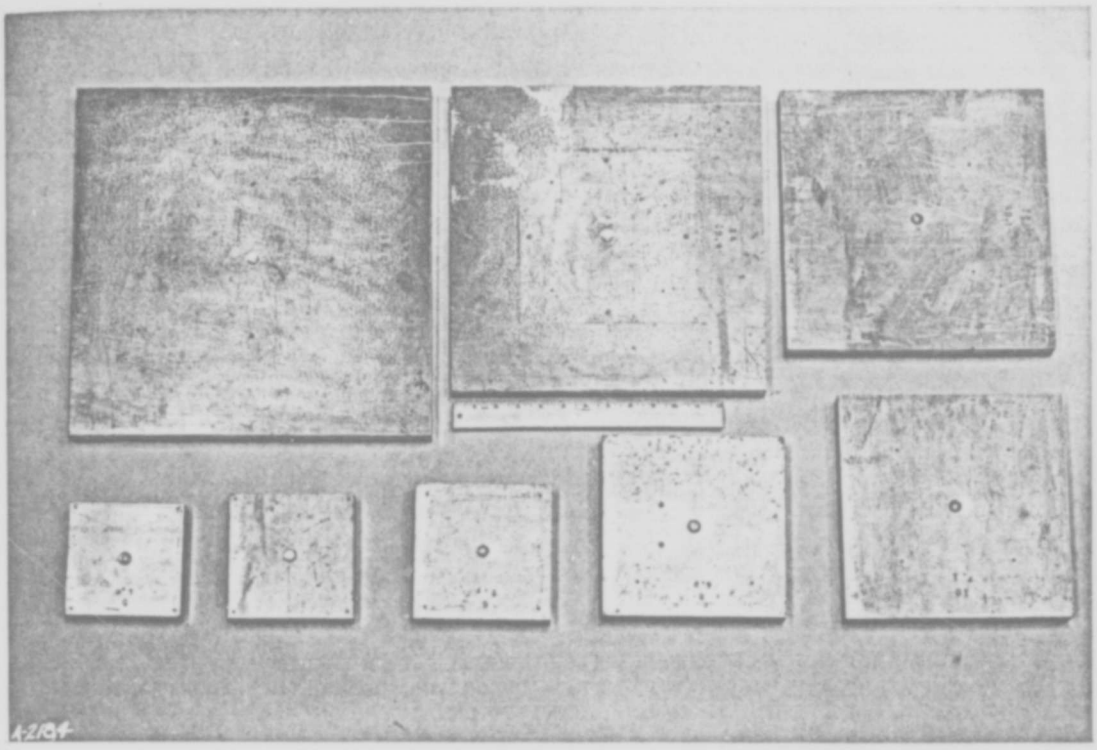

Fig. 5. Plates used in small-scale footing tests

plate-width ratios from one another and from soil-container boundaries than those described in the cart-width and test-spacing test series in Report 3. In that series, a spacing of 18 in. on centers was found to be sufficient to reduce test-location interference for 8-in.-wide plates to a negligible amount.[5] This spacing corresponds to a center-line distance to plate-width ratio of 2.25. However, this spacing criterion was slightly compromised to include an additional test in cart 19; the center-line distance to plate-width ratios for the spaces between tests 19-6 and 19-7 and between tests 19-7 and 19-8 are 2.1 and 2.0, respectively. No effects of this small decrease in spacing were apparent in the test data for these tests.

Test Results

19. The results of the soil tests made during cart construction, vane-resistance tests in the vicinity of each test location just prior to the footing tests, and the unit weight determinations after the footing

tests were completed are reported for the three cart specimens in tables 1-3.

20. The data on the undisturbed block samples taken from the soil-cart specimens and the results of UC tests conducted on small specimens from the blocks are reported in plates 1-3. Actual average values of wet unit weight, shear strength, and water content for each cart specimen as determined from the UC tests are tabulated below. Programed values are also given for comparison.

	Actual UC Average			Programed Values		
Cart No.	Shear Strength τ_f kips/sq ft	Wet Unit Wt γ_m lb/cu ft	Water Content w %	Shear Strength τ_f kips/sq ft	Wet Unit Wt γ_m lb/cu ft	Water Content w %
18	0.62	112.9	33.5	0.50	115.0	35.0
19	1.21	116.9	28.3	1.25	115.0	28.5
20	1.78	118.2	25.5	2.00	115.0	25.4

21. Results of the unconsolidated-undrained triaxial and consolidated-drained direct shear tests are given in plates 4-6. The envelopes of the Mohr diagrams for the unconsolidated-undrained triaxial tests on specimens from carts 18, 19, and 20 have slope angles of 1.0, 2.5, and 4.0 deg, respectively. Nearly all of the specimens tested were more than 85 percent saturated. Estimated values of shear strength and wet unit weight for each test location are tabulated below.

Test Number	Test Location	Estimated* Shear Strength τ_f kips/sq ft	Estimated** Wet Unit Wt γ_m lb/cu ft	Test Number	Test Location	Estimated Shear Strength τ_f kips/sq ft	Estimated** Wet Unit Wt γ_m lb/cu ft
18-1	2+00/20	0.60	113	18-5	9+50/20	0.65	112
2	3+50/20	0.55	113	6	12+00/20	0.65	113
3	5+00/20	0.60	111	7	15+00/20	0.60	114
4	7+00/20	0.65	113	8	19+00/20	0.60	113

(Continued)

* τ_f = avg UC shear strength for cart $\times \frac{\text{vane resistance near plate}}{\text{avg vane resistance for cart}}$.

** γ_m = avg UC wet unit wt for cart $\times \frac{\text{posttest wet unit wt near test}}{\text{avg posttest wet unit wt for cart}}$.

Test Number	Test Location	Estimated Shear Strength τ_f kips/sq ft	Estimated Wet Unit Wt γ_m lb/cu ft
19-1	2+00/20	1.20	118
2	3+50/20	1.20	115
3	5+00/20	1.20	118
4	7+00/20	1.25	117
5	9+50/20	1.20	115
6	12+00/20	1.20	115
7	14+50/20	1.20	116
8	16+50/20	1.25	118
9	19+00/20	1.25	118

Test Number	Test Location	Estimated Shear Strength τ_f kips/sq ft	Estimated Wet Unit Wt γ_m lb/cu ft
20-1	2+00/20	1.75	121
2	3+50/20	1.80	120
3	5+00/20	1.70	119
4	7+00/20	1.85	119
5	9+50/20	1.75	119
6	12+00/20	1.85	118
7	13+50/20	1.85	114
8	15+00/20	1.75	115
9	16+50/20	1.75	118
10	19+00/20	1.85	120

22. Results of the dynamic tests are reported in plates 7-30. The plates present computed column load, column acceleration, load cell reaction, and average plate displacement time histories for the dynamic tests. These time histories were determined from the test oscillograph records by using procedures that are described in Appendix A. Idealized versions of the column-load time histories are shown in plates 31-33 along with the column-load time histories actually computed.

23. Continuous footing load-displacement curves have been prepared in nondimensional form for each of the 24 dynamic footing tests and are given in plates 34-36. These plots of $\frac{R}{b^2 \tau_f}$ versus $\frac{z}{b}$ were prepared in lieu of dimensional load-displacement curves because the large range of footing sizes used in each cart made presentation of the dimensional curves unwieldy.

24. Load-displacement data for the three static tests are given in plate 37. The static tests in carts 18, 19, and 20 were all conducted on 10-in.-square plates and required 2.5, 2.6, and 3.3 hr, respectively, for completion.

25. The appearance of the surface of the soil specimen in the vicinity of the test locations after a static test was observed to be distinctly different from that observed after a dynamic test. After the static tests, considerable upheaval of the specimen surface was noted as well as significant radial and tangential cracking of the surface of the specimen. After the dynamic tests, upheaval of the specimen surface was noticed to be

considerably less than that in a static test with comparable maximum displacement, and little if any cracking was noted. Similar phenomena had been previously observed and reported in Report 3.[5] Rotation of the footings about the bearing tip during displacement was negligible; the maximum angle of rotation about the horizontal axis was 0.02 radians.

26. A summary of the dynamic test data is tabulated below.

	Controlled Parameters*							Dependent Parameters			
Test No.	Plate Width b in.	Maximum Dynamic** Input P_{max} kips	Input Rise Time t_r msec	Input Hold Time t_h msec	Total Pulse Time t_o msec	Shear Strength τ_f kips/sq ft	Wet Unit Weight γ_m lb/cu ft	Maximum Reaction R_{max} kips	Time to R_{max} $t(R_{max})$ msec	Maximum Displacement z_{max}, in.	Time to z_{max} $t(z_{max})$ msec
18-1	5.5	1.10	5	11	390	0.60	113	1.39	42	0.75	56
2	6	1.11	3	24	410	0.55	113	1.47	33	0.46	44
3	8	1.38	6	26	410	0.60	111	1.91	22	0.24	29
4	10	3.67	10	15	390	0.65	113	4.37	32	0.82	46
5	12	3.67	7	0	380	0.65	112	4.43	22	0.38	26
6	14	7.20	4	0	390	0.65	113	8.04	22	1.01	40
7	16	6.00	5	28	420	0.60	114	7.35	20	0.48	23
19-1	5	1.30	10	30	430	1.20	118	1.82	27	0.22	36
2	6	3.04	6	10	410	1.20	115	3.54	34	0.92	53
3	8	3.73	4	4	420	1.20	118	4.54	18	0.36	25
4	10	8.64	4	34	370	1.25	117	10.30	21	0.99	32
5	12	9.13	5	0	390	1.20	115	10.52	17	0.64	24
6	14	17.58	3	0	370	1.20	115	18.25	16	1.48	27
7	14	8.73	5	0	340	1.20	116	10.17	13	0.29	16
8	10	9.42	4	0	360	1.25	118	10.21	20	1.31	33
20-1	5	2.30	6	0	410	1.75	121	2.68	24	0.29	35
2	6	5.01	4	0	390	1.80	120	5.31	22	0.91	35
3	8	6.59	3	0	360	1.70	119	7.69	18	0.60	23
4	10	13.60	2	0	370	1.85	119	14.28	18	1.64	30
5	12	13.25	2	0	400	1.75	119	14.72	15	0.67	18
6	8	9.58	2	0	410	1.85	118	9.82	22	1.72	36
7	8	3.78	6	30	420	1.85	114	4.46	15	0.13	30
8	6	4.10	6	0	410	1.75	115	4.63	24	0.78	36
9	5	4.06	6	18	380	1.75	118	4.47	40	2.53	62

* Piston weight was 160 lb in all tests.

** Since the dynamic loading machine does not permit direct control of R_{max}, values of P_{max} to give the desired values of R_{max} were determined from preliminary tests on box specimens having approximately the same consistency as the cart specimen. These values of P_{max} which can be controlled by the machine, were programed for the tests.

The maximum dynamic column load P_{max} and input rise times, hold times, and positive-phase durations were determined from the idealized dynamic column-force curves in plates 31-33. The shear strength and wet unit weight are reprinted from the tabulation in paragraph 21. Maximum footing reaction R_{max}, the time of its occurrence $t(R_{max})$, maximum footing displacement z_{max}, and the time to maximum displacement $t(z_{max})$ were determined from plates 7-30.

27. Footing-response data are summarized in the following tabulation:

Test No.	Plate Width b in.	Maximum Load-cell Reaction R_{max} kips	Time to R_{max} $t(R_{max})$ msec	Maximum Plate Displacement z_{max} in.	Time to z_{max} $t(z_{max})$ msec	Final Plate Displacement z_{final} in.	Computed Maximum Velocity v_{max} ips	Time to v_{max} $t(v_{max})$ msec	Maximum Positive Acceleration a^+ g	Maximum Negative Acceleration a^- g
18-1	5.5	1.39	42	0.75	56	0.53	13.5	24	16.9	-1.7
2	6	1.47	33	0.46	44	0.25	14.3	17	11.3	-1.5
3	8	1.91	22	0.24	29	0.09	11.8	13	5.1	-2.4
4	10	4.37	32	0.82	46	0.46	36.4	19	15.1	-4.6
5	12	4.43	22	0.38	26	0.17	24.6	13	12.8	-5.5
6	14	8.04	22	1.01	40	0.57	52.9	12	31.2	-8.6
7	16	7.35	20	0.48	23	0.17	34.5	10	24.5	-8.9
19-1	5	1.82	27	0.22	36	0.11	9.9	17.5	8.6	-2.0
2	6	3.54	34	0.92	53	0.71	32.0	20	12.2	-3.7
3	8	4.54	18	0.36	25	0.18	28.7	10	17.4	-6.8
4	10	10.30	21	0.99	32	0.68	58.7	11	33.8	-10.2
5	12	10.52	17	0.64	24	0.41	46.1	11	32.6	-12.6
6	14	18.25	16	1.48	27	0.93	109.3	9.5	76.0	-22.9
7	14	10.17	13	0.29	16	0.08	34.9	7	27.2	-14.4
8	10	10.21	20	1.31	33	0.86	69.8	12	34.6	-12.6
20-1	5	2.68	24	0.29	35	0.15	14.5	14	9.6	-2.9
2	6	5.31	22	0.91	35	0.68	41.2	13	27.9	-6.8
3	8	7.69	18	0.60	23	0.36	41.2	9	22.4	-10.0
4	10	14.28	18	1.64	30	1.19	88.7	11	55.5	-16.7
5	12	14.72	15	0.67	18	0.37	66.5	8	71.0	-21.6
6	8	9.82	22	1.72	36	1.37	78.6	12	47.3	-12.7
7	8	4.46	15	0.13	30	0.04	14.0	9	7.7	-5.0
8	6	4.63	24	0.78	36	0.56	32.8	13	24.0	-4.5
9	5	4.47	40	2.53	62	2.27	64.7	26	21.8	-5.7

In addition to quantities already described in the tabulation in paragraph 26 (included for completeness), the preceding tabulation lists the final plate displacement determined several minutes after the completion of the test, the range of accelerations experienced by the load column, and the maximum velocity determined by numerical integration of the acceleration data.[7] These additional data have been included to give the reader a more complete picture of the footing response and the velocity and acceleration spectra encountered.

PART IV: DISCUSSION AND ANALYSIS

Comparison of Nondimensional Relations

28. Using the test data reported in paragraph 26 for carts 18-20, the resistance, strength, inertia, and displacement parameters were computed for each test. (For definitions of these dimensionless parameters, see paragraphs 8 and 9.) In the following paragraphs, these data will be presented and compared with the bands of data for each of the three nondimensional relations given in Part II of this report.

Resistance parameter versus displacement parameter

29. Fig. 6 is a plot of the resistance parameter versus the displacement parameter. The points represent the values of $\frac{R_{max}}{b^2 \tau_f}$ and $\frac{z_{max}}{b}$ for the 24 dynamic tests. The dotted band is the range of the Report 3 model test data from a similar plot (see fig. 2, page 19). Eighteen of the 24 data points fall within the band of the Report 3 data with the remaining six data points falling slightly above it. The new data appear to form a band that is shifted slightly above the Report 3 data.

30. Static resistance parameter-displacement parameter curves are also shown in fig. 6. The crosshatched zone represents the band of similar static test data from Report 3. In the early portion of the curves ($\frac{z}{b} \leq 0.1$) agreement with the Report 3 band is good. At large displacements the Report 3 test data, which were obtained using 4-1/2-, 6-, and 8-in. plates, lie somewhat above the curves for the tests on 10-in. plates reported herein. This may be due to difficulties in evaluation of the shear strength or differences in the conduct of the test. Although the same criteria were used to control the loading in both sets of tests, it is noted that the Report 3 static tests ranged from 1.7 to 2.2 hr in duration, while those reported for carts 18-20 ranged from 2.5 to 3.3 hr. Thus, it is possible that a creep

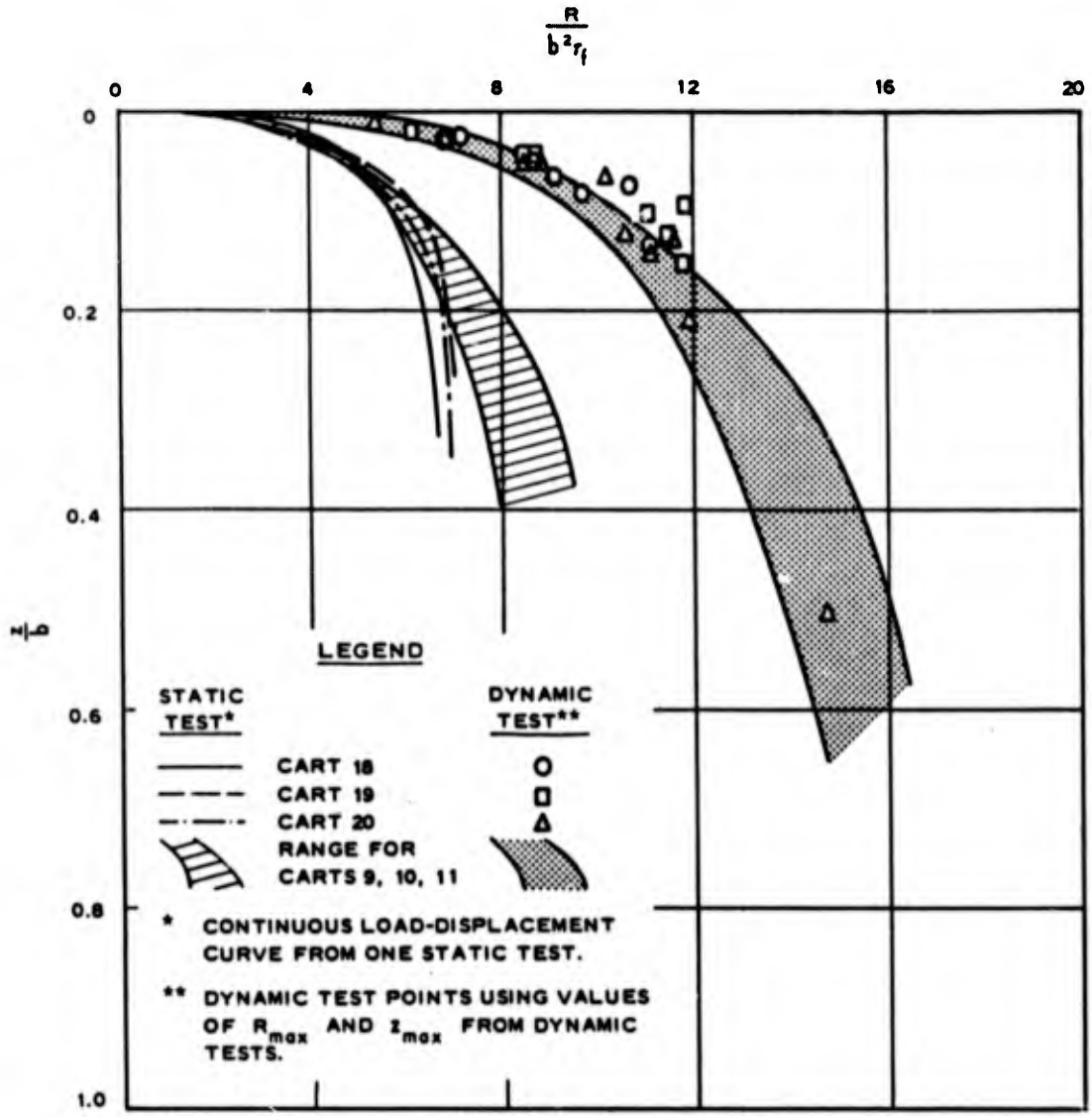

Fig. 6. Resistance parameter versus displacement parameter

type of displacement is responsible for the differences at larger deformations.

Strength parameter
versus displacement parameter

31. The second nondimensional relation under investigation, the relation between strength parameter $\frac{P_{max}}{b^2\tau_f}$ and displacement parameter $\frac{z_{max}}{b}$, is shown in fig. 7. The 24 dynamic tests yielded values of the strength parameter ranging from 4.60 to 13.37, a range nearly as

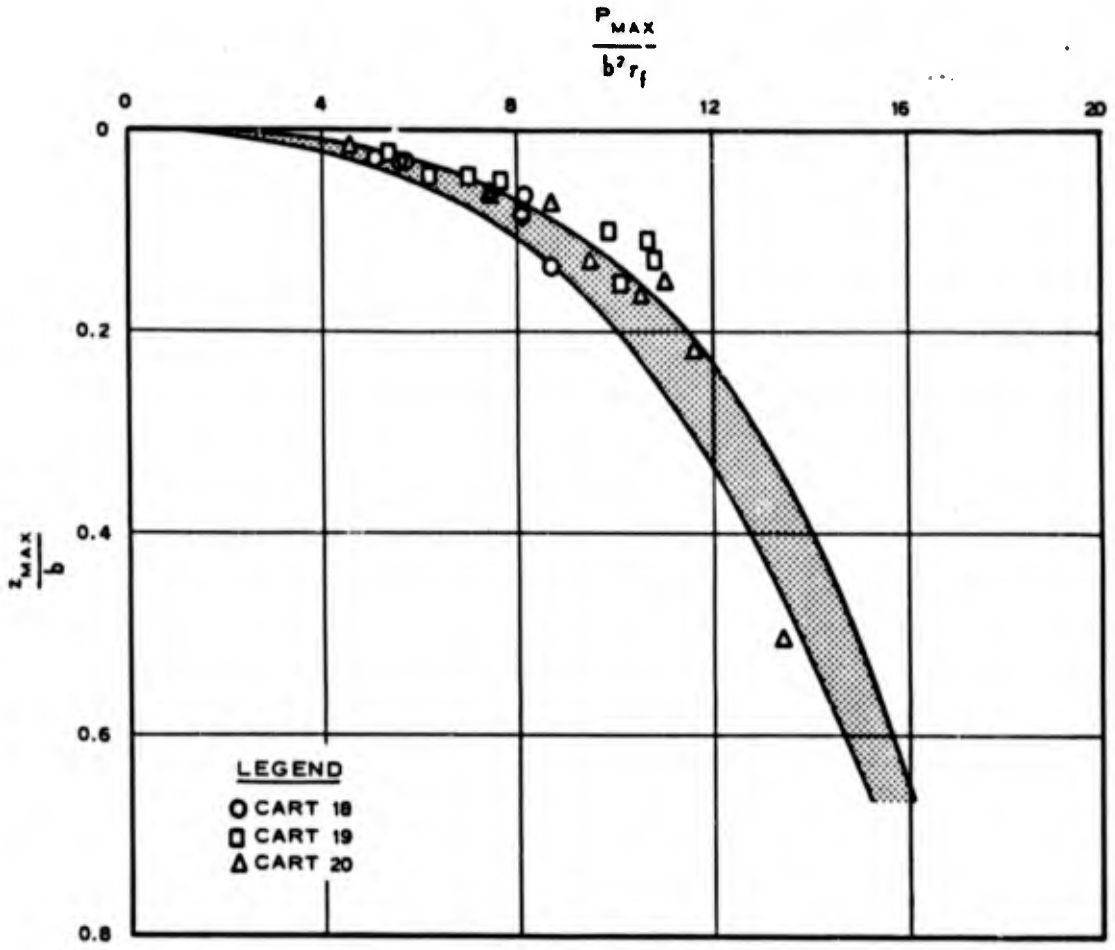

Fig. 7. Strength parameter versus displacement parameter

large as that of the Report 3 data (see fig. 3, page 20). The dotted band in fig. 7 indicates the range of points in the original nondimensional relation shown in fig. 3. Agreement between the data and the Report 3 band is good, but some points lie slightly above the band and one point, at a relatively large displacement, lies just below the band.

32. Comparing figs. 3 and 7, it was observed that there is only one point in fig. 3 in the region where the strength parameter lies between 8.0 and 11.5, while in fig. 7 there are 12. Thus, the weight of data suggests that the relation of strength parameter to displacement parameter would be better defined by the new data in this region.

Strength parameter
versus inertia parameter

33. The third nondimensional relation, that of strength parameter

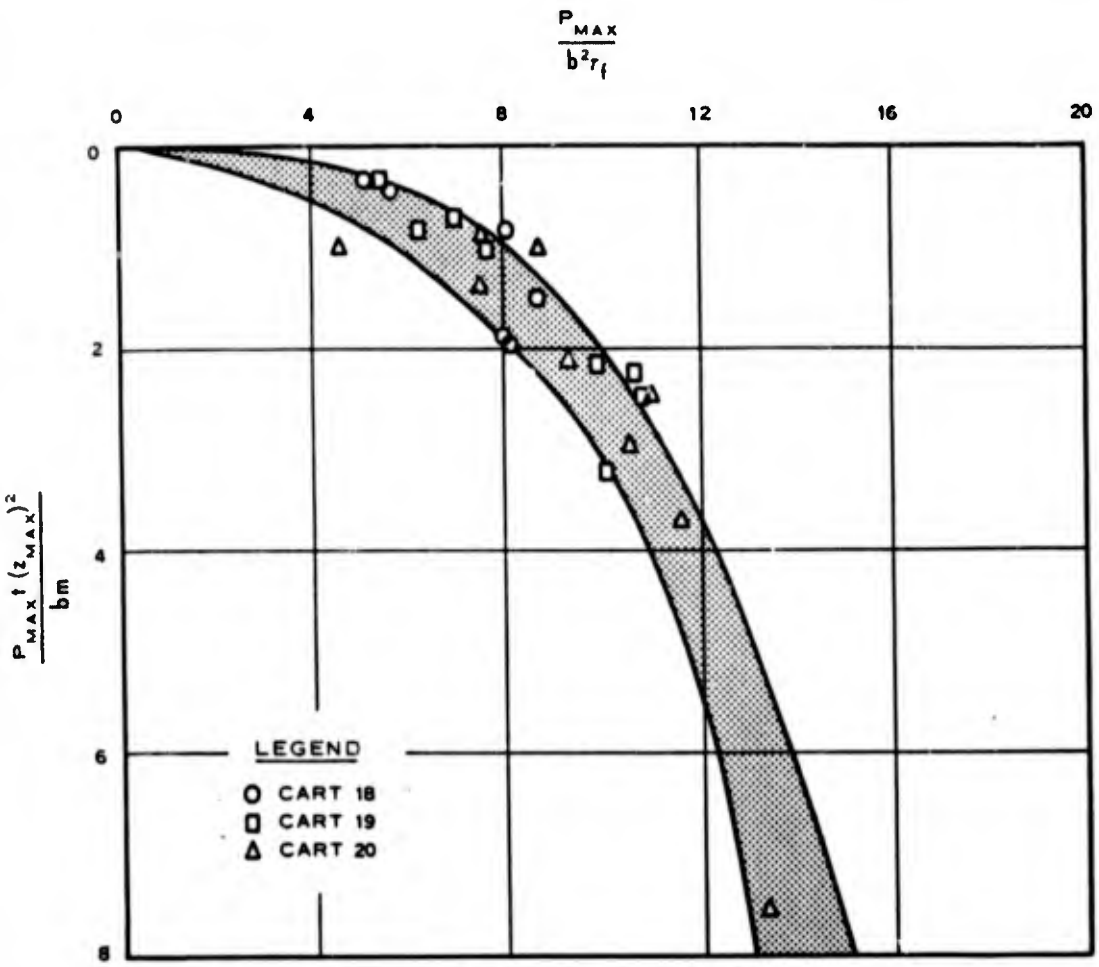

Fig. 8. Strength parameter versus inertia parameter

to inertia parameter, is shown in fig. 8. The data from carts 18-20 agree well with the dotted band which represents the range of data in the similar relation presented in Report 3 (see fig. 4, page 21). Although there are a few points outside the band, almost all of which lie above it and in the region where the strength parameter lies between 8.0 and 11.5, the agreement is generally good. The discussion on the relative weight of the two sets of data given in paragraph 32 applies equally well here.

Stress-strain relations

34. The evidence presented in the preceding paragraphs regarding the existence of the three nondimensional relations tends to imply identical or at least nearly identical nondimensional stress-strain relations for the three soil specimens tested. Nondimensional stress-strain curves for the three soil-cart specimens are shown in fig. 9.

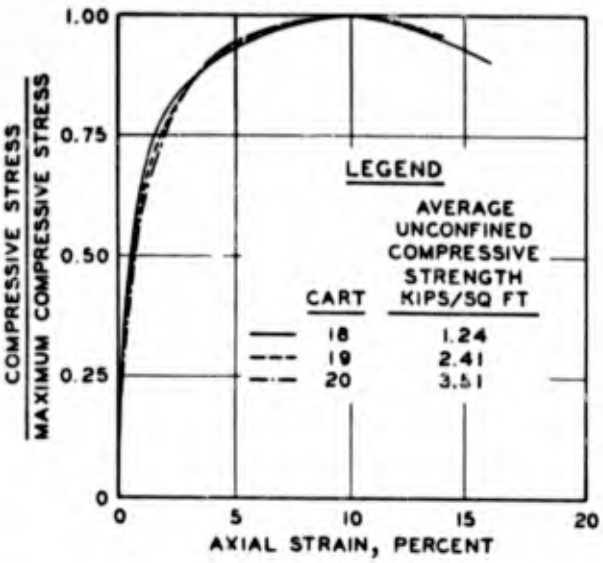

Fig. 9. Normalized UC stress-strain curves

These normalized curves were obtained by dividing the average UC test results shown in plates 1-3 by the respective maximum UC stresses. The figure shows that the curves are almost identical in form and that peak stress was reached at from 8.0 to 9.8 percent axial strain. On the basis of the work presented in Report 3, reasonably close agreement of the nondimensional stress-strain curves was anticipated. However, the agreement of the data shown in fig. 9 far surpassed expectations.

Limitations and use

35. Figures 6-9 have shown that the general forms of the three nondimensional relations developed in Report 3 have been reproduced in dynamic small-scale footing tests on compacted clay that were not interrelated by scaling relations. The maximum displacement of a dynamically loaded footing and the time of its occurrence, for the conditions herein described, can be predicted by using figs. 6-8. Within certain limits, of course, reasonable estimates perhaps can be made for other associated conditions. For confident predictions of displacements for other conditions, however, additional investigations covering a wider range of parameters are required.

Curve Fitting

36. Combining the data from carts 9-11 (Report 3) and that from carts 18-20 (this report) gives 39 points for each of the three nondimensional relations. Curve-fitting methods were applied in an attempt to obtain equations of best fit for each of the three nondimensional relations presented in the preceding section.

37. Because curve-fitting methods require prior knowledge or assumption of the general form of the equation that fits the data, the points which form nonlinear relations on arithmetic plots were replotted on log-log paper. Fig. 10 shows the log-log plots which yielded essentially

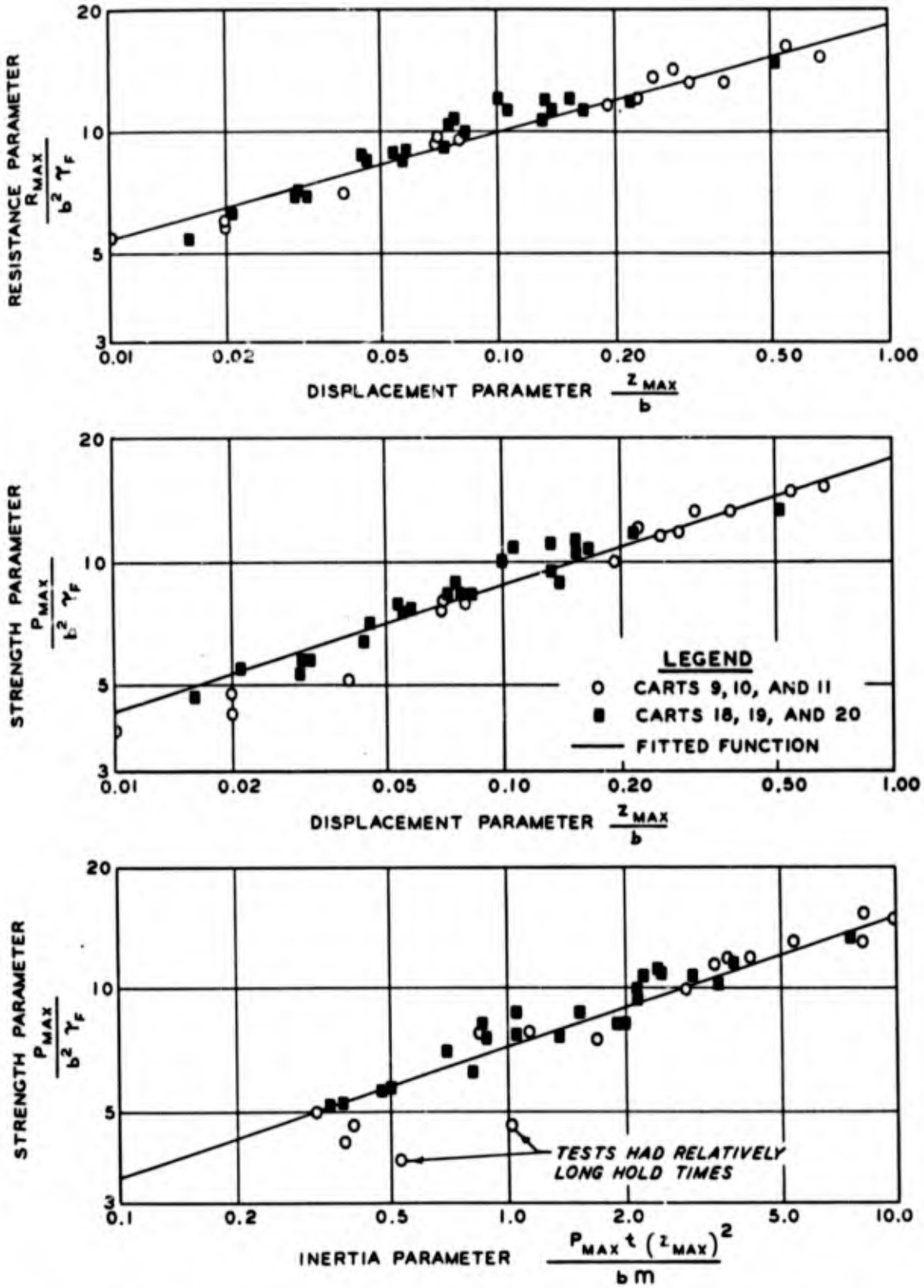

Fig. 10. Logarithmic plots of dimensionless quantities

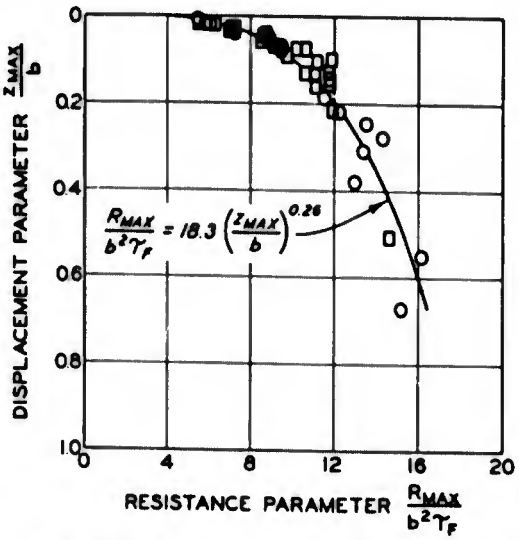

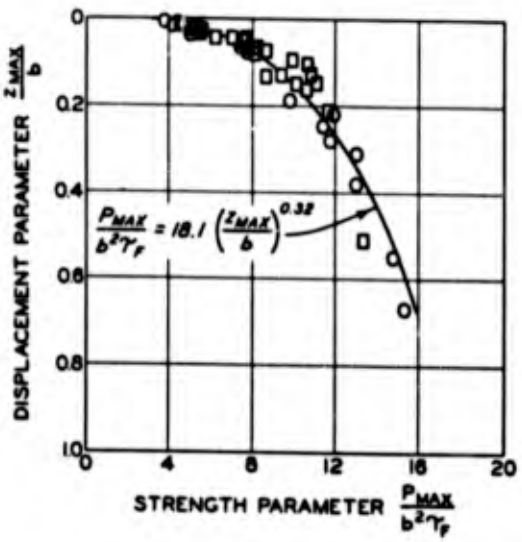

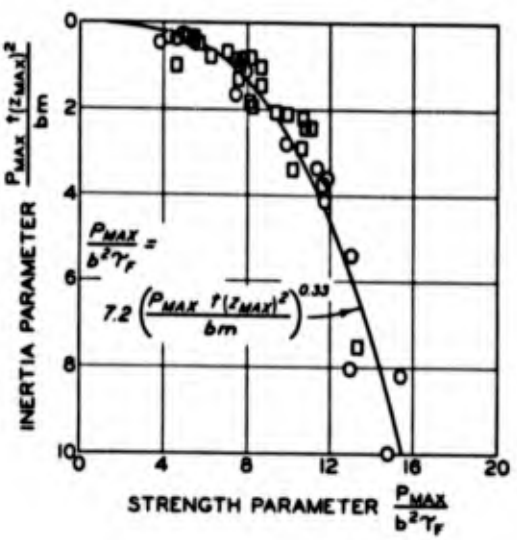

LEGEND
- ○ CARTS 9, 10, AND 11
- □ CARTS 18, 19, AND 20

straight-line relations. A straight line on a log-log plot is a power function similar to

$$Y = aX^n \tag{3}$$

where

Y = ordinate

X = abscissa

a, n = constants

The constants a and n were evaluated for the three nondimensional relations by using a successive approximation technique based on the general curve-fitting method for nonlinear formulas outlined by Scarborough[8] (pp 539-545). The power functions that best fit the data are given below.

$$\frac{R_{max}}{b^2\tau_f} = 18.3\left(\frac{z_{max}}{b}\right)^{0.26} \tag{4}$$

$$\frac{P_{max}}{b^2\tau_f} = 18.1\left(\frac{z_{max}}{b}\right)^{0.32} \tag{5}$$

$$\frac{P_{max}}{b^2\tau_f} = 7.2\left[\frac{P_{max}\, t(z_{max})^2}{bm}\right]^{0.33} \tag{6}$$

These equations are plotted in fig. 11 for comparison with the nondimensional data of interest.

Fig. 11. Comparison of fitted curves with nondimensional test data

38. It should be pointed out that the power functions, although fitting the data rather well, have not been shown to be the only form of equation which fits the data, and it is possible that another nonlinear function fits the data equally well. The equations in paragraph 37 are regarded as describing the data and not as the equations governing the physical process in the small-scale dynamic footing tests.

Comparison of Static and Dynamic Load-Displacement Curves

39. Comparison of the static and dynamic resistance parameter-displacement parameter plots, which are in reality dimensionless maximum footing load-maximum displacement plots, is given in fig. 12. Examination of these plots indicates that the dynamic test data can be approximated by multiplying the average static resistance parameter by a factor ranging from approximately 1.7 (at small values of $\frac{z}{b}$) to 1.9 (at large values of $\frac{z}{b}$). Dynamic-to-static load ratios of 1.5 to 1.7 were derived in Report 3 from similar comparisons. Static and dynamic unconsolidated-undrained triaxial tests of fat clays very similar to the clay used in

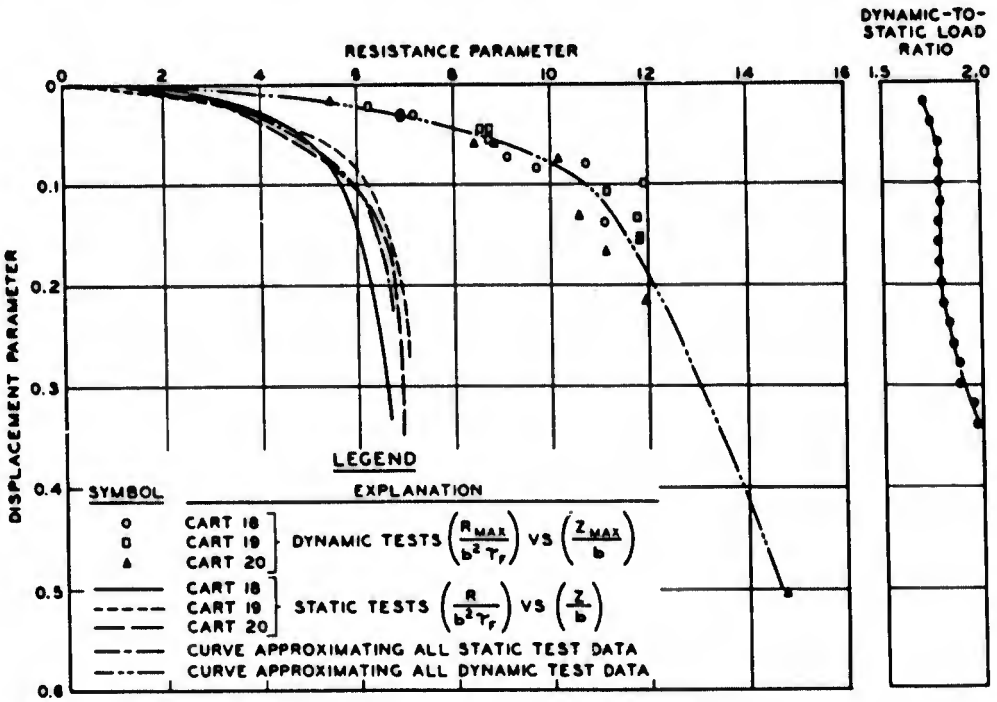

Fig. 12. Comparison of dynamic resistance parameter with static resistance parameter at equal values of displacement parameter

both footing studies showed that the ratios of dynamic-to-static shear strength, or strain-rate factors, are of the same magnitude (1.5 to 1.9) as the load ratios obtained from the footing tests.[9,10,11]

40. The laboratory triaxial tests also indicated that the ratio of dynamic-to-static shear strength decreased as water content and degree of saturation decreased.[10] Average dynamic-to-static load ratios were determined for each of the carts in the Report 3 model study and for each of those reported in this investigation. These ratios are plotted versus the average degree of saturation for the cart specimens in fig. 13.

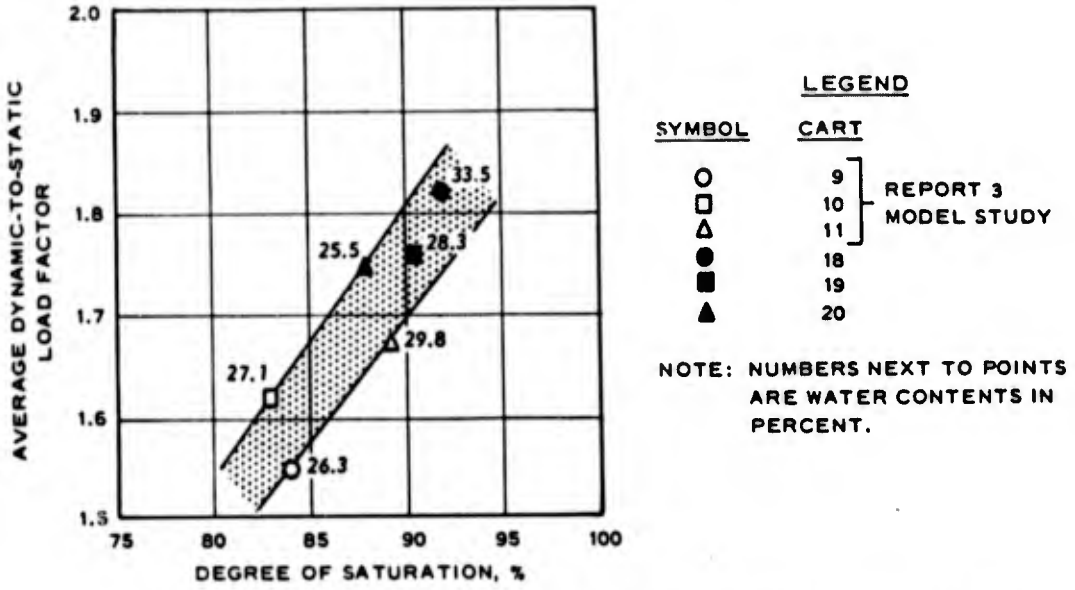

Fig. 13. Effect of degree of saturation and water content on dynamic-to-static load ratio

Report 3 specimens, which had lower dynamic-to-static load ratios, also had lower degrees of saturation. Thus, the differences in dynamic-to-static load ratios noted between the Report 3 data and the data in this footing test series may be related to changes in the ratio of static-to-dynamic shear strength caused by changes in water content and degree of saturation.

41. The static load-displacement curve for a 10-in.-square plate (test 18-8) and the dynamic load-displacement curve for the same size plate (test 18-4) on the same soil specimen are plotted in fig. 14. An estimated band of dynamic load-displacement relations obtained by multiplying the static load by dynamic-to-static load ratios of 1.5 and 1.9 is also shown. The lower band curve clearly provides a conservative estimate of

the maximum load-maximum displacement point. Similar trends are noted for static and dynamic tests on 10-in.-square plates in carts 19 and 20, as indicated in figs. 15 and 16.

42. In the tests reported, the time to maximum footing load ranged from 13 to 42 msec, and the average downward footing velocity ranged from 4.3 to 54.8 ips. As previously noted, dynamic unconsolidated-undrained

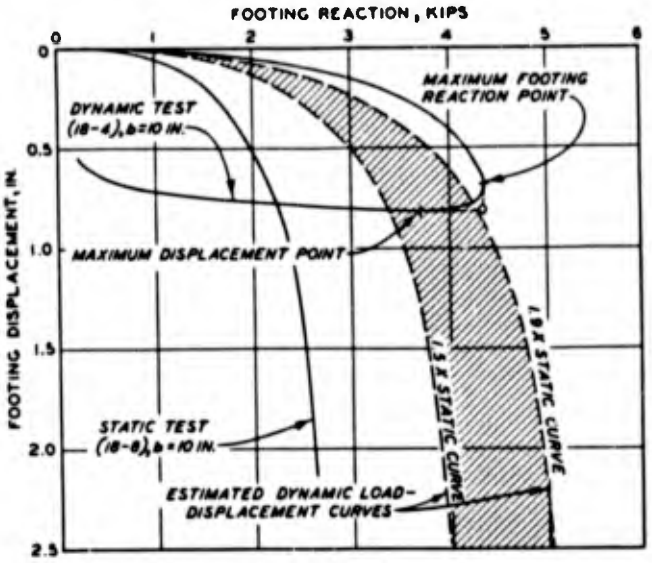

Fig. 14. Dynamic and static footing load-displacement curves from tests 18-4 and 18-8

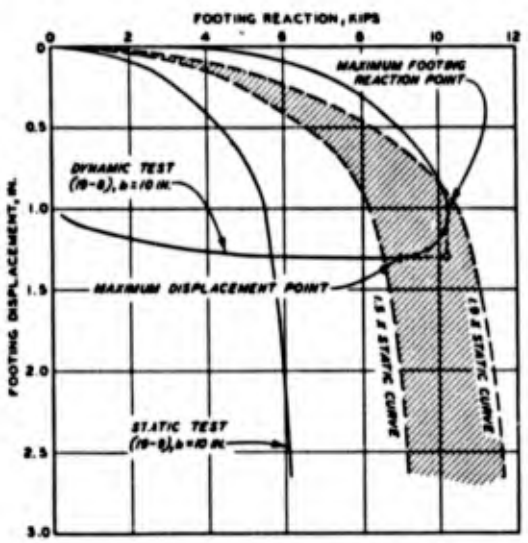

Fig. 15. Dynamic and static footing load-displacement curves from tests 19-8 and 19-9

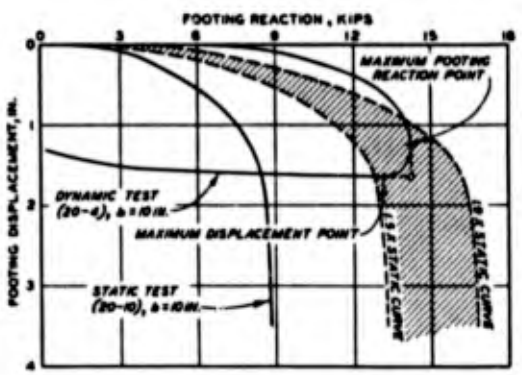

Fig. 16. Dynamic and static footing load-displacement curves from tests 20-4 and 20-10

shear strength of fat clays is dependent on the time of loading or strain rate. Use of the dynamic-to-static load ratios presented above with load-pulse time histories and rates of footing displacement outside the ranges tested should therefore be approached with caution. Additional testing is necessary to complete investigations of this type for the range of footing loadings and displacement rates possible in actual prototype conditions.

However, the observations noted here are believed to be of significance in estimating the response of dynamically loaded footings.

PART V: CONCLUSIONS AND RECOMMENDATIONS

Conclusions

43. Based on the footing tests conducted (those reported both here and in Report 3) and the analysis of the data, the following conclusions concerning the three nondimensional dynamic footing test relations originally developed in Report 3 are presented:

a. The nondimensional relations given in figs. 6-8 are independent of the Report 3 model scaling relations.

b. For the range of footing load-pulse durations and shapes investigated, the maximum displacement of clay-supported square footings can be predicted from the relations between $\frac{R_{max}}{b^2\tau_f}$ and $\frac{z_{max}}{b}$ given in fig. 6 or equation 4.

c. For the range of column-load pulses investigated and the piston mass used, the maximum displacement can also be predicted from the relation between $\frac{P_{max}}{b^2\tau_f}$ and $\frac{z_{max}}{b}$ given in fig. 7 or equation 5.

d. For the conditions given in subparagraph 43c, time to maximum displacement can be predicted approximately from the relation between $\frac{P_{max}}{b^2\tau_f}$ and $\frac{P_{max}\, t(z_{max})^2}{bm}$ given in fig. 8 or equation 6.

44. The following additional conclusions resulting from the conduct and analysis of the tests are offered:

a. The ratio of dynamic-to-static resistance parameters for equal values of displacement parameter ranged from 1.7 to 1.9. This range differs somewhat from the 1.5 to 1.7 range reported in Report 3.

b. For the range of footing sizes and shear strengths tested, the dynamic load-displacement curve for a footing on the clay tested can be conservatively approximated up to the point of maximum displacement by multiplying the load in

a static load-displacement curve for the same soil and footing by a factor of 1.5.

Recommendations

45. To extend the nondimensional foundation response prediction relations for use with more realistic protective structure problems, the following investigations are recommended:

a. A study of the effect of structure (piston) mass on the three relations developed to predict the response of dynamically loaded, clay-supported footings.

b. A study of the effect of depth of burial on footing load-displacement curves as a step toward predicting the response of buried protective structures.

c. A study of the effect of major variations in the duration of the dynamic footing load pulse (positive-phase duration) under relatively large, intermediate, and low footing-load levels.

d. A study of the effect of footing-load rise time (time to maximum reaction) with emphasis on the effect of rise time on the magnitude of the dynamic-to-static load ratio.

LITERATURE CITED

1. Triandifalidis, G. E., Analytical Study of Dynamic Bearing Capacity of Foundations. Prepared by University of Illinois under contract DA-22-079-eng-240 for the U. S. Army Engineer Waterways Experiment Station, CE, Vicksburg, Miss. January 1961.

2. U. S. Army Engineer Waterways Experiment Station, CE, Theoretical Study of the Displacement of Long Footings by Dynamic Loads. Miscellaneous Paper No. 3-418, Vicksburg, Miss., March 1961.

3. _____, Dynamic Bearing Capacity of Soils; Dynamic Loading Machine and Preliminary Small-Scale Footing Tests, by R. C. Sloan. Technical Report No. 3-599, Report 1, Vicksburg, Miss., June 1962.

4. _____, Dynamic Bearing Capacity of Soils; Dynamically Loaded Small-Scale Footing Tests on Dry Dense Sand. Technical Report No. 3-599, Report 2, Vicksburg, Miss. (In preparation.)

5. _____, Dynamic Bearing Capacity of Soils; The Application of Similitude to Small-Scale Footing Tests, by J. G. Jackson, Jr., and P. F. Hadala. Technical Report No. 3-599, Report 3, Vicksburg, Miss., December 1964.

6. Murphy, Glenn, Similitude in Engineering. Ronald Press, New York, N. Y., 1950.

7. U. S. Army Engineer Waterways Experiment Station, CE, A CK-225 Computer Program for Numerical Integration with Automatic Method Selection, by J. B. Cheek, Jr. Miscellaneous Paper No. 5-583, Vicksburg, Miss., June 1963.

8. Scarborough, J. B., Numerical Mathematical Analysis, 5th ed. Johns Hopkins Press, Baltimore, Md., 1962.

9. Casagrande, Arthur, and Shannon, W. L., "Strength of soils under dynamic loads." Transactions, American Society of Civil Engineers, vol 114 (1949).

10. Massachusetts Institute of Technology, First Interim Report on Dynamic Soil Tests. DASA-1162, Cambridge, Mass., October 1959.

11. Whitman, R. V., Richardson, A. M., and Nasim, N. M., Strength of Saturated Fat Clay. Massachusetts Institute of Technology, Cambridge, Mass., June 1962.

12. U. S. Army Engineer Waterways Experiment Station, CE, The Unified Soil Classification System. Technical Memorandum No. 3-357, vol 1, Vicksburg, Miss., March 1953 (revised April 1960).

13. Hvorslev, M. J., Subsurface Exploration and Sampling of Soils for Civil Engineering Purposes. Report on Research Project of ASCE, edited and printed by U. S. Army Engineer Waterways Experiment Station, CE, Vicksburg, Miss., November 1949.

14. Perry, C. C., and Lissner, H. R., "Strain gage instrumentation." Shock and Vibration Handbook, C. M. Harris and C. E. Crede, eds. (McGraw-Hill Book Company, Inc., New York, N. Y., 1961), vol 1, Chap. 17.

15. U. S. Army Engineer Waterways Experiment Station, CE, Laboratory Test Procedures. Prepared and distributed for the Office, Chief of Engineers, Department of the Army, Washington, D. C.

16. Turnbull, W. J., and Foster, C. R., "Stabilization of materials by compaction." Transactions, American Society of Civil Engineers, vol 123 (1958), pp 1-26.

Table 1

Vane Shear Resistance and Unit Weight Tests, Cart 18

(A) Construction Control Tests

Compaction-Layer Depth in.	In-Place Unit Wt: Station ft	Offset in.	Water Content %	Wet Unit Wt lb/cu ft	Dry Unit Wt lb/cu ft	Vane Resistance: Average kips/sq ft	Range kips/sq ft
0-3	1+00	24	35.1	113.9	84.3	0.81	0.68-0.95
	4+00	62	34.8	111.4	82.6		
	8+00	24	35.0	111.3	82.4		
	12+00	62	36.0	110.5	81.3		
	16+00	24	35.9	109.7	80.7		
	20+00	62	35.4	111.5	82.3		
3-6	1+00	24	31.4	114.3	87.0	0.80	0.64-0.92
	4+00	62	33.5	111.5	83.5		
	8+00	24	32.6	112.4	84.8		
	12+00	62	32.7	112.1	84.5		
	16+00	24	33.5	111.6	83.6		
	20+00	62	32.8	113.2	85.2		
6-9	1+00	43	37.3	109.3	79.6	0.79	0.66-0.96
	4+00	43	36.9	109.5	80.0		
	8+00	43	37.0	110.0	80.3		
	12+00	43	34.6	112.1	83.3		
	16+00	43	36.6	110.7	81.0		
	20+00	43	34.1	112.8	84.1		
9-12	4+00	43	38.0	thin lift*		0.64	0.50-0.85
	8+00	43	36.7	thin lift			
	12+00	43	36.8	thin lift			
	16+00	43	36.9	thin lift			
	20+00	43	38.0	thin lift			
Avg			35.3	111.5	82.8	0.76	

(B) Pretest Vane Tests

Test No.	Plate Location: Station ft	Offset in.	Average Vane Resistance: Near Plate (27 Tests) kips/sq ft	Under Plate (3 Tests) kips/sq ft
18-1	2+00	43	1.01	1.02
18-2	3+50	43	0.96	0.96
18-3	5+00	43	1.04	1.02
18-4	7+00	43	1.10	1.18
18-5	0+90	43	1.05	1.09
18-6	12+00	43	1.09	1.10
18-7	15+00	43	1.03	0.95
18-8	19+00	43	1.04	1.02
Avg			1.04	

(C) Posttest Unit Wt Tests

Station ft	Offset in.	Water Content %	Wet Unit Wt lb/cu ft	Dry Unit Wt lb/cu ft
2+00	62	34.2	111.6	83.2
3+00	24	34.3	111.2	82.8
5+00	62	33.8	109.8	82.1
7+00	24	34.6	111.1	82.5
9+50	62	35.0	110.6	81.9
12+00	24	34.8	111.5	82.7
13+00	24	34.6	110.3	81.9
15+00	62	34.8	112.1	83.2
17+00	24	35.4	110.9	81.9
19+00	24	36.4	111.6	82.9
19+00	62	34.3	111.8	83.2
20+00	43	34.8	111.4	82.6
Avg		34.6	111.2	82.6

* This layer was actually approximately 2.5 in. thick, which is slightly too thin for the satisfactory operation of the Little Rock control sampler.

Table 2

Vane Shear Resistance and Unit Weight Tests, Cart 19

(A) Construction Control Tests

Compaction-Layer Depth in.	In-Place Unit Wt: Station ft	Offset in.	Water Content %	Wet Unit Wt lb/cu ft	Dry Unit Wt lb/cu ft	Vane Resistance: Average kips/sq ft	Range kips/sq ft
0-3	2+00	24	29.2	116.7	90.3	1.52	1.31-1.74
	4+00	62	29.4	115.4	89.2		
	8+00	24	28.7	116.5	90.5		
	12+00	62	29.4	116.8	90.3		
	16+00	24	29.2	115.9	89.7		
	19+00	62	29.6	116.1	89.6		
3-6	2+00	24	27.0	118.2	92.9	2.19	1.53-2.49
	4+00	62	27.2	118.2	92.7		
	8+00	24	26.9	118.4	93.0		
	12+00	62	26.8	118.8	93.5		
	16+00	24	27.2	117.4	92.1		
	19+00	62	27.1	118.8	93.2		
6-9	2+00	43	28.8	117.6	91.3	1.99	1.74-2.38
	4+00	43	27.2	118.6	93.2		
	8+00	43	28.1	117.7	91.9		
	12+00	43	28.2	117.6	91.7		
	16+00	43	28.6	116.7	90.7		
	19+00	43	28.7	116.9	90.8		
9-12	2+00	43	27.5	118.3	92.8	1.85	1.63-2.01
	4+00	43	27.2	118.8	93.4		
	8+00	43	27.1	117.7	92.6		
	12+00	43	28.0	117.2	91.6		
	16+00	43	28.3	117.0	91.2		
	19+00	43	27.5	118.5	92.9		
Avg			28.0	117.5	91.7	1.88	

(B) Pretest Vane Tests

Test No.	Plate Location: Station ft	Offset in.	Average Vane Resistance: Near Plate (27 Tests) kips/sq ft	Under Plate (3 Tests) kips/sq ft
19-1	2+00	43	2.18	2.21
19-2	3+50	43	2.18	2.20
19-3	5+00	43	2.24	2.09
19-4	7+00	43	2.29	1.98
19-5	9+50	43	2.19	2.16
19-6	12+00	43	2.25	2.03
19-7	14+50	43	2.24	2.26
19-8	16+50	43	2.29	2.46
19-9	19+00	43	2.32	2.48
Avg			2.24	

(C) Posttest Unit Wt Tests

Station ft	Offset in.	Water Content %	Wet Unit Wt lb/cu ft	Dry Unit Wt lb/cu ft
2+00	62	29.4	117.0	90.4
3+50	24	28.3	113.8	88.7
5+00	62	29.2	116.9	90.5
7+00	24	28.9	115.5	89.6
9+50	62	30.1	113.8	87.5
12+00	24	29.4	113.8	87.9
14+50	62	29.2	114.3	88.5
16+50	24	29.2	117.0	90.6
18+00	24	28.7	116.2	90.3
18+00	62	29.4	116.9	90.3
20+00	24	29.1	116.8	90.5
20+00	62	29.3	115.3	89.2
Avg		29.2	115.6	89.5

Table 3

Table 3

Vane Shear Resistance and Unit Weight Tests, Cart 20

(A) Construction Control Tests								(B) Pretest Vane Tests				
Compaction-Layer Depth in.	In-Place Unit Wt					Vane Resistance		Test No.	Plate Location		Average Vane Resistance	
	Station ft	Offset in.	Water Content %	Wet Unit Wt lb/cu ft	Dry Unit Wt lb/cu ft	Average kips/sq ft	Range kips/sq ft		Station ft	Offset in.	Near Plate (27 Tests) kips/sq ft	Under Plate (3 Tests) kips/sq ft
0-3	2+00	24	25.8	120.5	95.8	2.98	2.84-3.11	20-1	2+00	43	3.37	2.93
	4+00	62	25.5	119.5	95.2			20-2	3+50	43	3.44	3.23
	8+00	24	25.8	119.8	95.2			20-3	5+00	43	3.31	3.13
	12+00	62	26.0	119.1	94.5			20-4	7+00	43	3.53	3.64
	16+00	24	26.0	118.9	94.4			20-5	9+50	43	3.39	3.41
	19+00	62	25.8	119.6	95.1			20-6	12+00	43	3.53	3.37
								20-7	13+50	43	3.53	3.69
3-6	2+00	24	25.6	120.0	95.5	2.65	2.52-2.86	20-8	15+00	43	3.37	3.52
	4+00	62	26.1	120.1	95.2			20-9	16+50	43	3.42	3.37
	8+00	24	26.6	118.3	93.4			20-10	19+00	43	3.53	3.31
	12+00	62	26.3	119.4	94.5							
	16+00	24	26.3	119.1	94.3			Avg			3.44	
	19+00	62	25.8	119.2	94.8							
6-9	2+00	43	26.1	120.0	95.2	3.05	2.90-3.23	(C) Posttest Unit Wt Tests				
	4+00	43	26.2	118.8	94.1			Station ft	Offset in.	Water Content %	Wet Unit Wt lb/cu ft	Dry Unit Wt lb/cu ft
	8+00	43	25.5	119.4	95.1			2+00	62	26.1	119.7	94.9
	12+00	43	25.8	119.4	94.9			3+50	24	26.1	119.4	94.7
	16+00	43	25.6	119.1	94.8			5+00	62	26.2	118.1	93.6
	19+00	43	26.0	119.4	94.8			7+00	24	26.0	118.1	93.7
9-12	2+00	43	25.1	120.8	96.6	2.66	2.07-3.64	9+50	62	26.6	117.6	92.9
	4+00	43	27.4	117.9	92.4			12+00	24	25.9	117.1	93.0
	8+00	43	26.6	118.3	93.4			13+50	62	26.3	113.2	89.6
	12+00	43	26.1	119.5	94.8			15+00	24	26.2	113.3	89.8
	16+00	43	27.6	117.2	91.8			15+00	62	25.9	115.5	91.7
	18+00	43	26.5	119.6	94.5			17+00	24	26.2	117.2	92.9
								17+00	62	26.4	116.2	91.9
								20+50	24	26.2	119.7	94.8
								20+50	62	26.1	119.1	94.4
Avg			26.1	119.3	94.6	2.84		Avg			26.2	117.2	92.9

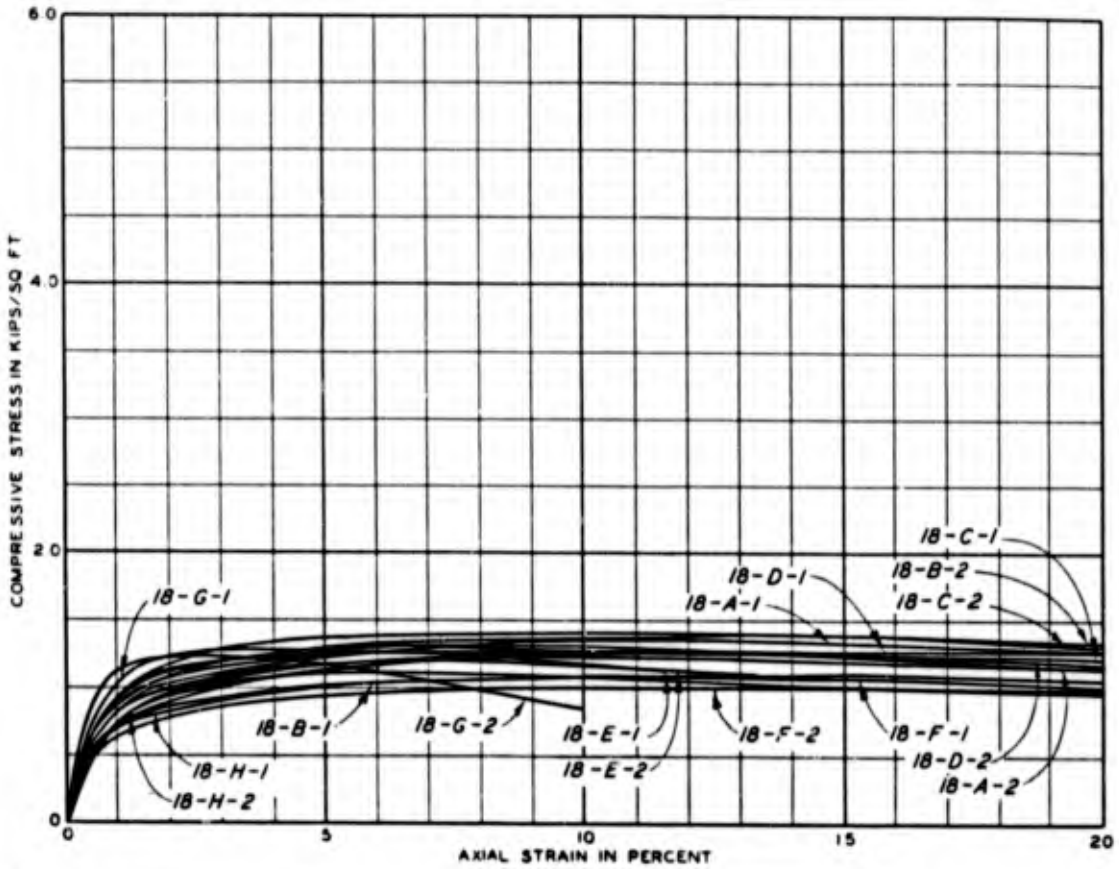

BLOCK				TEST*	INITIAL CONDITIONS				UNCONF COMP STRESS	SHEAR STRESS	TIME** TO FAILURE	FAILURE STRAIN
NUMBER	LOCATION				WATER CONTENT	DRY UNIT WT LB PER CU FT	VOID RATIO	SAT.				
	STATION FT	OFFSET IN.	DEPTH IN.		%			%	KIPS PER SQ FT	KIPS PER SQ FT	MIN	%
18-A	2+00	24	0-12	18-A-1	33.1	84.3	0.991	89.8	1.37	0.69	7	11.0
				18-A-2	32.9	84.8	0.979	90.4	1.34	0.67	5	7.0
18-B	3+50	62	0-12	18-B-1	33.6	83.6	1.008	89.7	1.12	0.56	4	6.6
				18-B-2	33.4	84.8	0.979	91.8	1.42	0.71	5	10.0
18-C	5+00	24	0-12	18-C-1	33.7	84.5	0.987	91.9	1.28	0.64	5	9.0
				18-C-2	32.9	85.3	0.968	91.4	1.39	0.70	7	12.5
18-D	7+00	62	0-12	18-D-1	33.6	84.7	0.982	92.0	1.28	0.64	7	13.3
				18-D-2	33.5	84.6	0.984	91.6	1.24	0.62	7	13.3
18-E	9+50	24	0-12	18-E-1	33.4	84.7	0.982	91.5	1.26	0.63	4	6.6
				18-E-2	33.5	83.8	1.003	89.8	1.21	0.61	4	6.6
18-F	12+00	62	0-12	18-F-1	34.3	84.6	0.984	93.8	1.08	0.54	8	12.5
				18-F-2	33.7	83.9	1.001	90.6	1.00	0.50	8	13.0
18-G	15+00	24	0-12	18-G-1	33.2	85.5	0.963	92.7	1.30	0.65	4	5.4
				18-G-2	35.0	83.6	1.008	93.4	1.22	0.61	1	2.3
18-H	17+00	62	0-12	18-H-1	33.2	85.3	0.968	92.3	1.11	0.56	8	12.5
				18-H-2	33.1	86.0	0.952	93.5	1.29	0.62	7	13.0
				AVERAGE	33.5	84.6	0.984	91.6	1.24	0.62	6	9.7

* STRAIN-CONTROLLED TEST ON 1.4-IN.-DIAM × 3.01-IN.-HIGH SPECIMEN TAKEN FROM 0- TO 4-IN. DEPTH OF THE BLOCK SAMPLE.

** RATE OF STRAIN CHANGED FROM 1% PER MINUTE TO 2.5% PER MINUTE AT FROM 4 TO 8% AXIAL STRAIN.

UNCONFINED COMPRESSION TEST RESULTS

CART 18

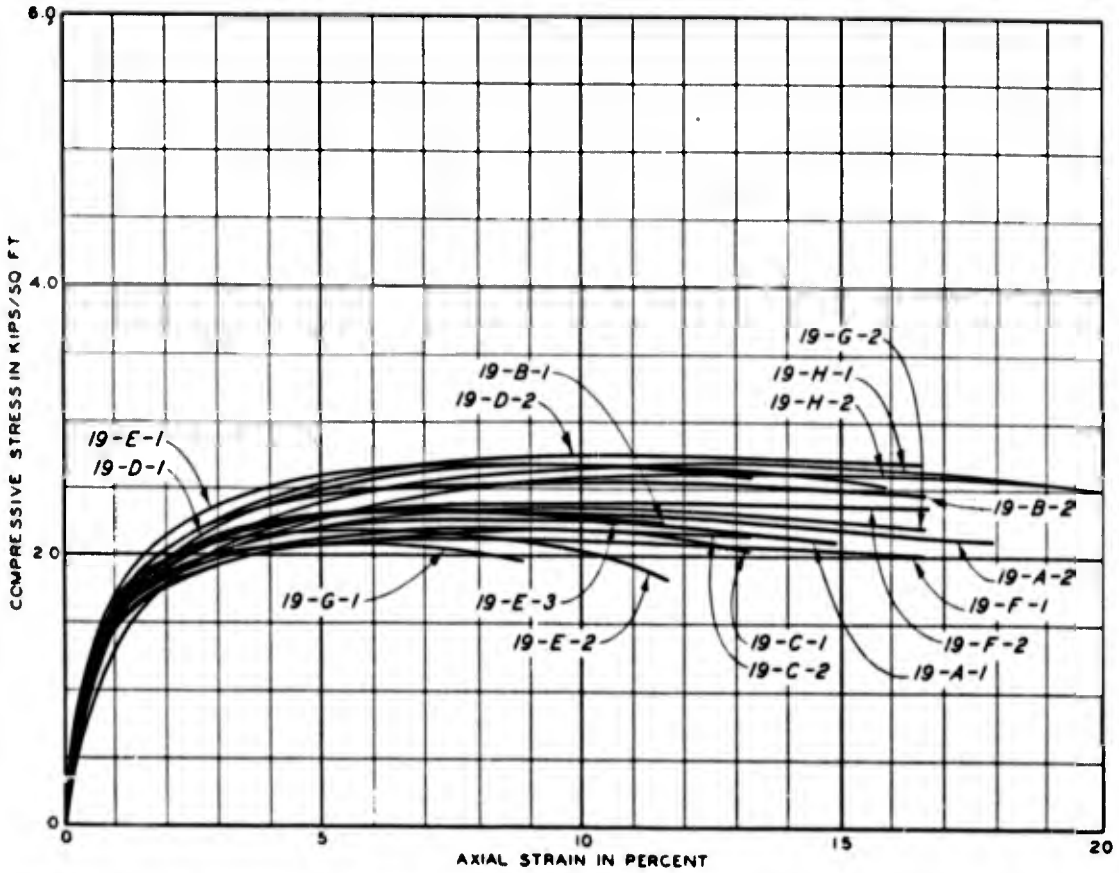

BLOCK				TEST*	INITIAL CONDITIONS				UNCONF COMP STRESS	SHEAR STRESS	TIME** TO FAILURE	FAILURE STRAIN
NUMBER	LOCATION				WATER CONTENT	DRY UNIT WT LB PER CU FT	VOID RATIO	SAT.				
	STATION FT	OFFSET IN.	DEPTH IN.		%			%	KIPS PER SQ FT	KIPS PER SQ FT	MIN	%
19-A	2+00	24	0-12	19-A-1	28.2	90.7	0.851	89.1	2.29	1.15	5	8.3
				19-A-2	28.7	90.4	0.857	90.1	2.35	1.18	5	8.3
19-B	3+50	62	0-12	19-B-1	28.4	91.1	0.843	90.6	2.35	1.18	4	6.6
				19-B-2	28.4	92.0	0.825	92.6	2.57	1.29	7	11.6
19-C	5+00	24	0-12	19-C-1	28.0	91.2	0.841	89.6	2.21	1.11	5	10.0
				19-C-2	28.6	91.1	0.843	91.3	2.23	1.12	5	8.3
19-D	7+00	62	0-12	19-D-1	27.4	92.5	0.815	90.4	2.68	1.34	6	10.0
				19-D-2	27.3	93.4	0.797	92.1	2.76	1.38	7	11.0
19-E	9+50	24	0-12	19-E-1	28.0	91.0	0.845	89.1	2.69	1.35	6	8.3
				19-E-2	28.0	90.2	0.861	87.5	2.19	1.10	4	5.7
				19-E-3	27.7	90.2	0.861	86.5	2.36	1.18	4	7.0
19-F	12+00	62	0-12	19-F-1	29.1	89.8	0.869	90.1	2.12	1.06	5	9.0
				19-F-2	29.1	90.4	0.857	91.3	2.39	1.20	7	11.0
19-G	14+50	20	0-12	19-G-1	28.7	90.0	0.865	89.3	2.08	1.04	4	5.9
				19-G-2	28.6	90.9	0.847	90.8	2.34	1.17	6	9.6
19-H	16+50	62	0-12	19-H-1	28.0	91.8	0.829	90.9	2.68	1.34	7	13.0
				19-H-2	28.4	91.9	0.827	92.4	2.61	1.31	8	13.5
AVERAGE					28.3	91.1	0.843	90.2	2.41	1.21	6	9.2

* STRAIN-CONTROLLED TEST ON 1.4-IN.-DIAM × 3.01-IN.-HIGH SPECIMEN TAKEN FROM 0- TO 4-IN. DEPTH OF THE BLOCK SAMPLE.

** RATE OF STRAIN CHANGED FROM 1% PER MINUTE TO 2.5% PER MINUTE AT FROM 4 TO 8% AXIAL STRAIN.

UNCONFINED COMPRESSION TEST RESULTS
CART 19

PLATE 2

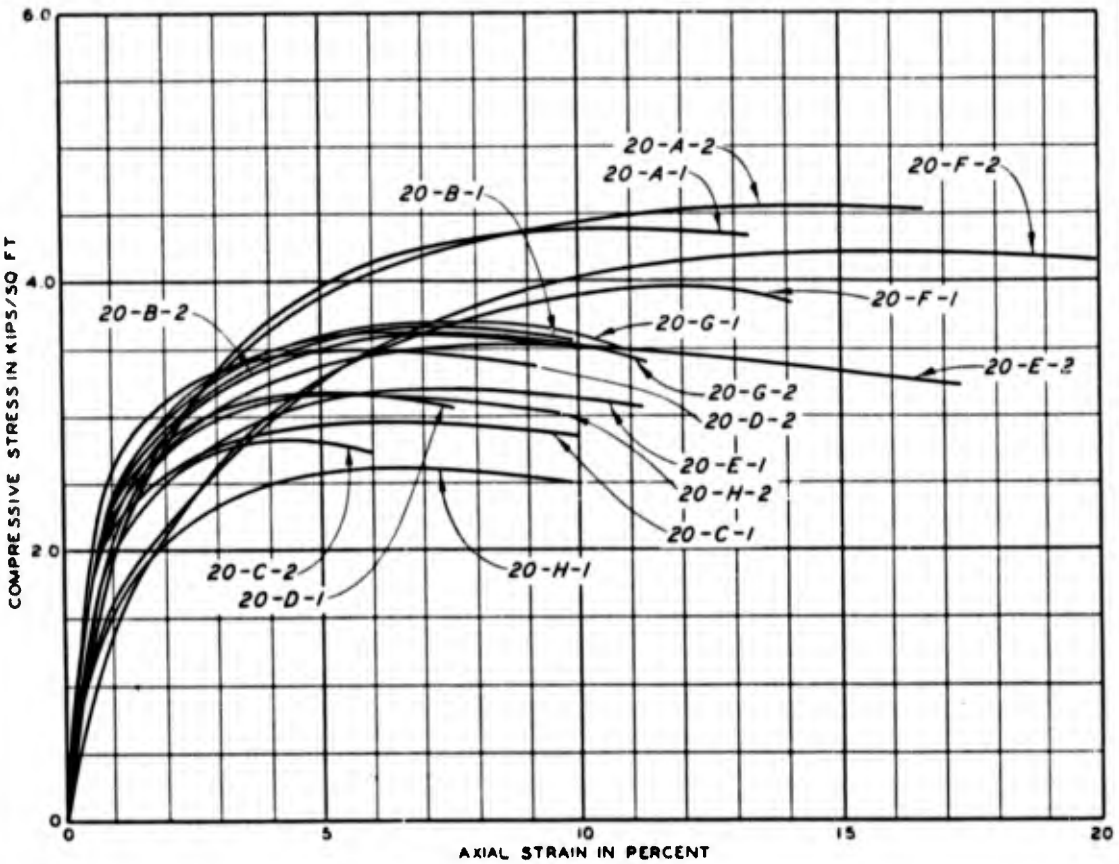

BLOCK				TEST*	INITIAL CONDITIONS				UNCONF COMP STRESS	SHEAR STRESS	TIME** TO FAILURE	FAILURE STRAIN
NUMBER	LOCATION				WATER CONTENT	DRY UNIT WT LB PER CU FT	VOID RATIO	SAT.	KIPS PER SQ FT	KIPS PER SQ FT	MIN	%
	STATION FT	OFFSET IN.	DEPTH IN.		%			%				
20-A	2+00	24	0-12	20-A-1	25.1	96.0	0.749	90.1	4.41	2.21	6	10.0
				20-A-2	25.7	95.8	0.752	91.9	4.56	2.28	8	13.3
20-B	3+50	62	0-12	20-B-1	25.6	95.1	0.765	90.0	3.67	1.84	4	7.0
				20-B-2	25.3	95.1	0.765	89.0	3.59	1.80	4	7.0
20-C	5+00	24	0-12	20-C-1	25.7	92.7	0.811	85.2	2.95	1.48	3	6.0
				20-C-2	25.4	91.5	0.835	81.8	2.83	1.42	2	4.4
20-D	7+00	62	0-12	20-D-1	25.4	93.1	0.803	85.1	3.17	1.59	3	5.1
				20-D-2	25.2	94.2	0.782	86.7	3.49	1.75	3	5.6
20-E	9+50	24	0-12	20-E-1	26.3	94.0	0.786	90.0	3.21	1.61	4	7.2
				20-E-2	25.7	94.8	0.771	89.7	3.52	1.76	5	8.2
20-F	12+00	62	0-12	20-F-1	25.4	95.3	0.761	89.8	3.97	1.99	6	11.9
				20-F-2	25.4	96.2	0.745	91.7	4.23	2.12	8	15.8
20-G	13+50	24	0-12	20-G-1	25.5	93.8	0.790	86.8	3.70	1.85	4	7.4
				20-G-2	25.3	93.6	0.793	85.8	3.62	1.81	4	6.5
20-H	16+00	62	0-12	20-H-1	25.7	93.6	0.793	87.2	2.61	1.31	3	6.4
				20-H-2	25.6	93.0	0.805	85.5	3.16	1.58	3	5.8
				AVERAGE	25.5	94.2	0.782	87.9	3.54	1.78	4	8.0

* STRAIN-CONTROLLED TEST ON 1.4-IN.-DIAM × 3.01-IN.-HIGH SPECIMEN TAKEN FROM 0- TO 4-IN. DEPTH OF THE BLOCK SAMPLE.

** RATE OF STRAIN CHANGED FROM 1% PER MINUTE TO 2.5% PER MINUTE AT FROM 4 TO 8% AXIAL STRAIN.

UNCONFINED COMPRESSION TEST RESULTS

CART 20

PLATE 4

UNCONSOLIDATED-UNDRAINED TRIAXIAL TEST *

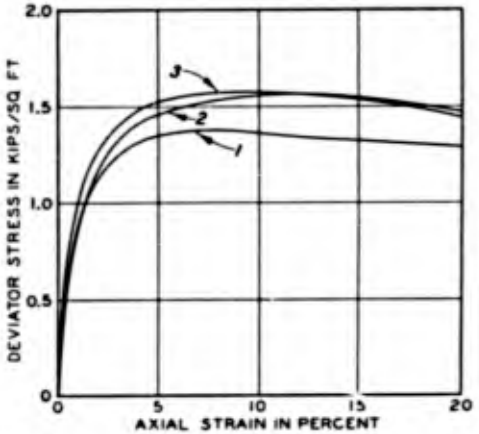

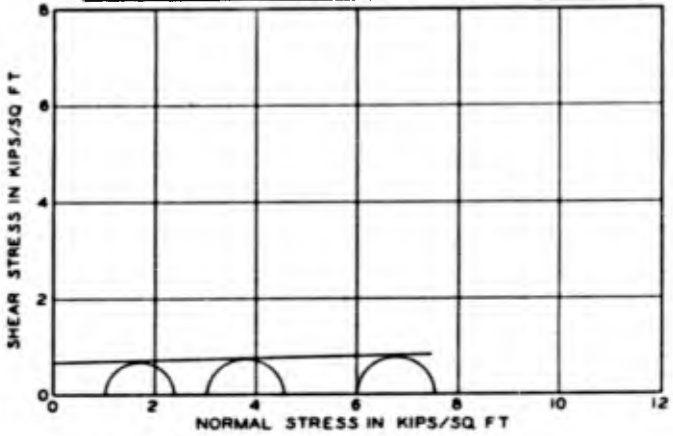

BLOCK	18-C		
STATION	5+00		
OFFSET, IN.	24		
DEPTH, IN.	0-12		
SAMPLE	1	2	3
WATER CONTENT, %	33.6	33.3	33.2
DRY UNIT WT, LB/CU FT	83.9	85.9	85.8
VOID RATIO	1.002	0.954	0.959
SATURATION, %	90.2	94.0	93.2
MAXIMUM DEVIATOR STRESS, KIPS/SQ FT	1.38	1.56	1.58
MINOR PRINCIPAL STRESS, KIPS/SQ FT	1.00	3.00	6.00
MAJOR PRINCIPAL STRESS, KIPS/SQ FT	2.38	4.56	7.58
TIME TO FAILURE, MIN	4	6	6
FAILURE STRAIN, %	8.3	11.6	9.5
APPARENT COHESION, KIPS/SQ FT	0.70		
APPARENT ANGLE OF SHEARING RESISTANCE, DEGREES	1.0		

CONSOLIDATED-DRAINED DIRECT SHEAR TEST **

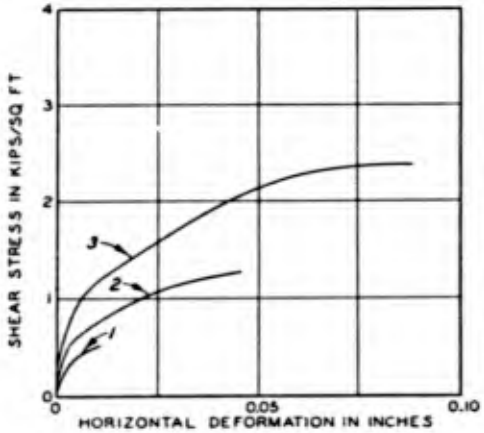

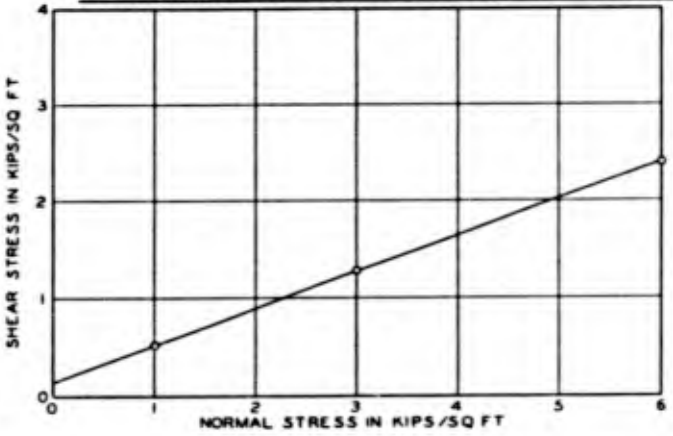

BLOCK	18-C		
STATION	5+00		
OFFSET, IN.	24		
DEPTH, IN.	0-12		
SAMPLE	1	2	3
WATER CONTENT, %	32.8	32.9	33.3
DRY UNIT WT, LB/CU FT	86.7	86.1	85.8
VOID RATIO	0.937	0.950	0.957
SATURATION, %	94.2	93.1	93.7
NORMAL STRESS, KIPS/SQ FT	1.00	3.00	6.00
MAXIMUM SHEAR STRESS, KIPS/SQ FT	0.52	1.28	2.48
WATER CONTENT AFTER TEST, %	34.1	32.1	29.4
DURATION OF TEST, MIN	360	360	315
APPARENT COHESION, KIPS/SQ FT	0.14		
APPARENT ANGLE OF SHEARING RESISTANCE, DEGREES	21.0		

* STRAIN-CONTROLLED TEST ON 1.4-IN.-DIAM BY 3.01-IN.-HIGH SPECIMENS OBTAINED FROM 0- TO 4-IN. DEPTH.

** STRESS-CONTROLLED TEST ON 2.4- BY 2.4- BY 0.4-IN.-HIGH SPECIMENS OBTAINED FROM 0- TO 4-IN. DEPTH.

LABORATORY STRENGTH TESTS
CART 18

UNCONSOLIDATED-UNDRAINED TRIAXIAL TEST*

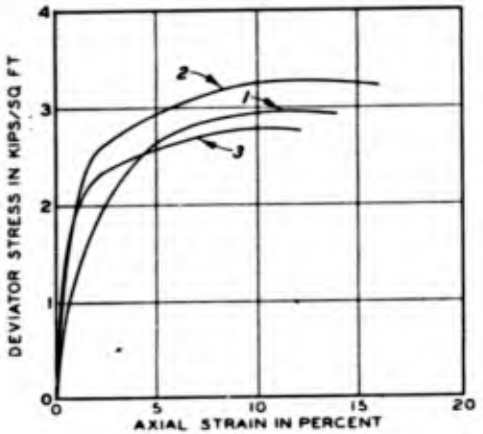

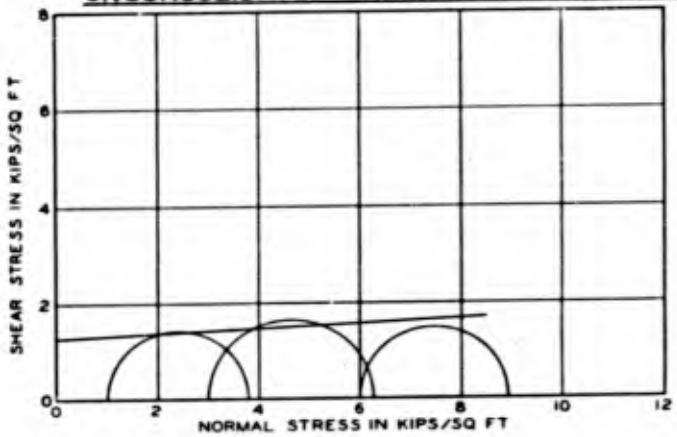

BLOCK	19-B		
STATION	3+50		
OFFSET, IN.	62		
DEPTH, IN.	0-12		
SAMPLE	1	2	3
WATER CONTENT, %	28.2	28.1	28.2
DRY UNIT WT, LB/CU FT	91.0	92.4	88.6
VOID RATIO	0.846	0.817	0.896
SATURATION, %	89.7	92.4	84.7
MAXIMUM DEVIATOR STRESS, KIPS/SQ FT	2.80	3.29	2.95
MINOR PRINCIPAL STRESS, KIPS/SQ FT	1.00	3.00	6.00
MAJOR PRINCIPAL STRESS, KIPS/SQ FT	3.80	6.29	8.95
TIME TO FAILURE, MIN	5	6	6
FAILURE STRAIN, %	10.0	12.0	12.0
APPARENT COHESION, KIPS/SQ FT	1.25		
APPARENT ANGLE OF SHEARING RESISTANCE, DEGREES	2.5		

CONSOLIDATED-DRAINED DIRECT SHEAR TEST**

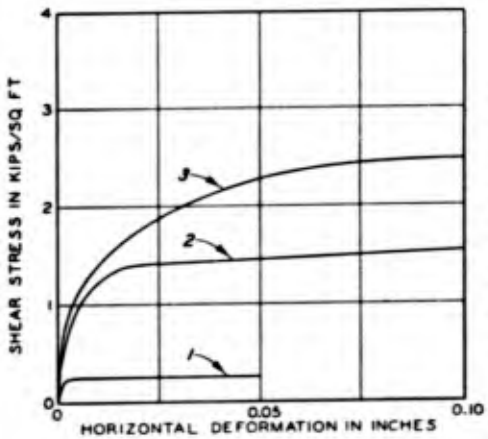

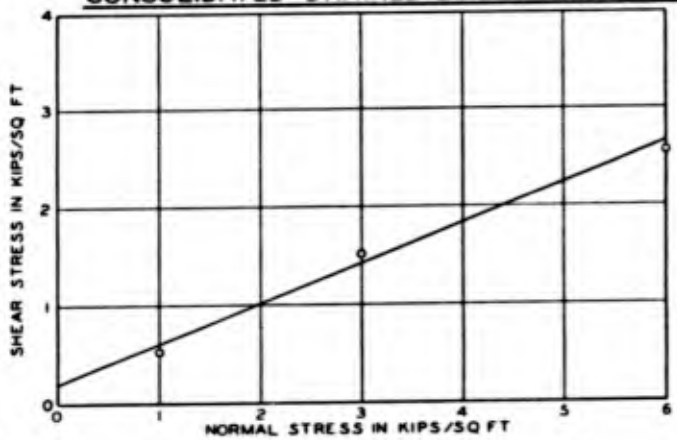

BLOCK	19-B		
STATION	3+50		
OFFSET, IN.	62		
DEPTH, IN.	0-12		
SAMPLE	1	2	3
WATER CONTENT, %	27.2	27.1	27.3
DRY UNIT WT, LB/CU FT	94.5	94.4	93.9
VOID RATIO	0.778	0.779	0.789
SATURATION, %	94.1	93.7	93.2
NORMAL STRESS, KIPS/SQ FT	1.00	3.00	6.00
MAXIMUM SHEAR STRESS, KIPS/SQ FT	0.52	1.52	2.58
WATER CONTENT AFTER TEST, %	29.2	29.1	27.5
DURATION OF TEST, MIN	405	405	315
APPARENT COHESION, KIPS/SQ FT	0.20		
APPARENT ANGLE OF SHEARING RESISTANCE, DEGREES	22.5		

* STRAIN-CONTROLLED TEST ON 1.4-IN.-DIAM BY 3.01-IN.-HIGH SPECIMENS OBTAINED FROM 0- TO 4-IN. DEPTH.

** STRESS-CONTROLLED TEST ON 2.4- BY 2.4- BY 0.4-IN.-HIGH SPECIMENS OBTAINED FROM 0- TO 4-IN. DEPTH.

LABORATORY STRENGTH TESTS
CART 19

PLATE 5

PLATE 6

UNCONSOLIDATED-UNDRAINED TRIAXIAL TEST*

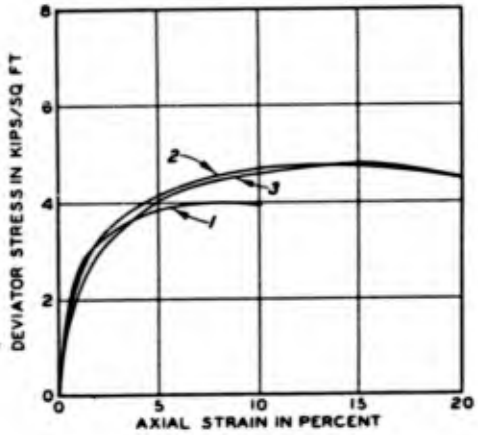

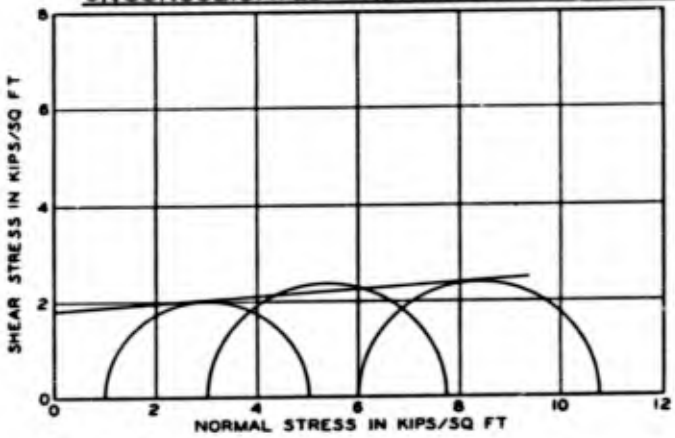

BLOCK	20-G		
STATION	3+50		
OFFSET, IN.	62		
DEPTH, IN.	0-12		
SAMPLE	1	2	3
WATER CONTENT, %	25.2	25.3	25.3
DRY UNIT WT, LB/CU FT	94.6	95.8	94.9
VOID RATIO	0.776	0.752	0.768
SATURATION, %	87.3	90.3	88.6
MAXIMUM DEVIATOR STRESS, KIPS/SQ FT	4.01	4.76	4.79
MINOR PRINCIPAL STRESS, KIPS/SQ FT	1.00	3.00	6.00
MAJOR PRINCIPAL STRESS, KIPS/SQ FT	5.01	7.76	10.79
TIME TO FAILURE, MIN	4	7	8
FAILURE STRAIN, %	7	15	15
APPARENT COHESION, KIPS/SQ FT	1.80		
APPARENT ANGLE OF SHEARING RESISTANCE, DEGREES	4.0		

CONSOLIDATED-DRAINED DIRECT SHEAR TEST**

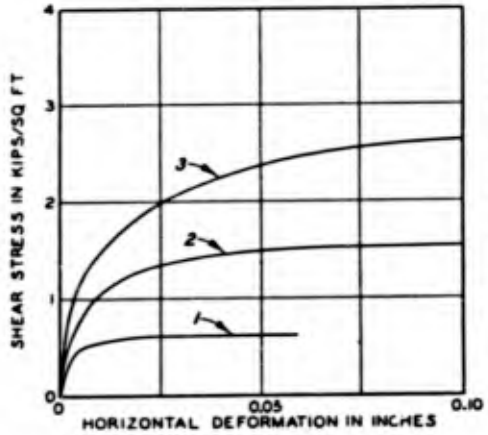

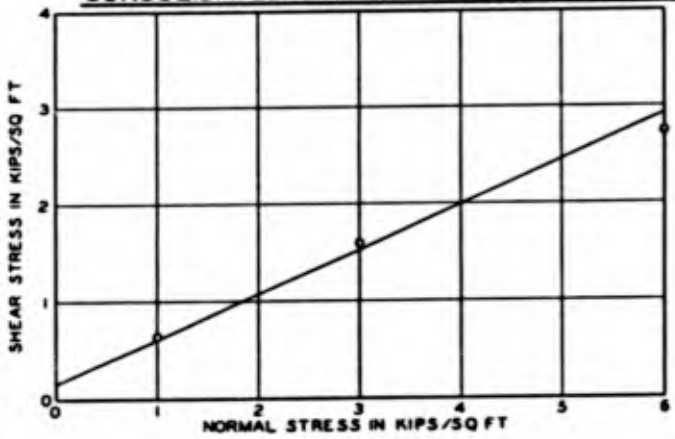

BLOCK	20-G		
STATION	3+50		
OFFSET, IN.	62		
DEPTH, IN.	0-12		
SAMPLE	1	2	3
WATER CONTENT, %	25.6	25.6	25.5
DRY UNIT WT, LB/CU FT	96.4	96.0	95.8
VOID RATIO	0.742	0.750	0.752
SATURATION, %	92.9	91.7	91.2
NORMAL STRESS, KIPS/SQ FT	1.00	3.00	6.00
MAXIMUM SHEAR STRESS, KIPS/SQ FT	0.64	1.60	2.72
WATER CONTENT AFTER TEST, %	28.6	27.8	27.5
DURATION OF TEST, MIN	435	435	345
APPARENT COHESION, KIPS/SQ FT	0.16		
APPARENT ANGLE OF SHEARING RESISTANCE, DEGREES	24.5		

* STRAIN-CONTROLLED TEST ON 1.4-IN.-DIAM BY 3.01-IN.-HIGH SPECIMENS OBTAINED FROM 0- TO 4-IN. DEPTH.

** STRESS-CONTROLLED TEST ON 2.4- BY 2.4- BY 0.8-IN.-HIGH SPECIMENS OBTAINED FROM 0- TO 4-IN. DEPTH.

LABORATORY STRENGTH TESTS
CART 20

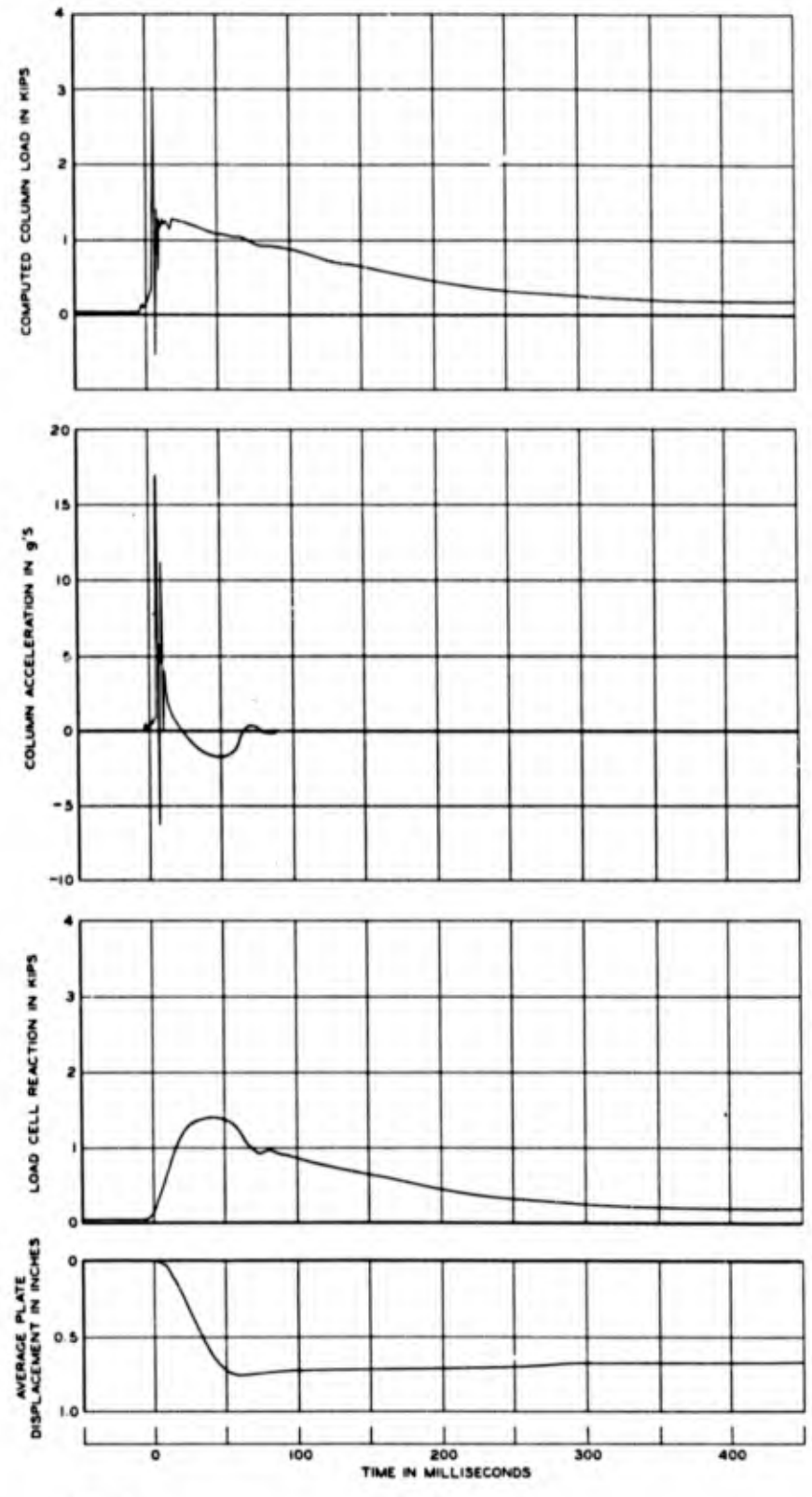

b = 5.5 IN.

Y_r = 0.60 KIPS/SQ FT

DYNAMIC TEST
18 - 1

PLATE 7

OBTAINED FROM C TO 24H. DEPTH.

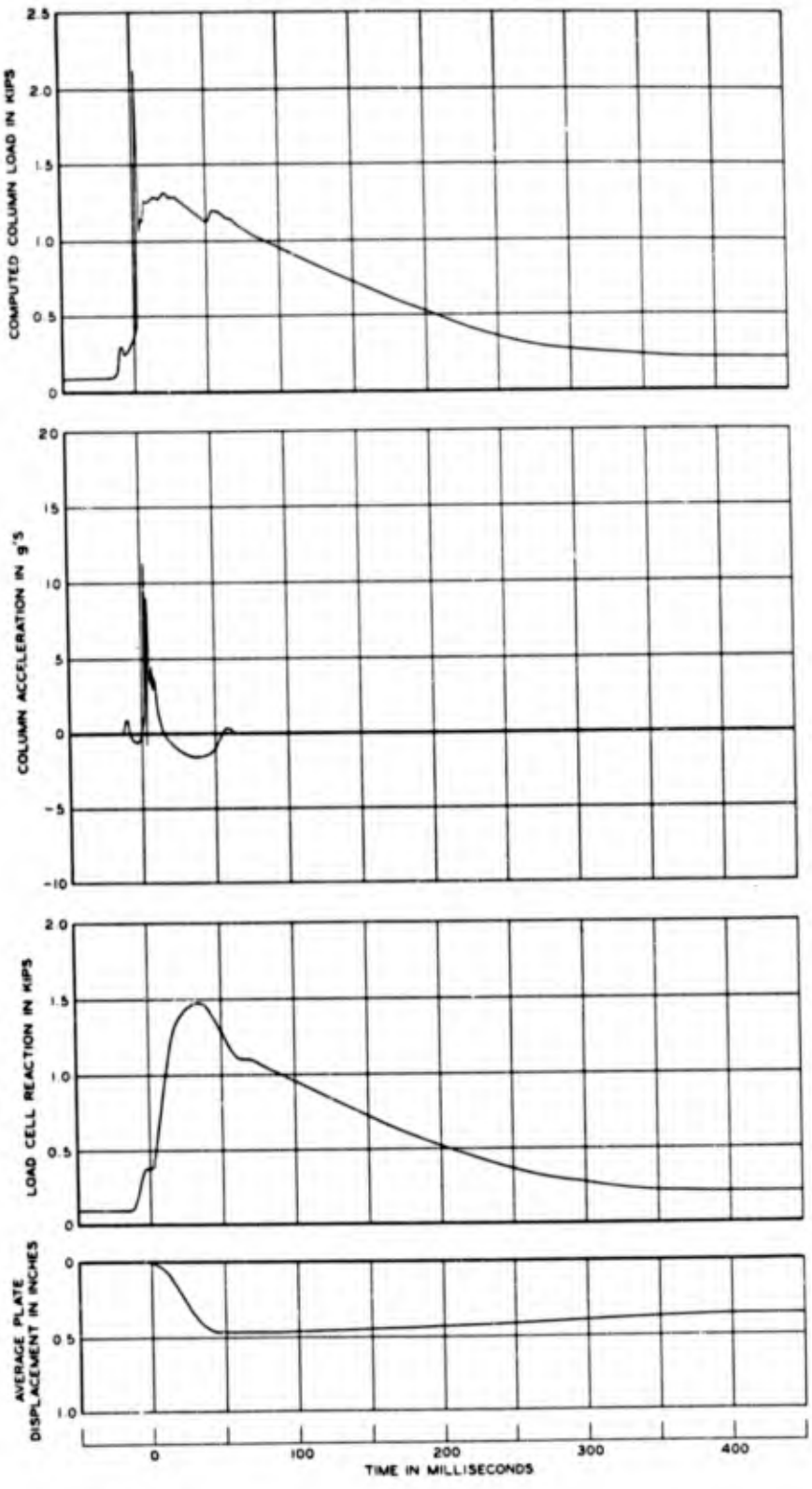

b = 6 IN

τ_r = 0.55 KIPS/SQ FT

DYNAMIC TEST

18-2

PLATE 8

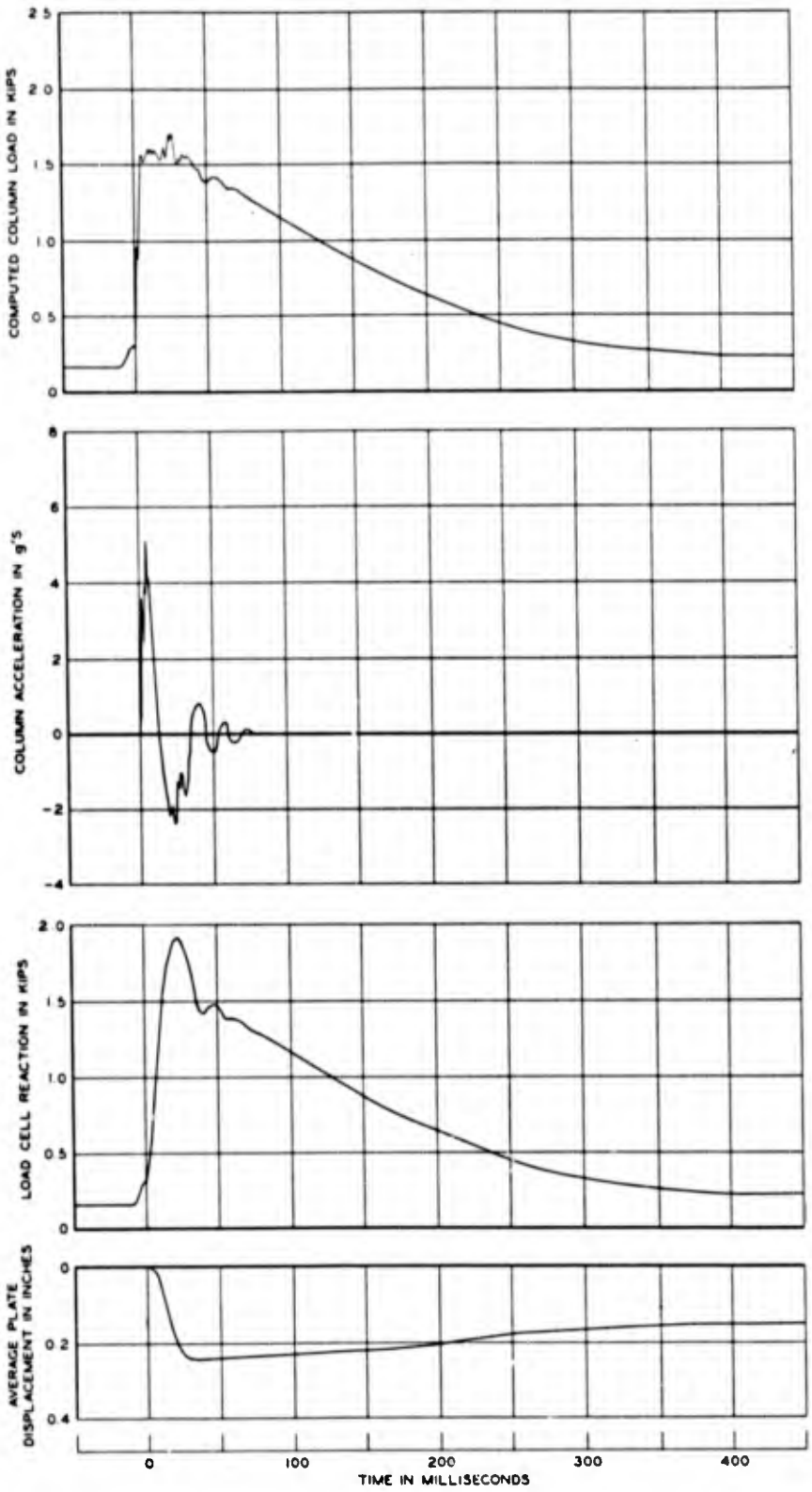

b = 8 IN

T_r = 0.60 KIPS/SQ FT

DYNAMIC TEST
18-3

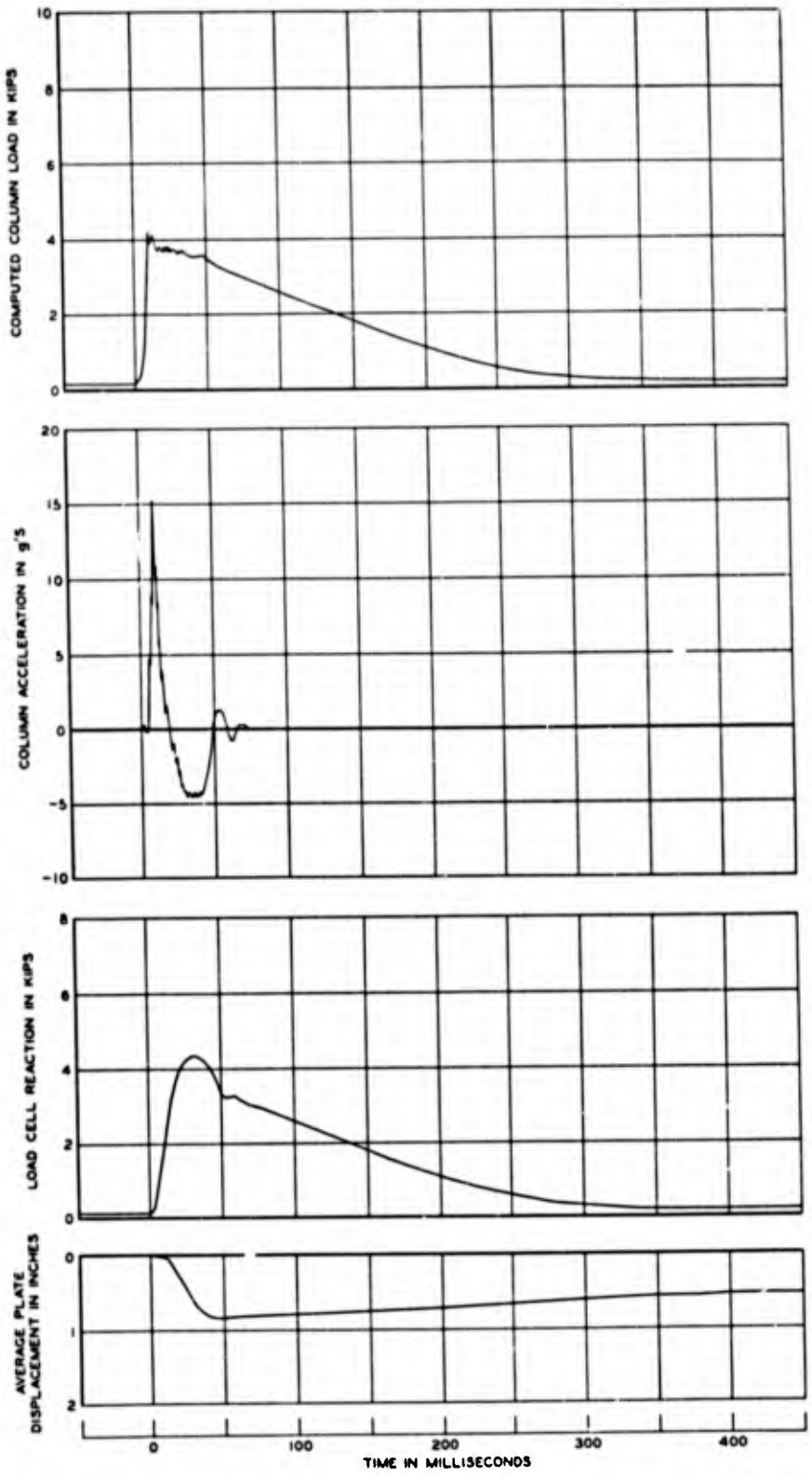

b = 10 IN.

T_r = 0.65 KIPS/SQ FT

DYNAMIC TEST

18-4

PLATE 10

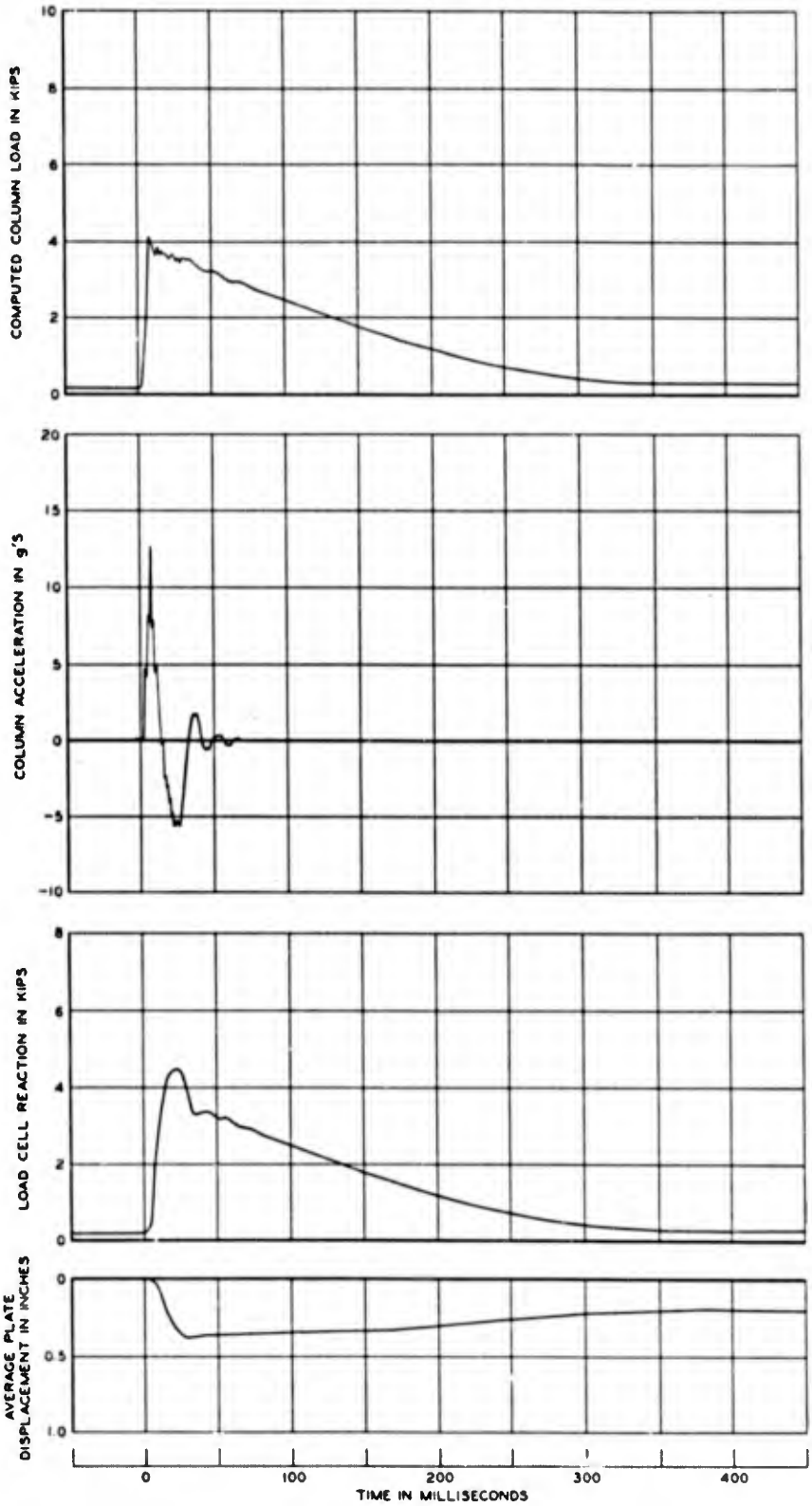

b = 12 IN.

T_v = 0.65 KIPS/SQ FT

DYNAMIC TEST
18-5

PLATE II

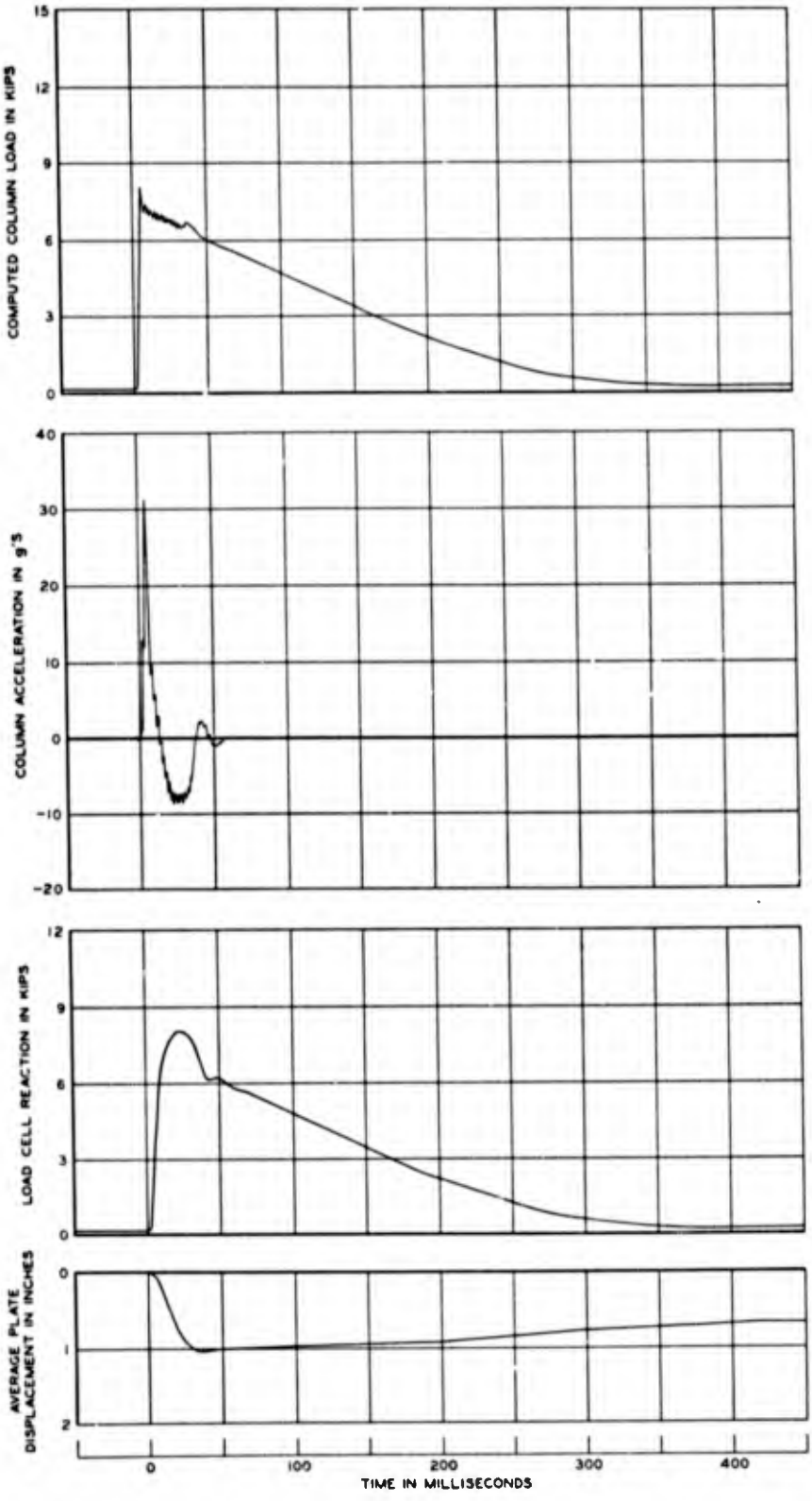

b = 14 IN

T_v = 0.65 KIPS/SQ FT

DYNAMIC TEST

18-6

PLATE 12

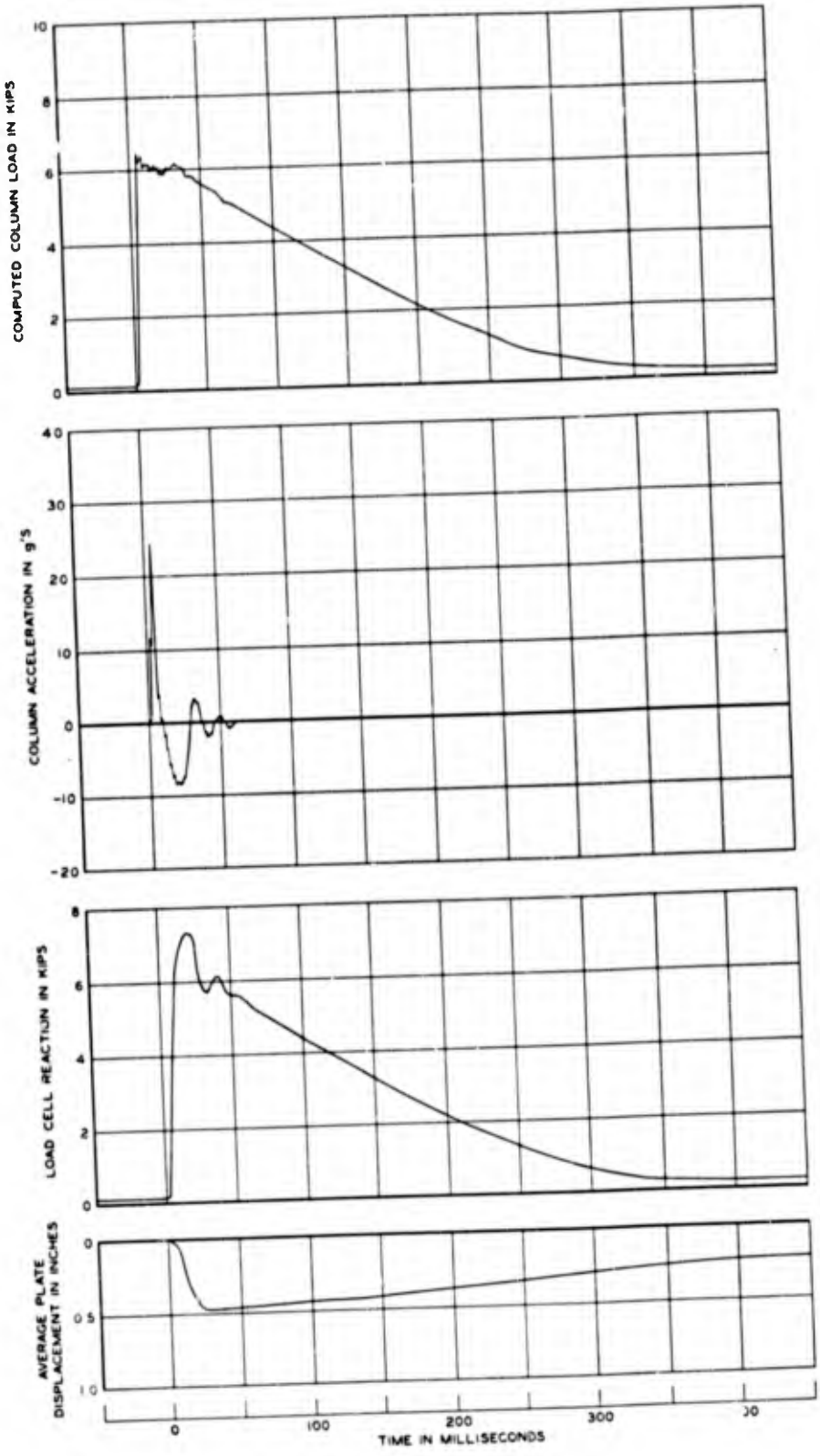

b = 16 IN

τ_r = 0.60 KIPS/SQ FT

DYNAMIC TEST
18-7

PLATE 13

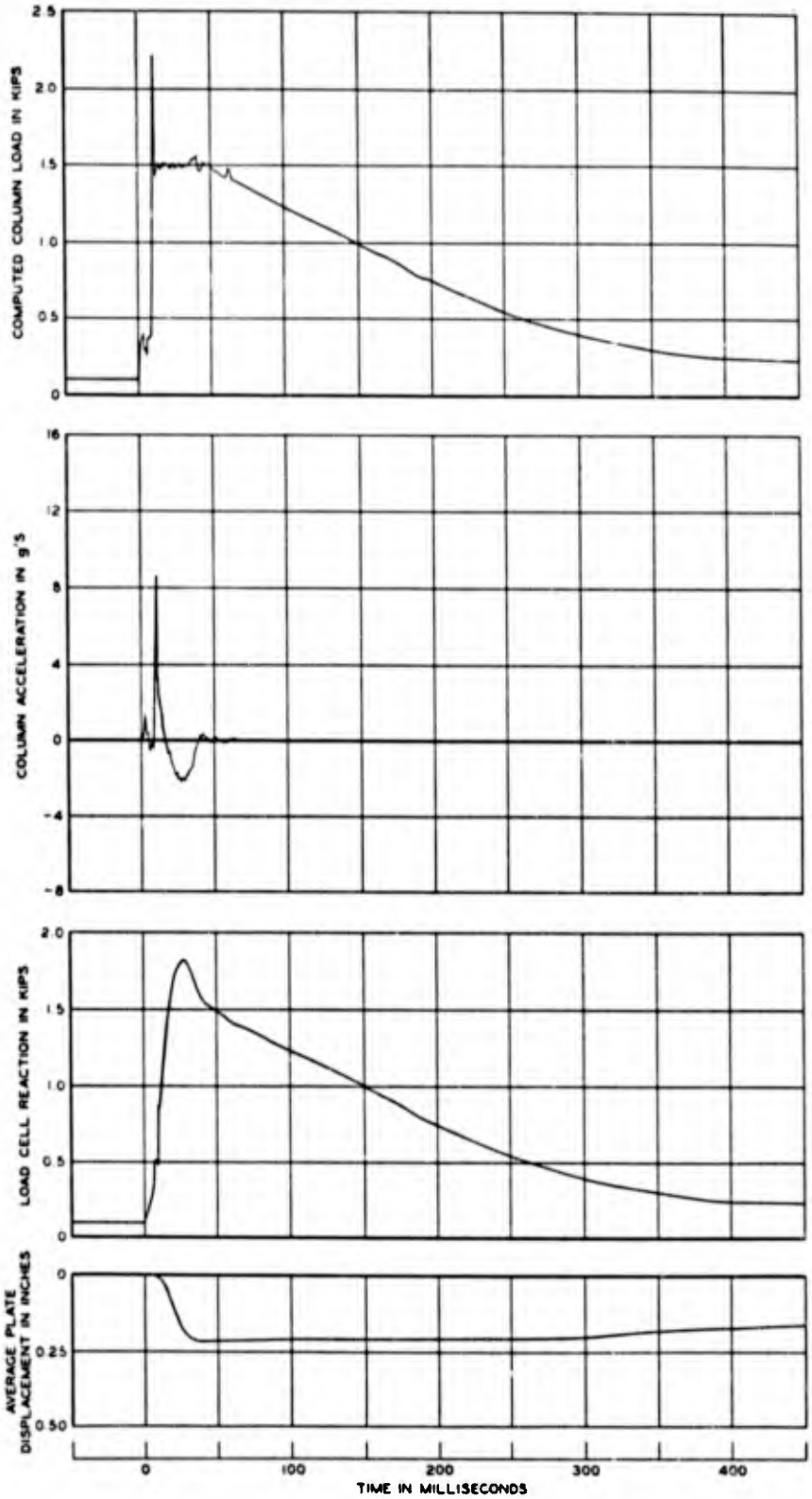

b = 5 IN.

T_r = 1.20 KIPS/SQ FT

DYNAMIC TEST

19 – 1

PLATE 14

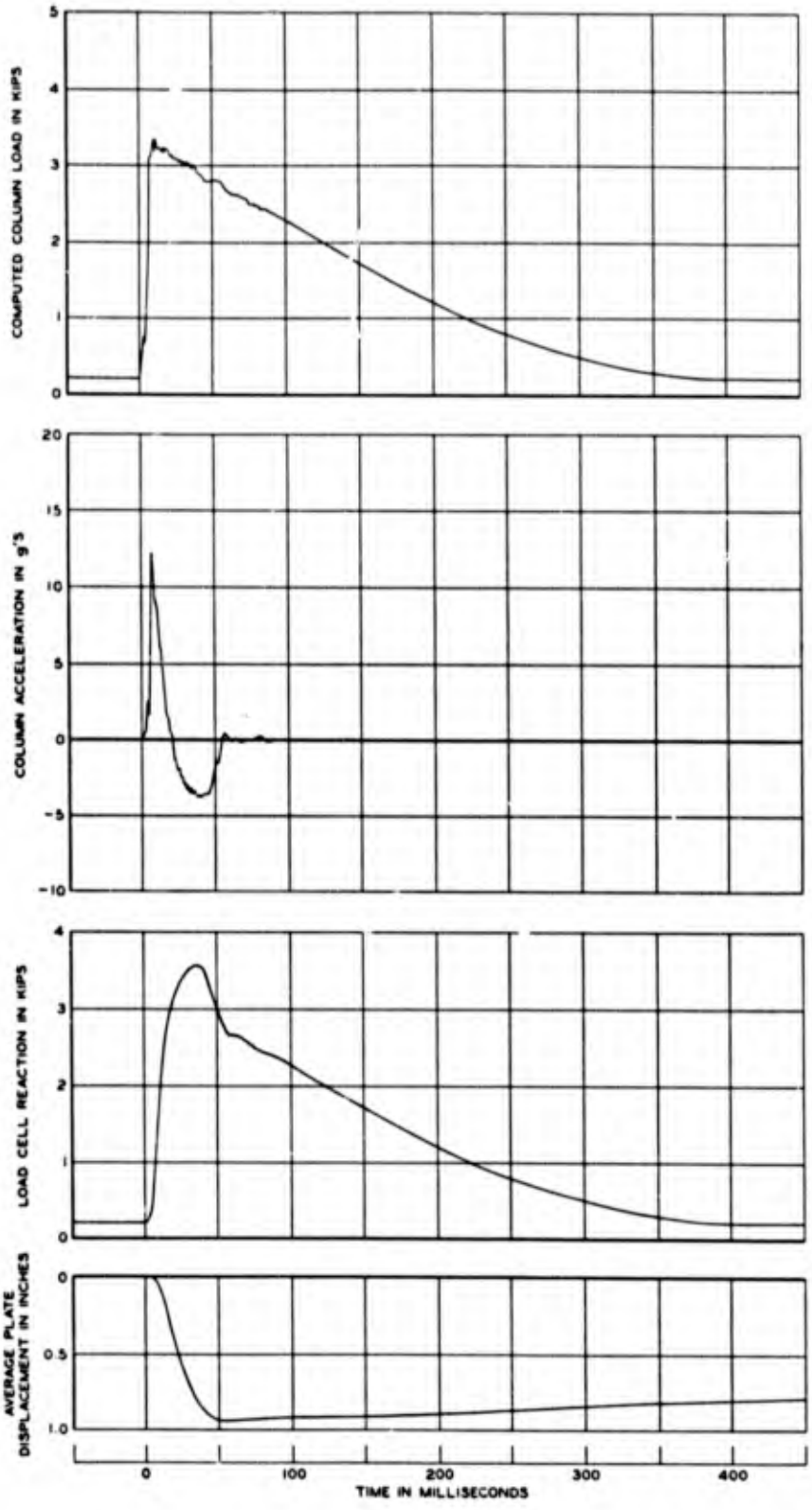

b = 6 IN.

Y_t = 1.20 KIPS/SQ FT

DYNAMIC TEST
19-2

PLATE 15

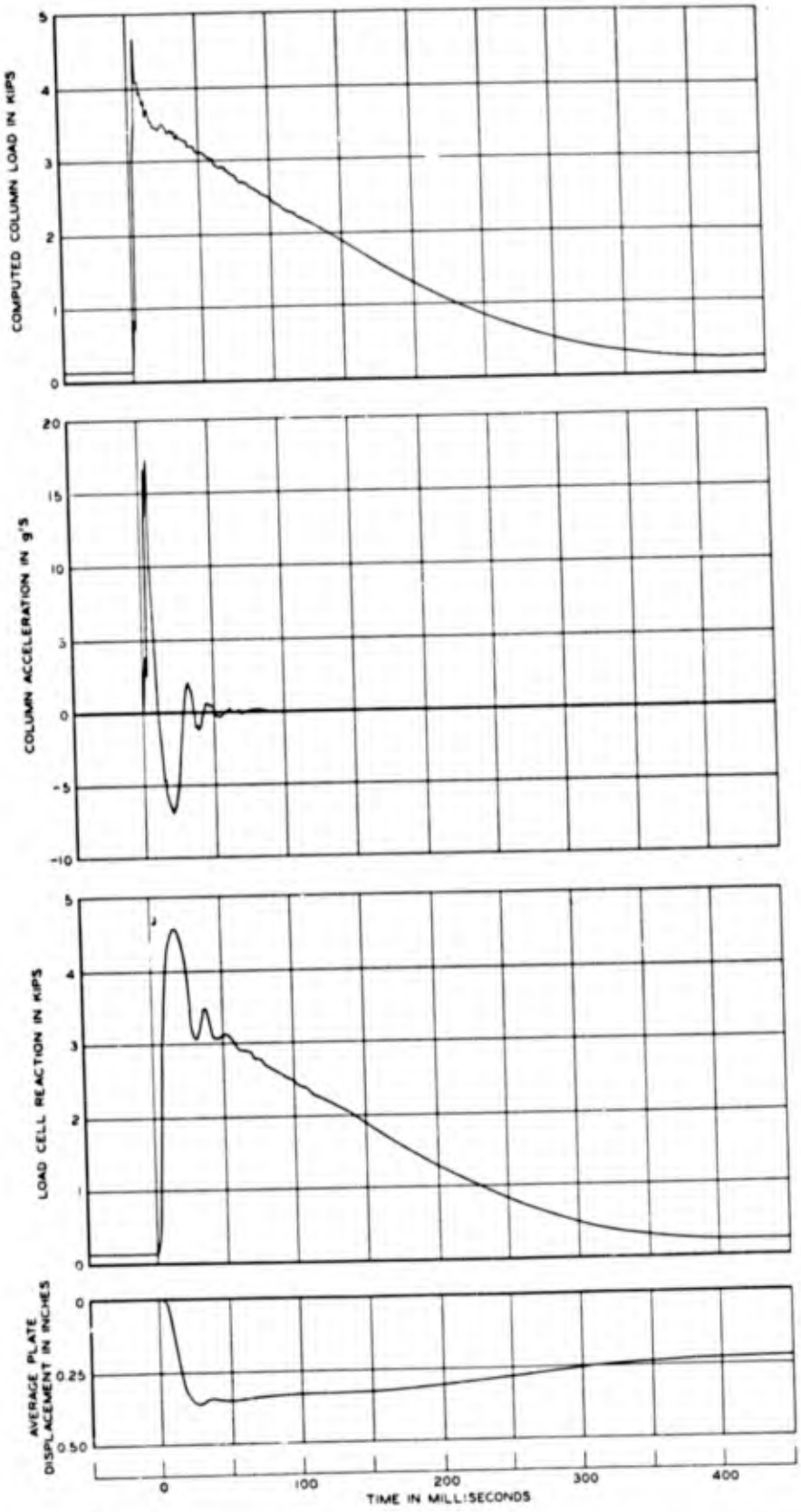

b = 8 in

γ_c = 120 #IPS/SQ FT

DYNAMIC TEST

19-3

PLATE 16

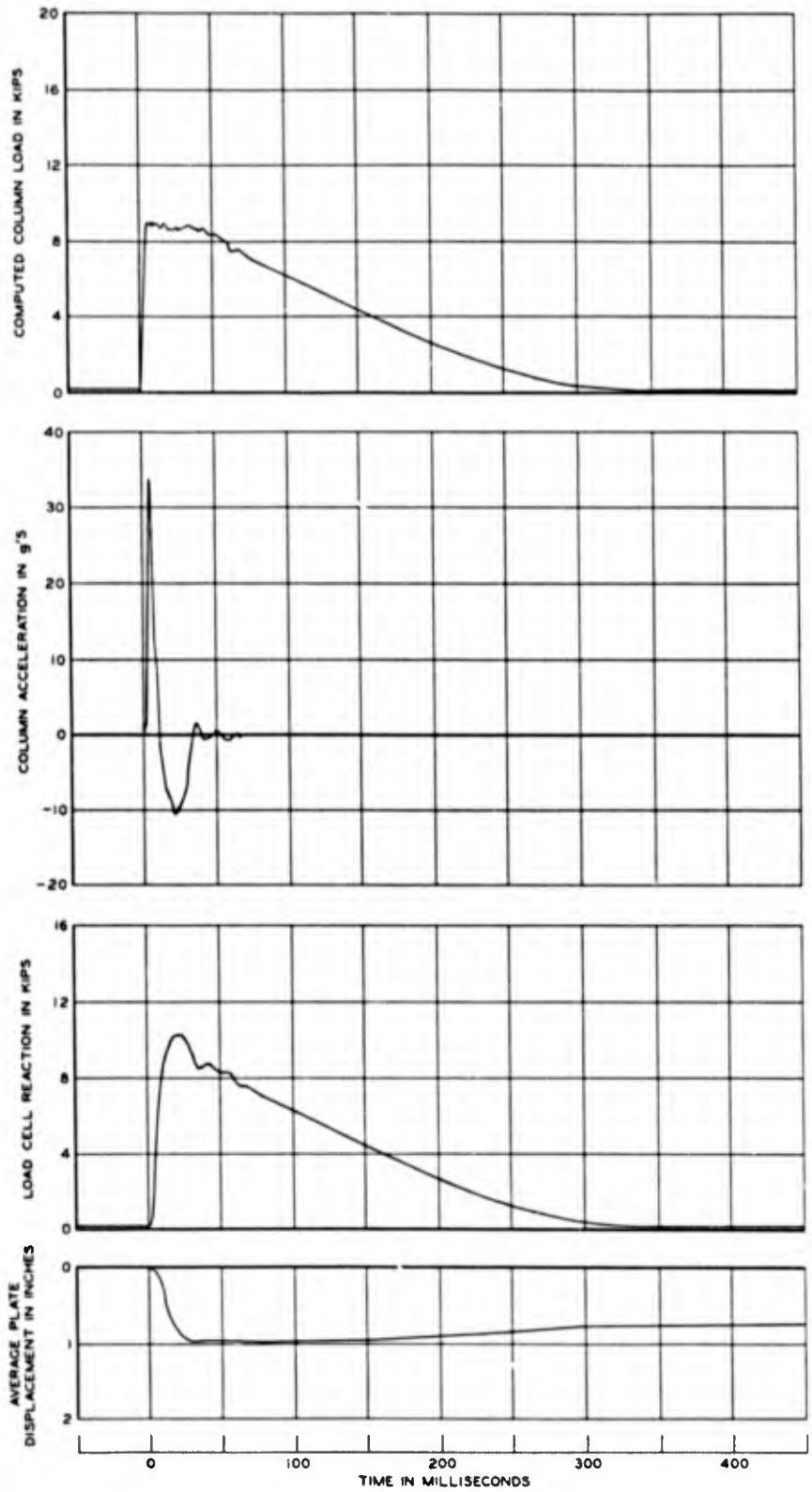

b = 10 IN

T_1 = 1.25 KIPS/SQ FT

DYNAMIC TEST
19-4

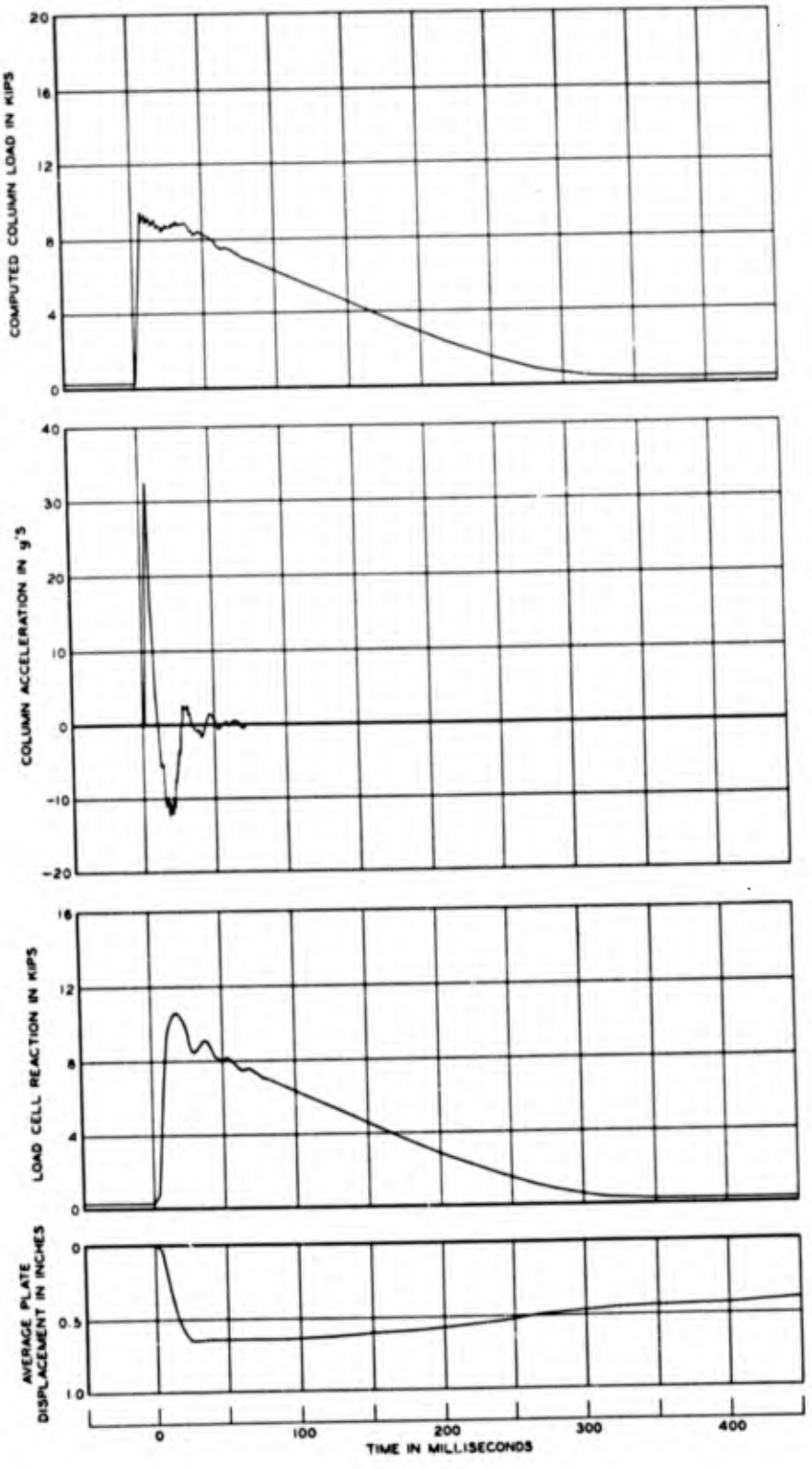

b = 12 IN.

τ_r = 1.20 KIPS/SQ FT

DYNAMIC TEST
19-5

PLATE 18

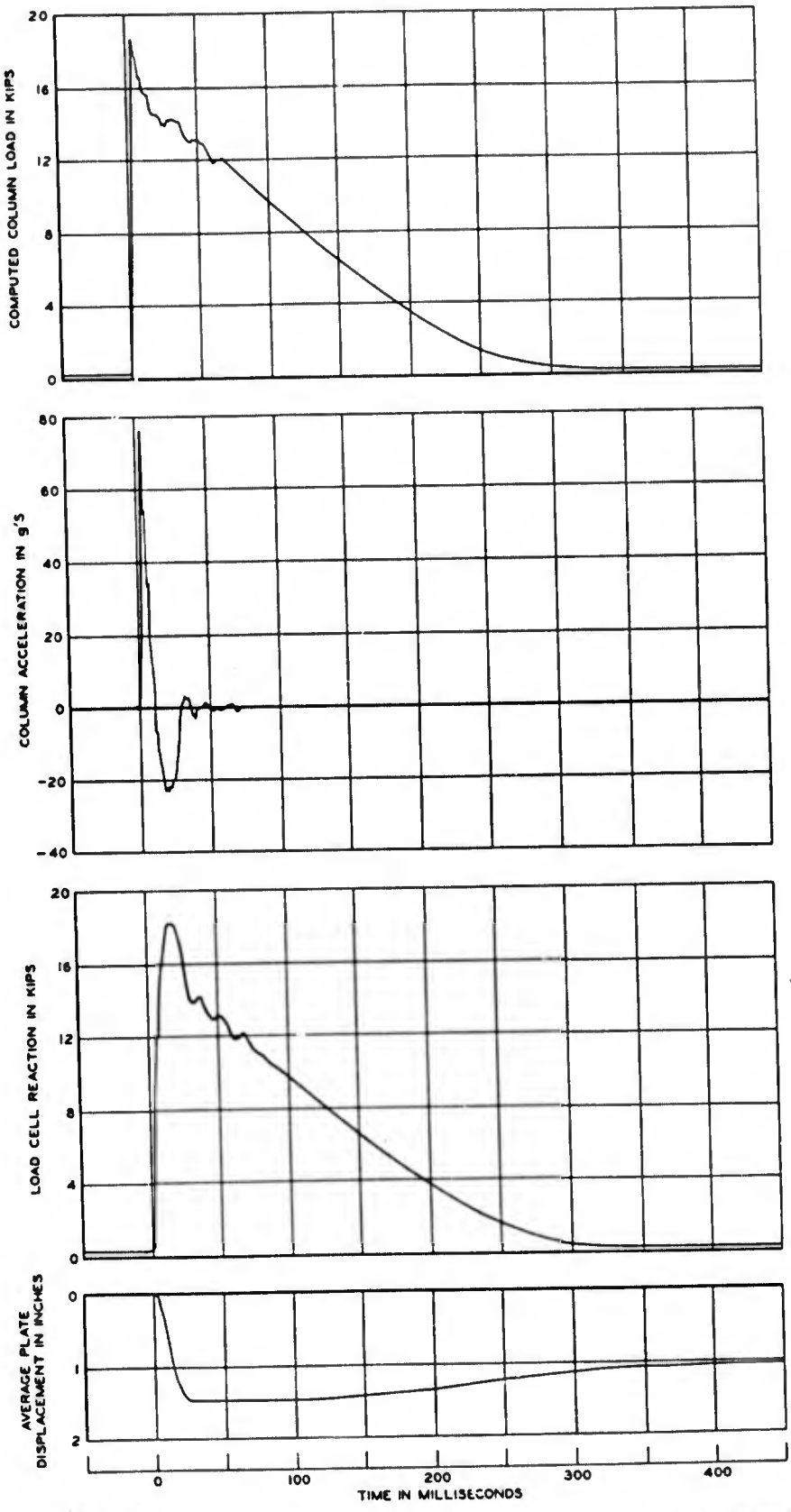

b = 14 IN.

T_v = 1.20 KIPS/SQ FT

DYNAMIC TEST
19-6

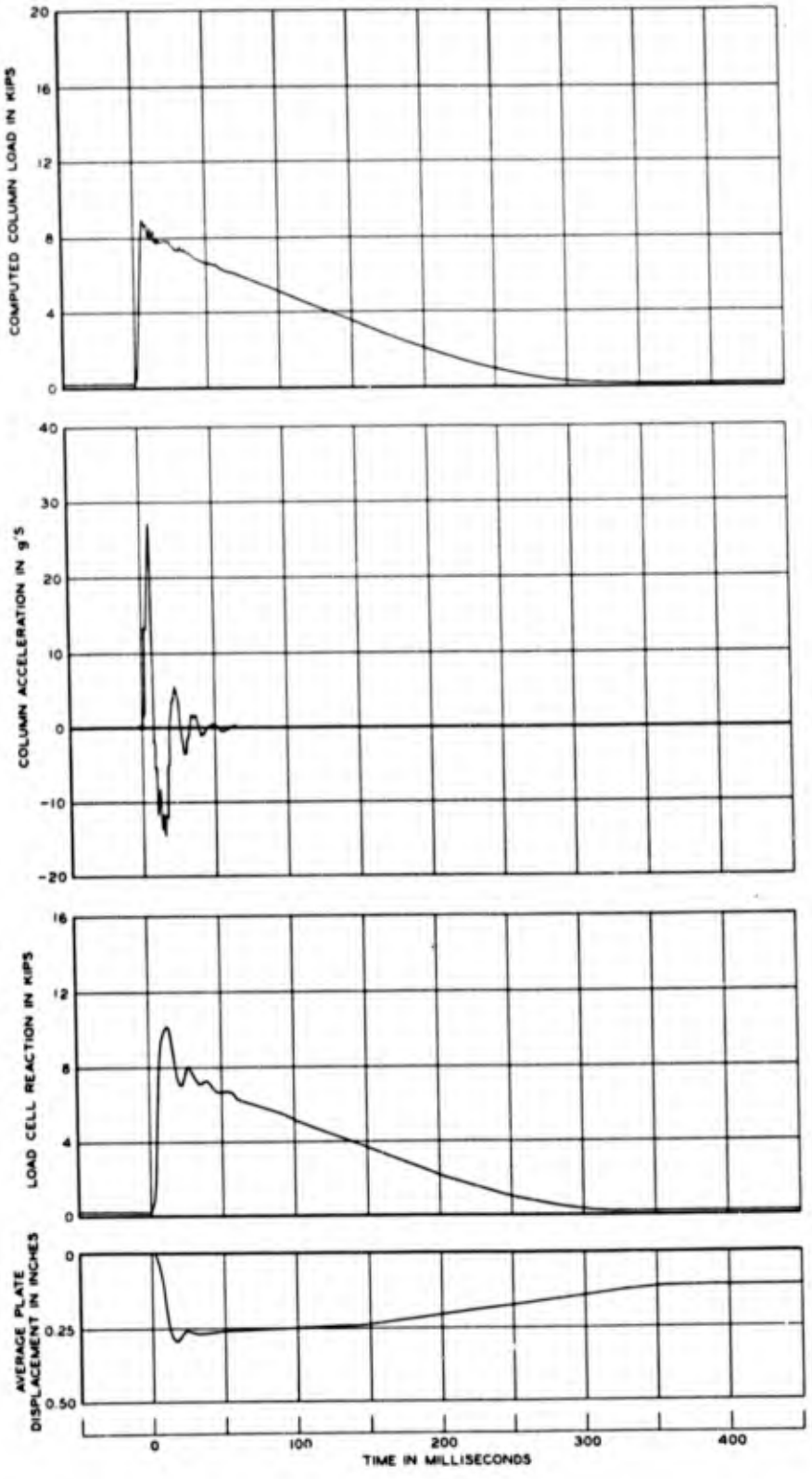

b = 14 IN.

T_r = 1.20 KIPS/SQ FT

DYNAMIC TEST
19-7

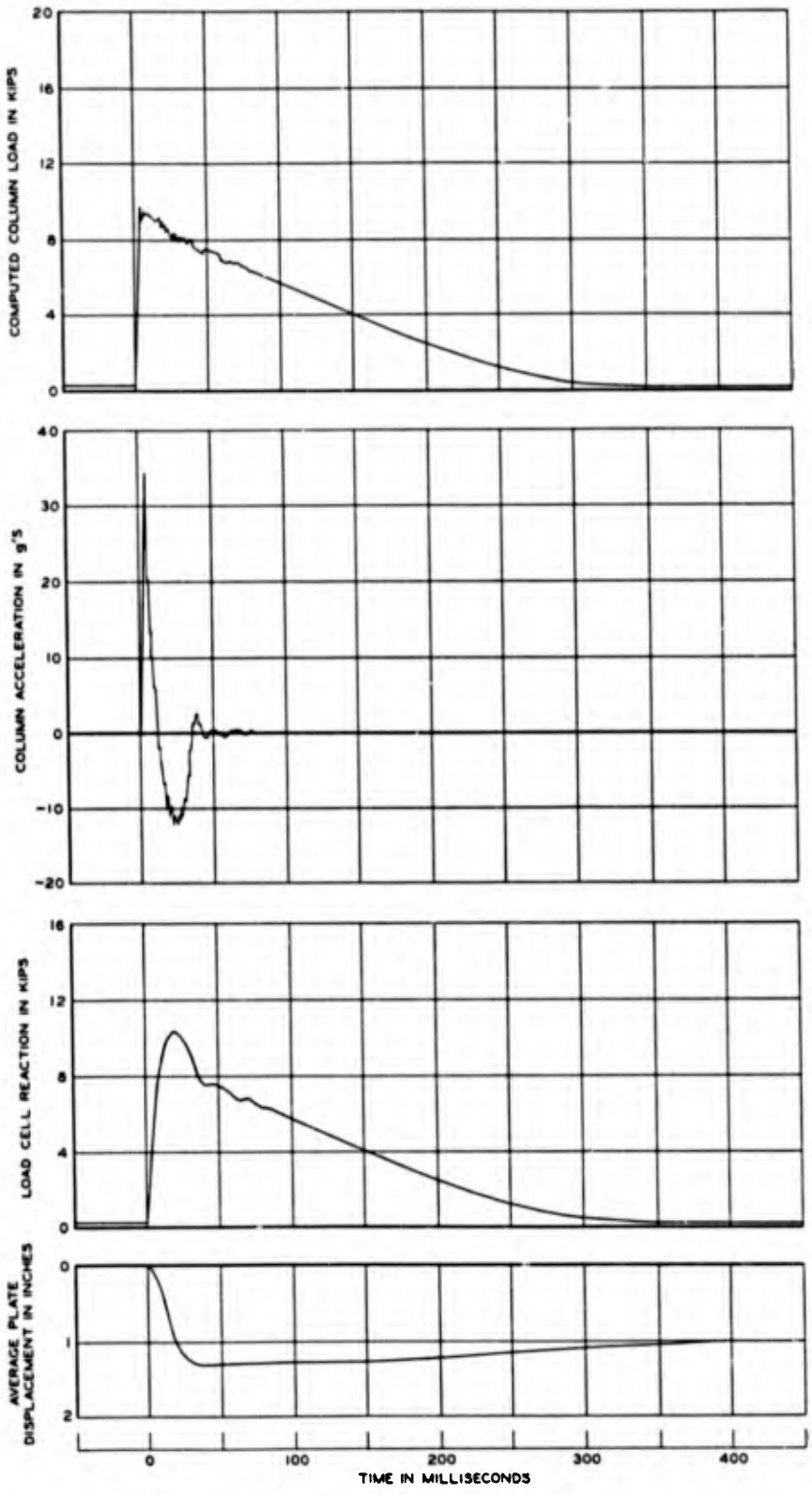

b = 10 IN.

T_r = 1.25 KIPS/SQ FT

DYNAMIC TEST
19-8

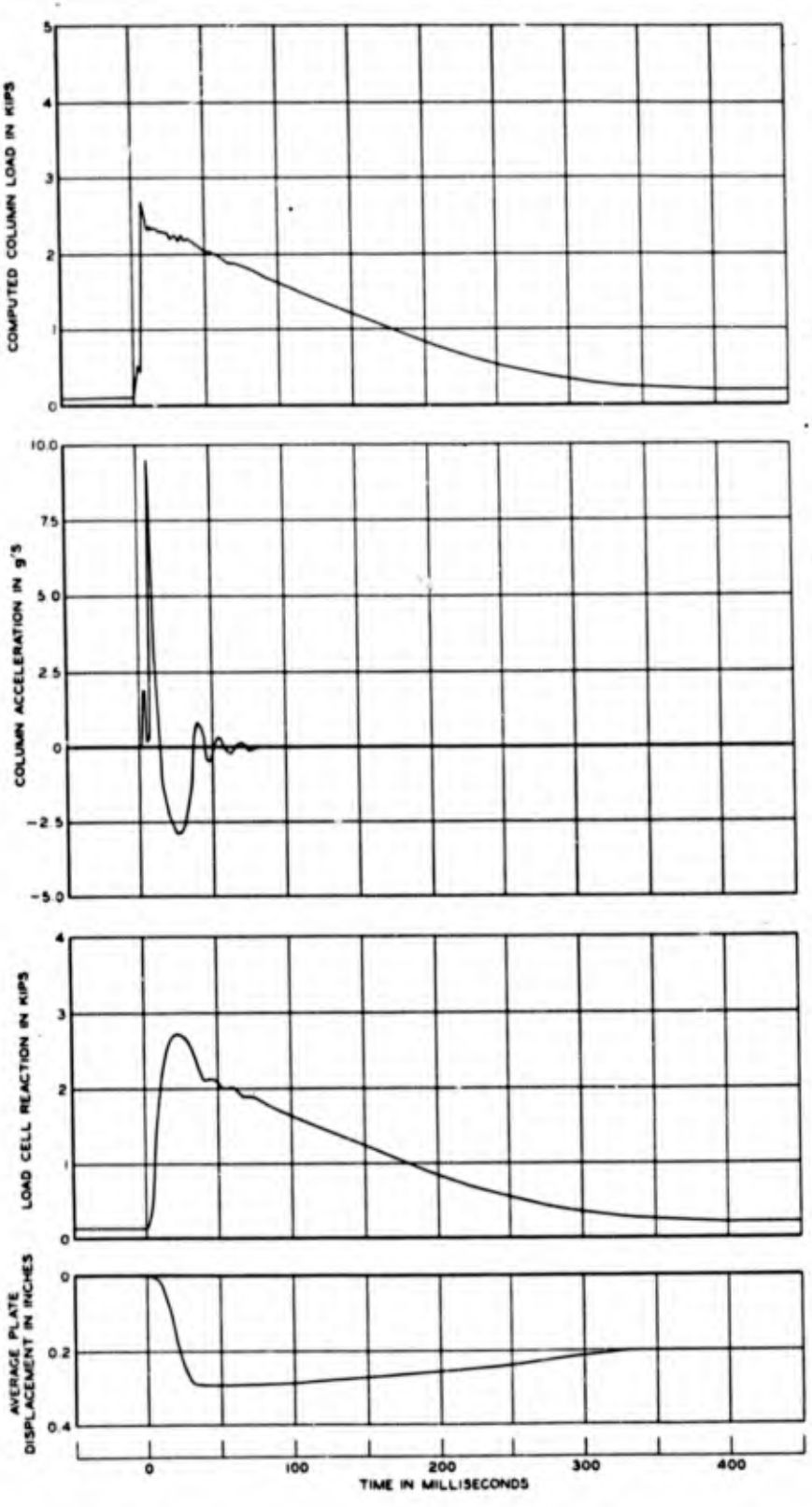

b = 5 IN.

τ_r = 1.75 KIPS/SQ FT

DYNAMIC TEST
20-1

PLATE 22

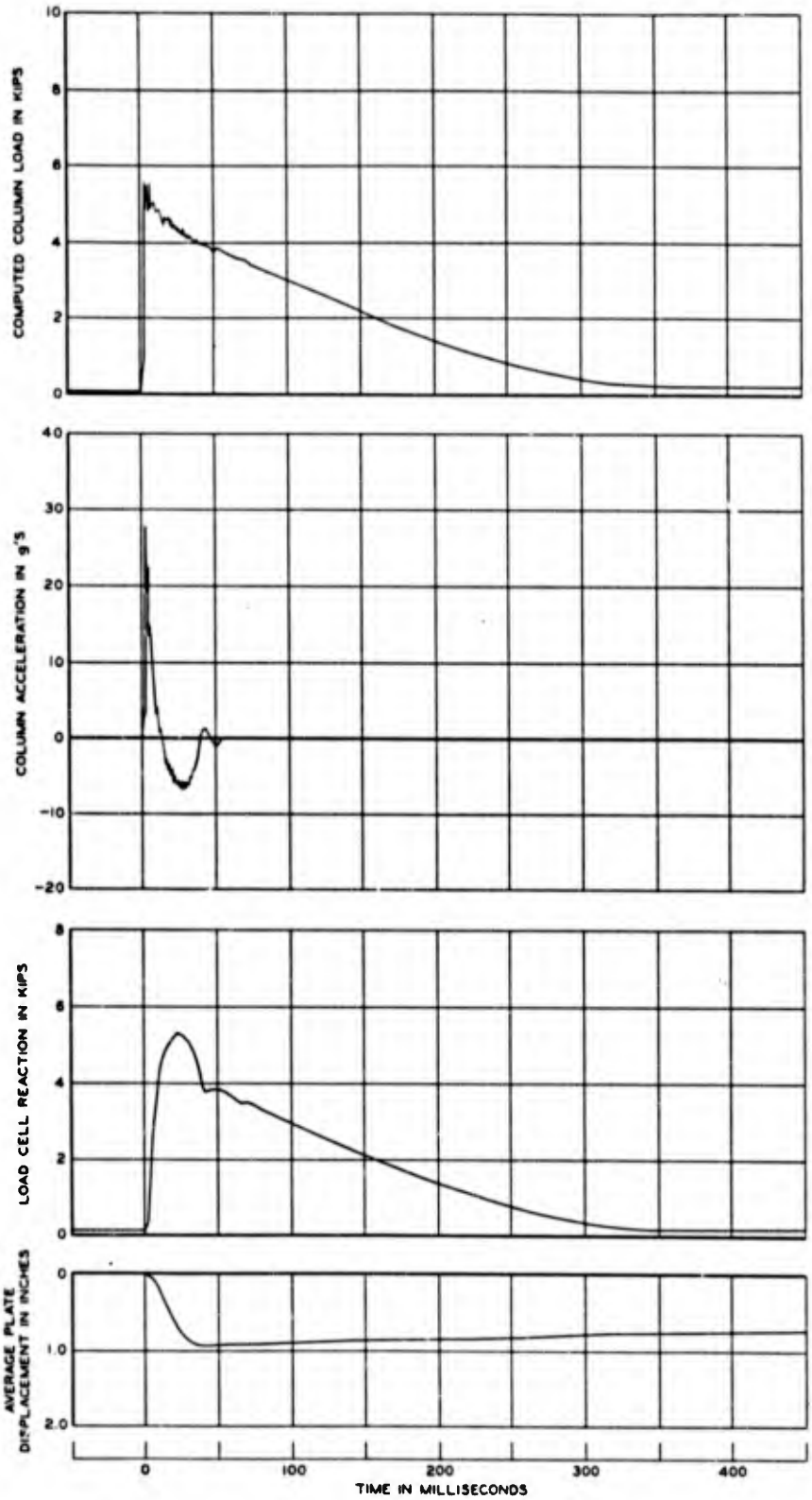

b = 6 IN.

T_ϕ = 1.80 KIPS/SQ FT

DYNAMIC TEST
20-2

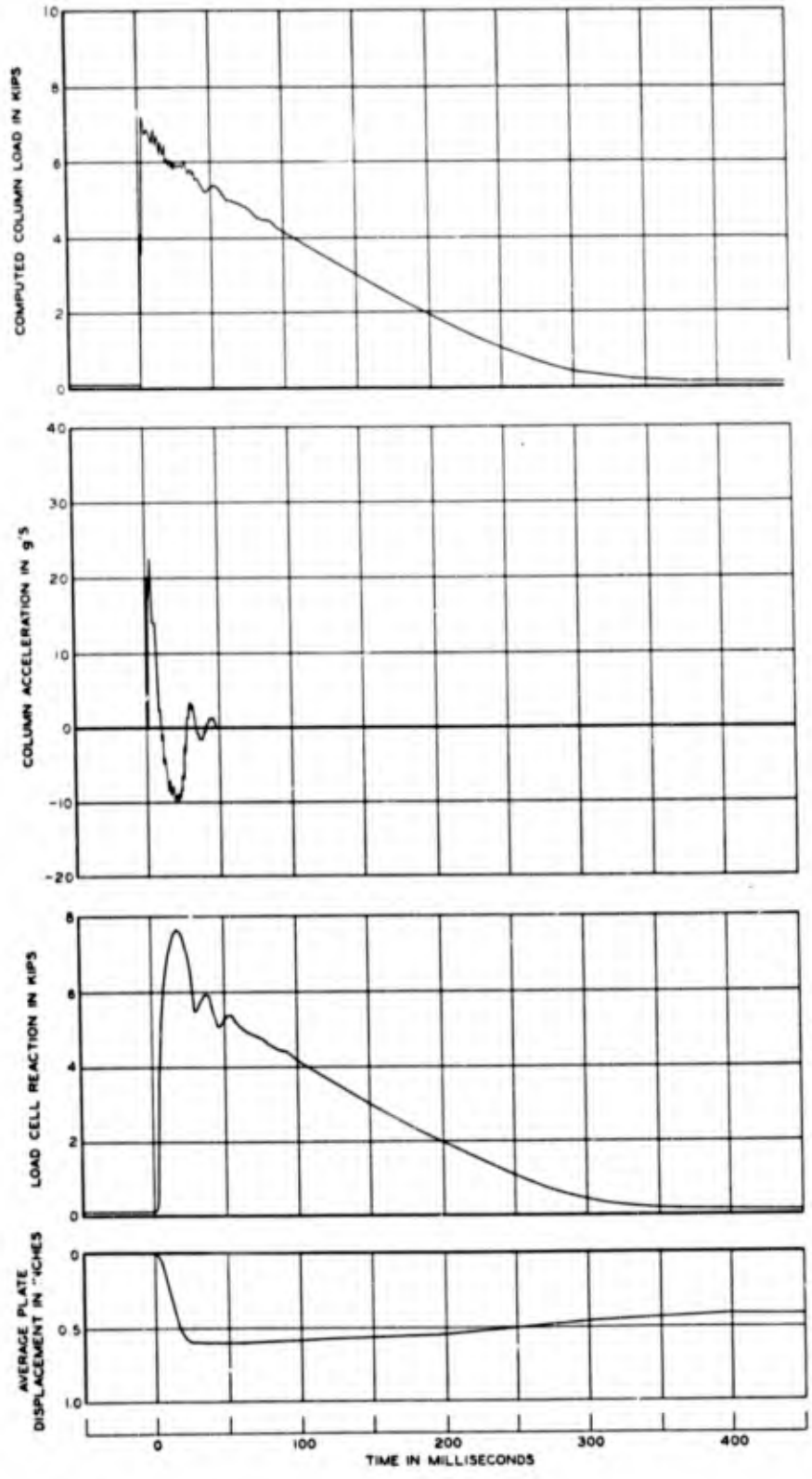

b = 8 IN.

T_f = 1.70 KIPS/SQ FT

DYNAMIC TEST
20-3

PLATE 24

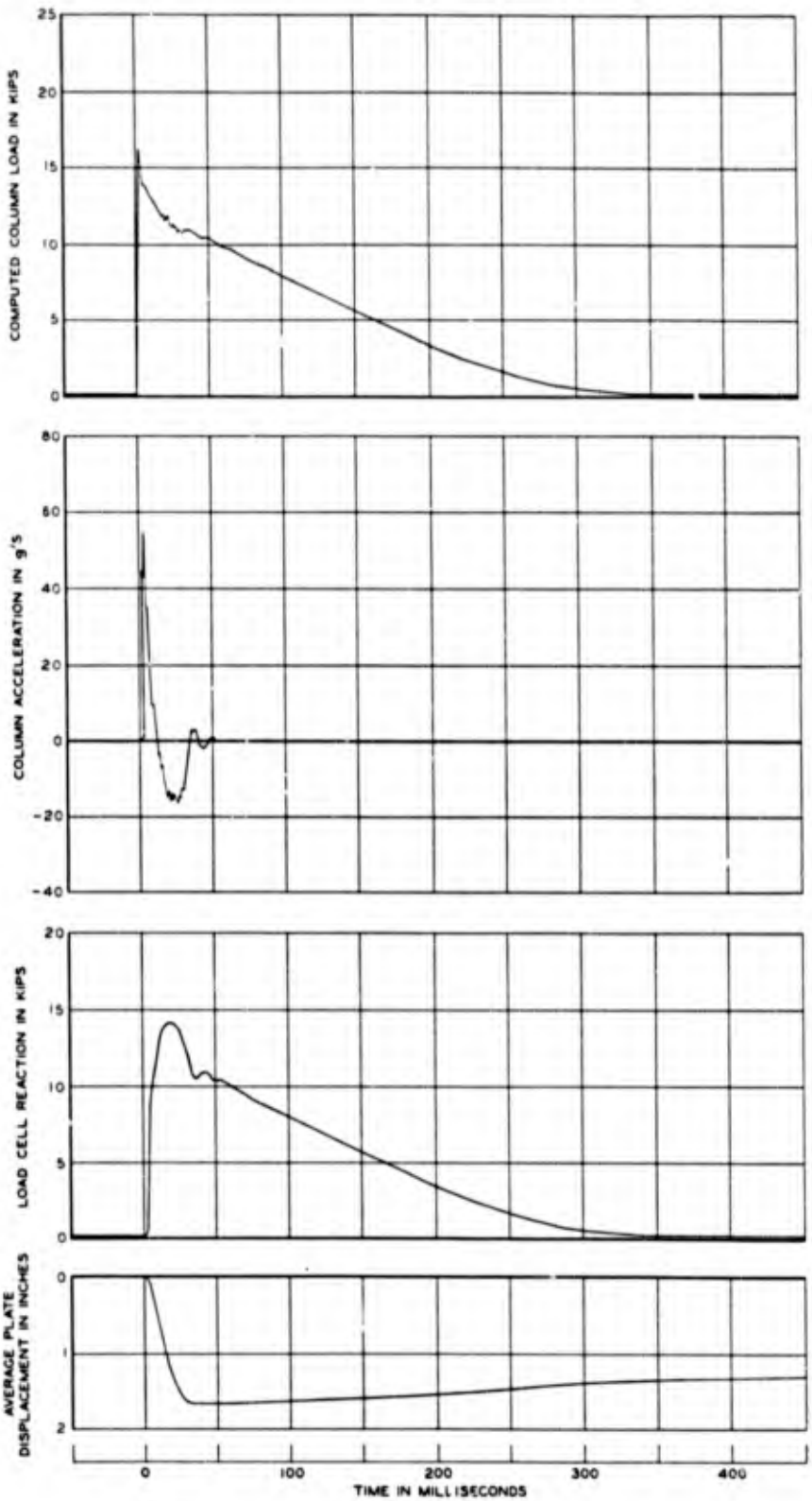

b = 10 IN

T_f = 1.85 KIPS/50 FT

DYNAMIC TEST

20-4

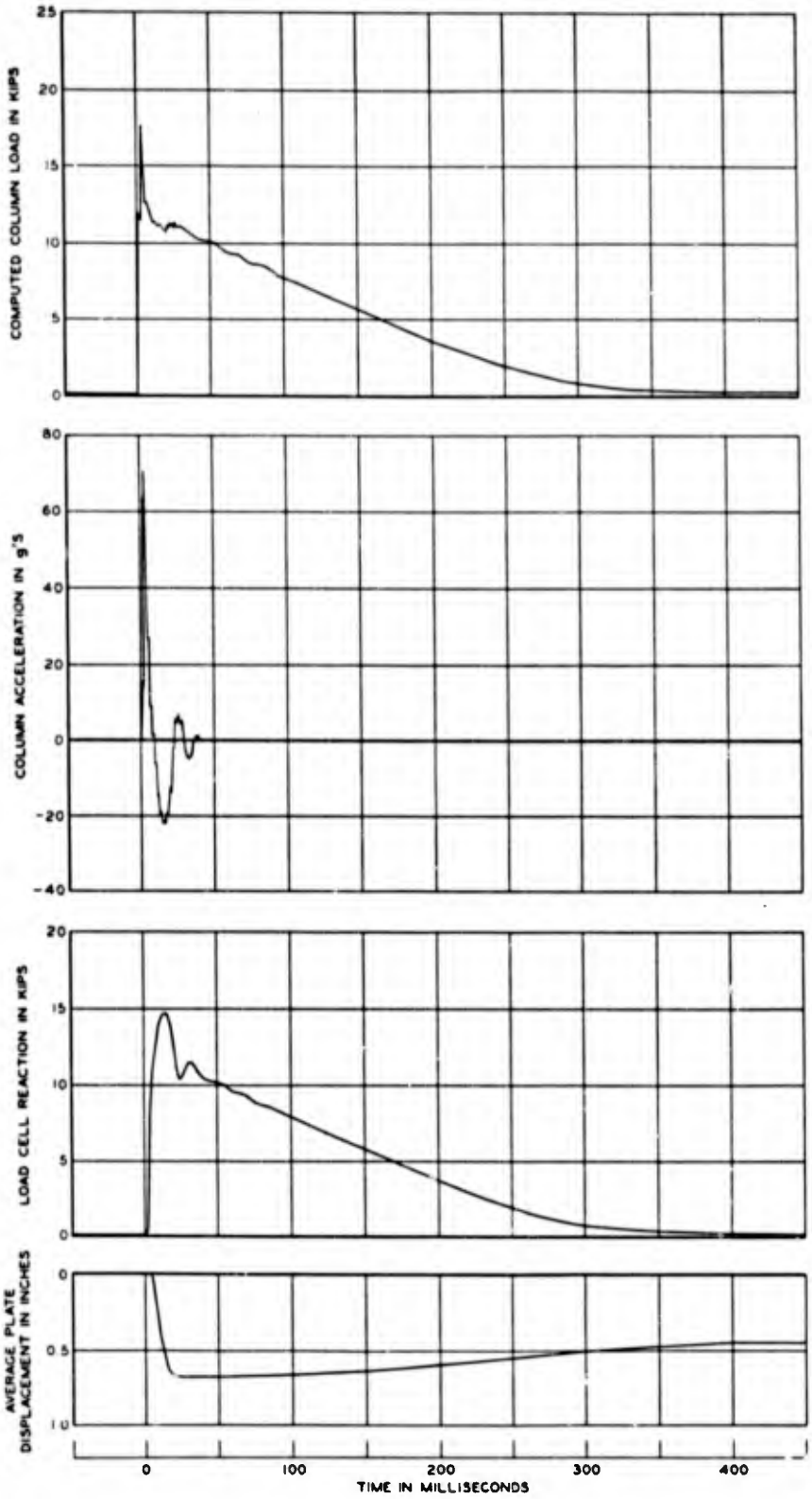

b = 12 IN.

T_f = 175 KIPS/SQ FT

DYNAMIC TEST
20-5

PLATE 26

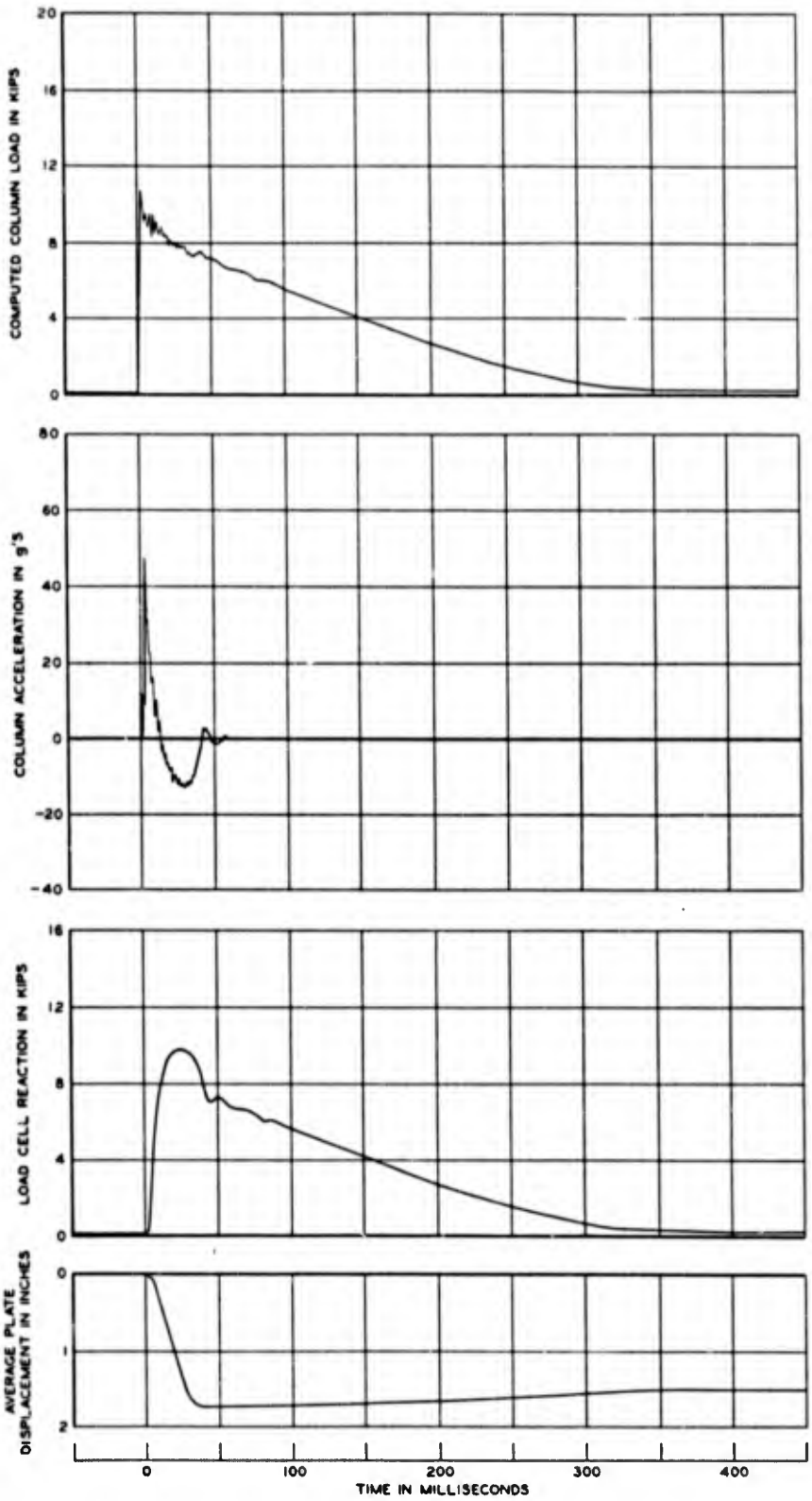

b = 8 IN.

τ = 1.85 KIPS/SQ FT

DYNAMIC TEST
20-6

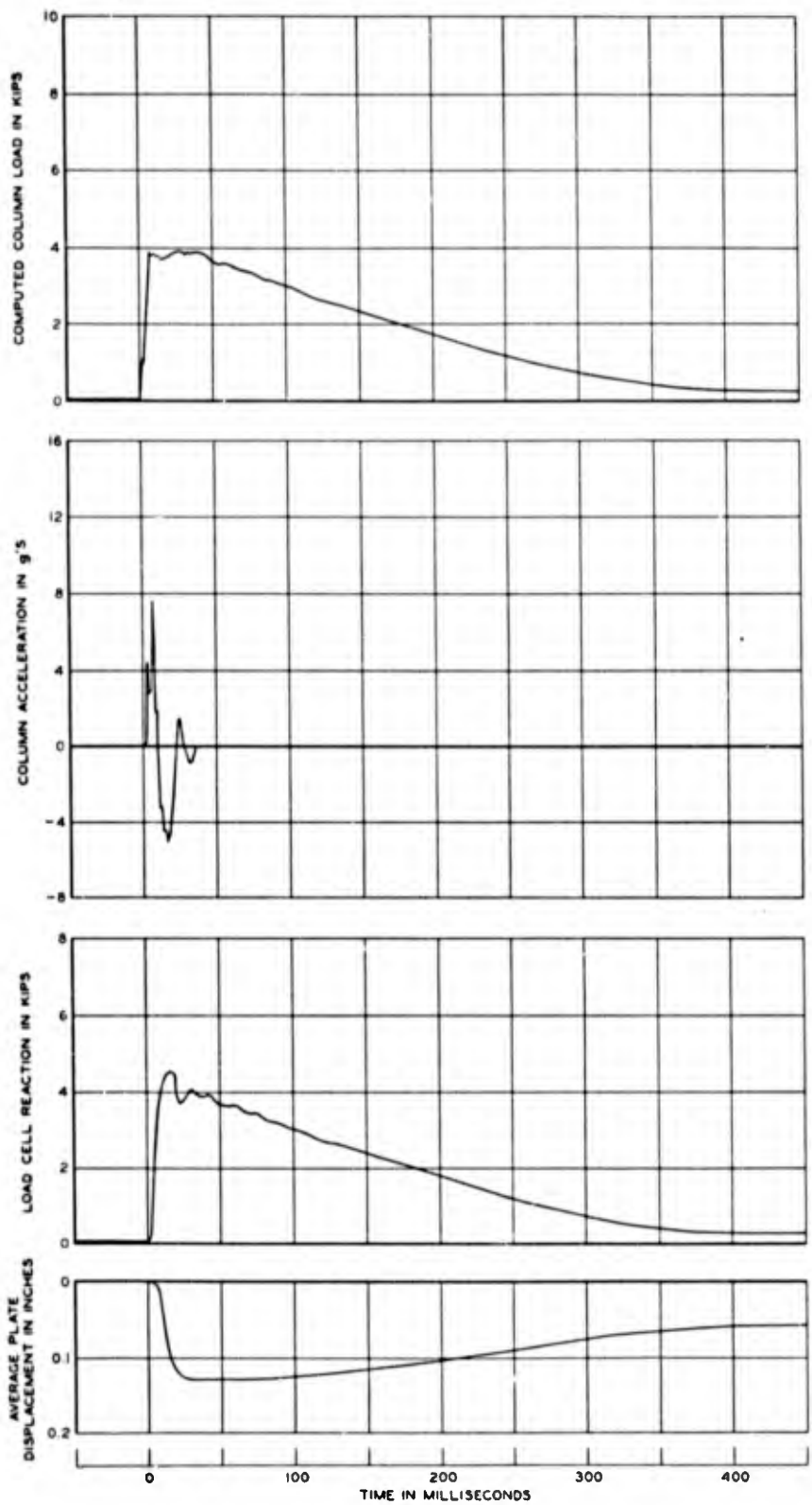

b = 8 IN

γ_f = 1.85 KIPS/SQ FT

DYNAMIC TEST

20-7

PLATE 28

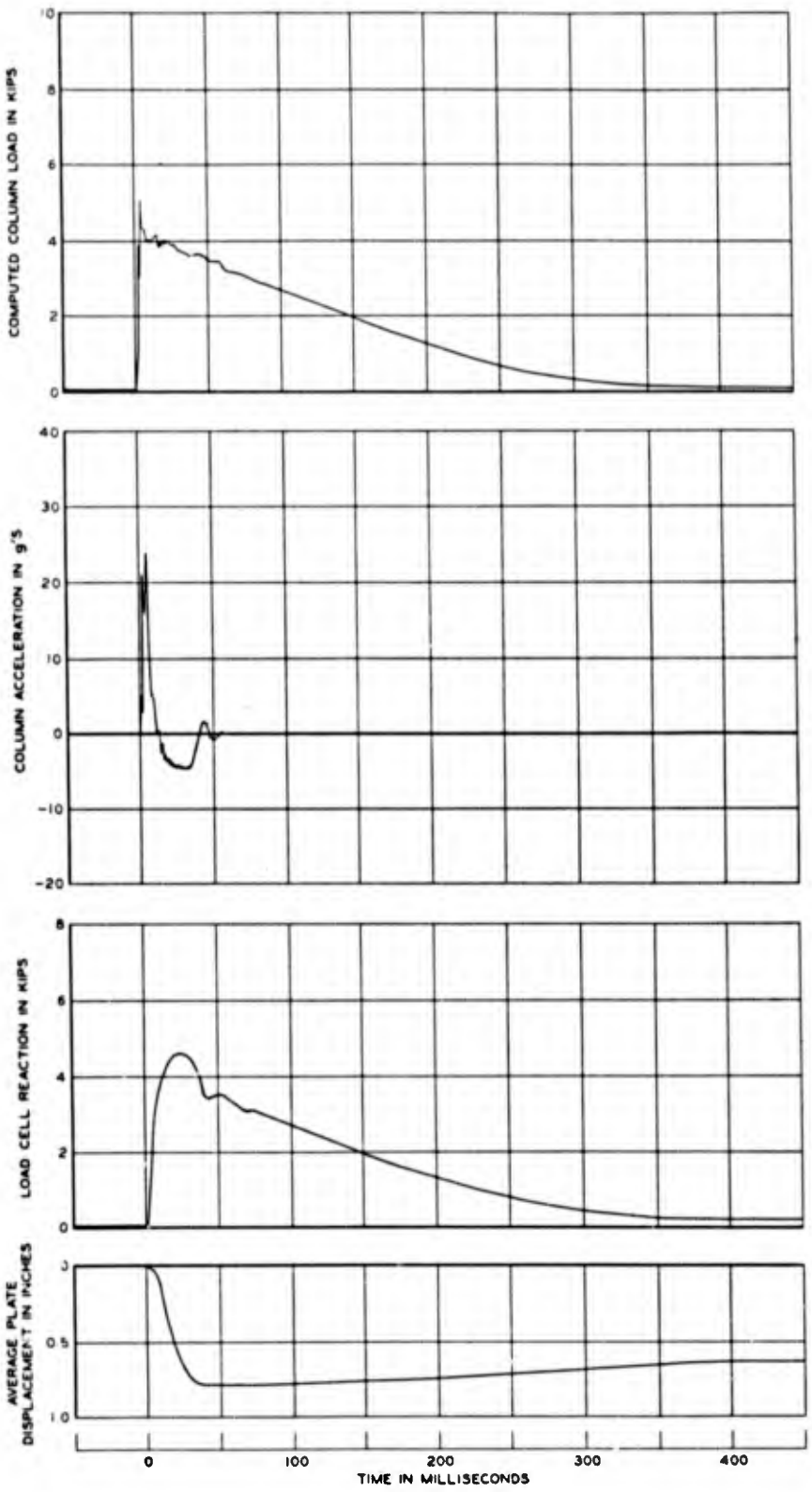

b = 6 IN

T_f = 1.75 KIPS/SQ FT

DYNAMIC TEST
20-8

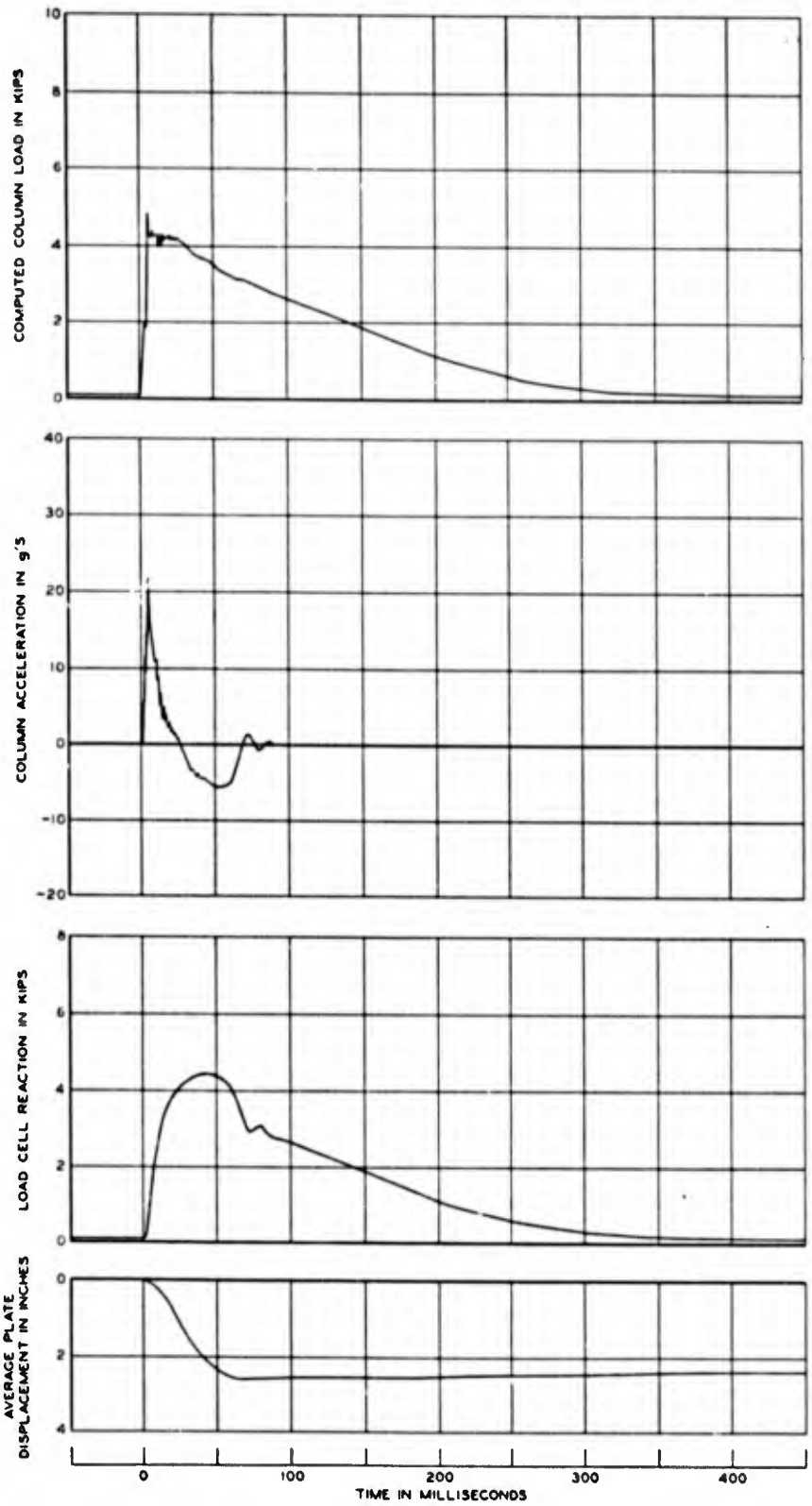

b = 5 IN

T_r = 175 KIPS/SQ FT

DYNAMIC TEST
20-9

PLATE 30

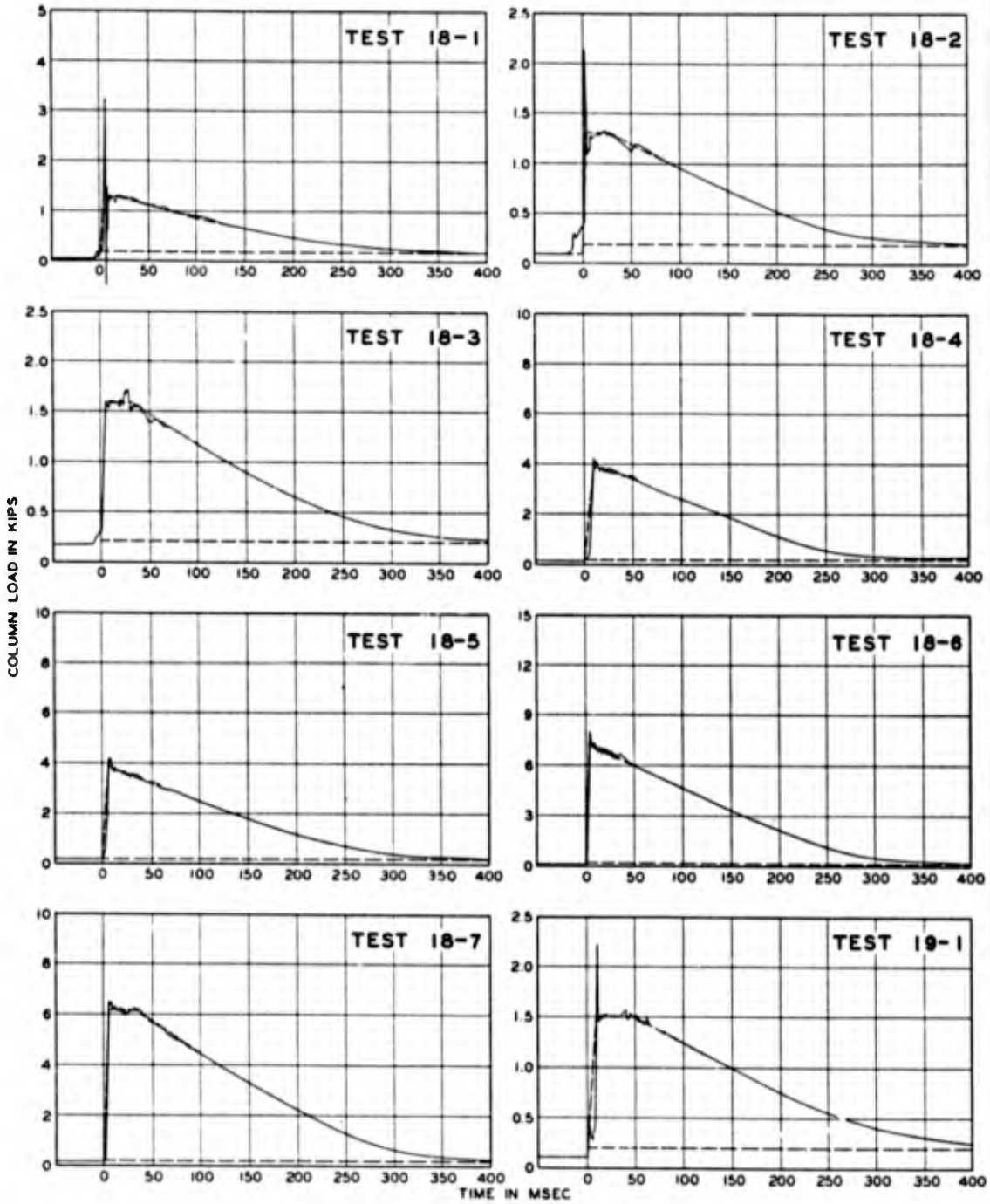

COMPUTED AND IDEALIZED COLUMN LOAD - TIME CURVES FOR DYNAMIC TESTS 18-1 THROUGH 19-1

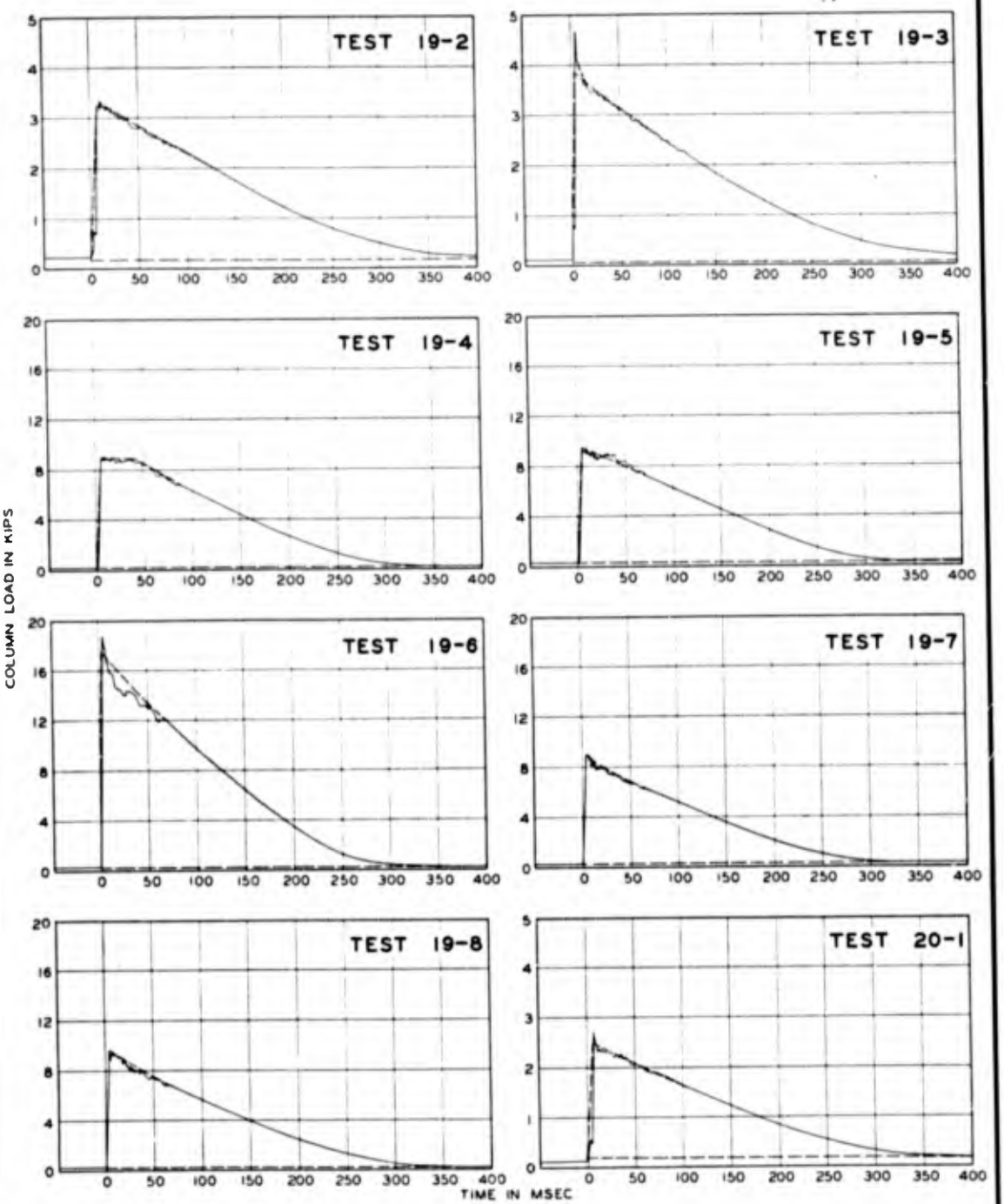

COMPUTED AND IDEALIZED COLUMN LOAD - TIME CURVES FOR DYNAMIC TESTS 19--2 THROUGH 20-1

PLATE 32

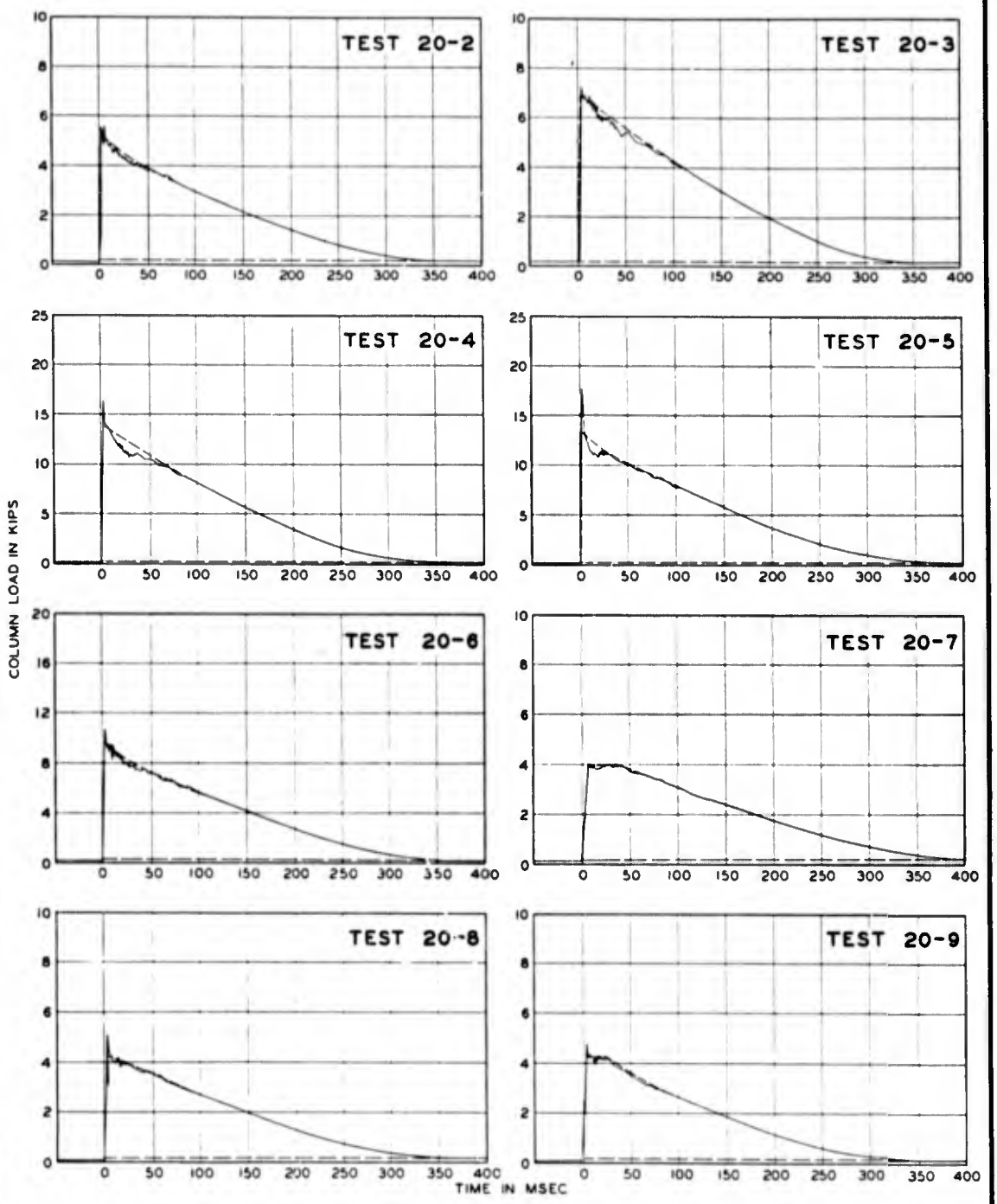

COMPUTED AND IDEALIZED COLUMN LOAD - TIME CURVES FOR DYNAMIC TESTS 20-2 THROUGH 20-9

PLATE 34

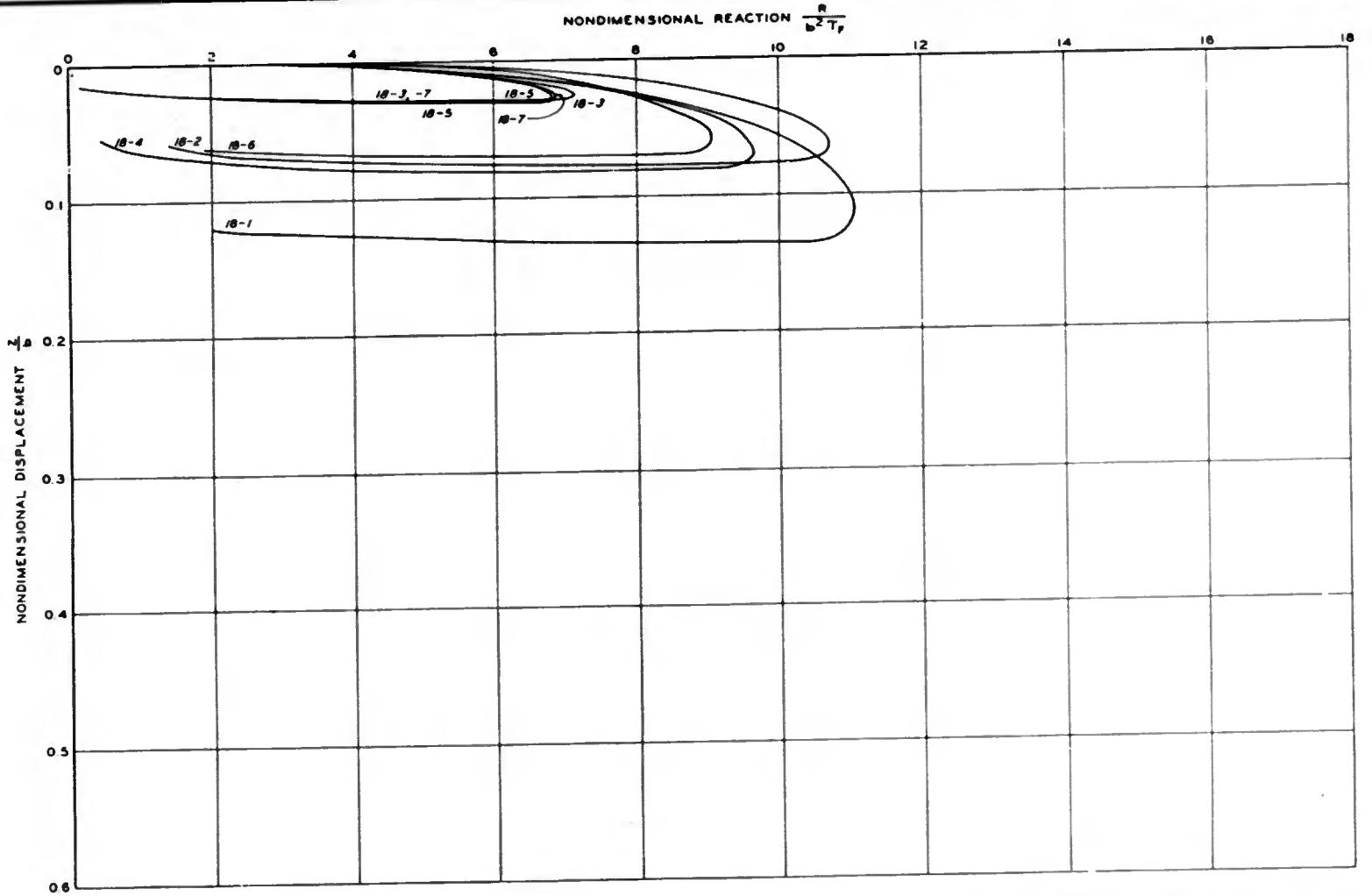

NONDIMENSIONAL FOOTING
LOAD-DISPLACEMENT CURVES

CART 18

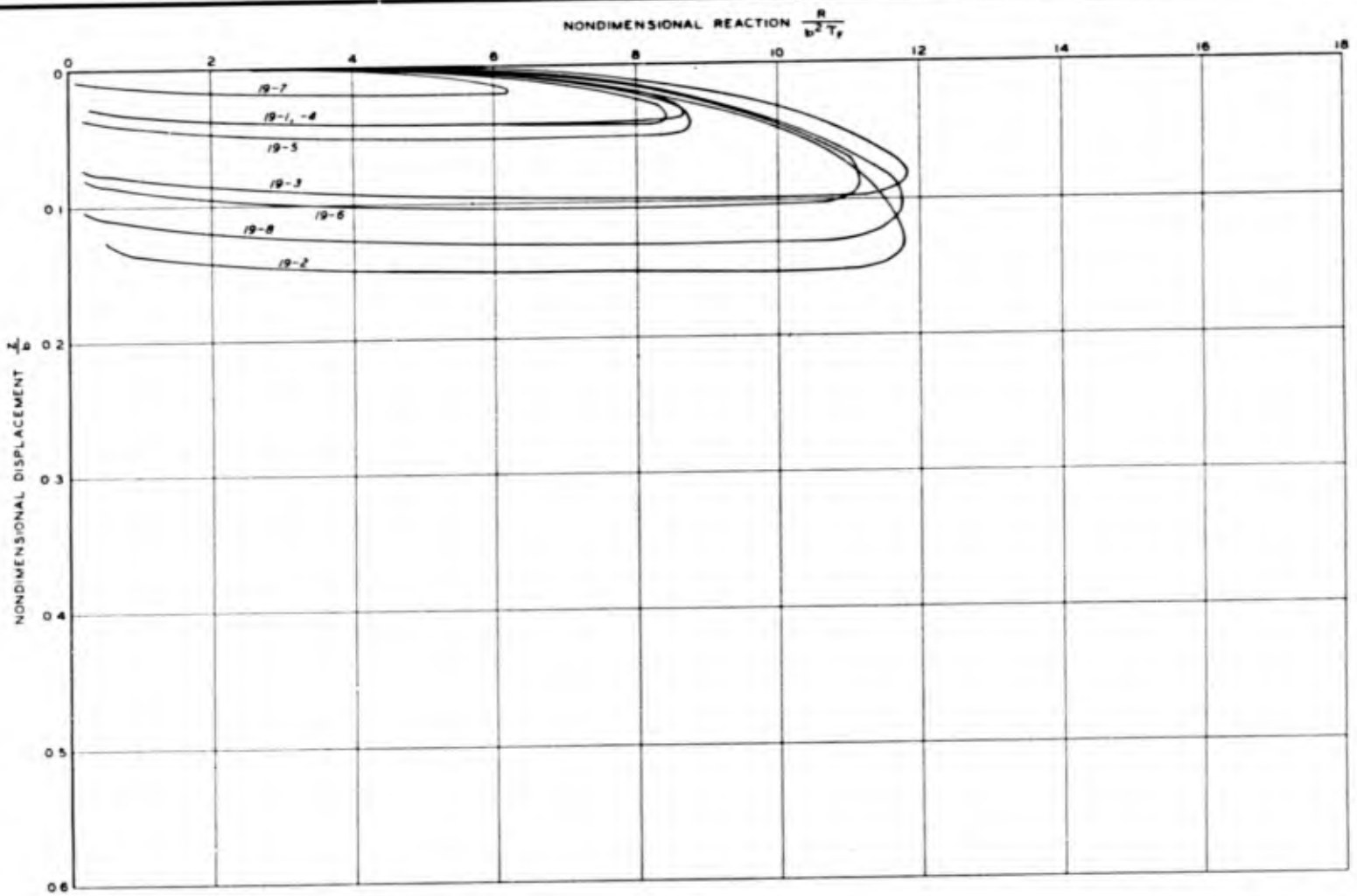

NONDIMENSIONAL FOOTING
LOAD-DISPLACEMENT CURVES

CART 19

PLATE 35

PLATE 36

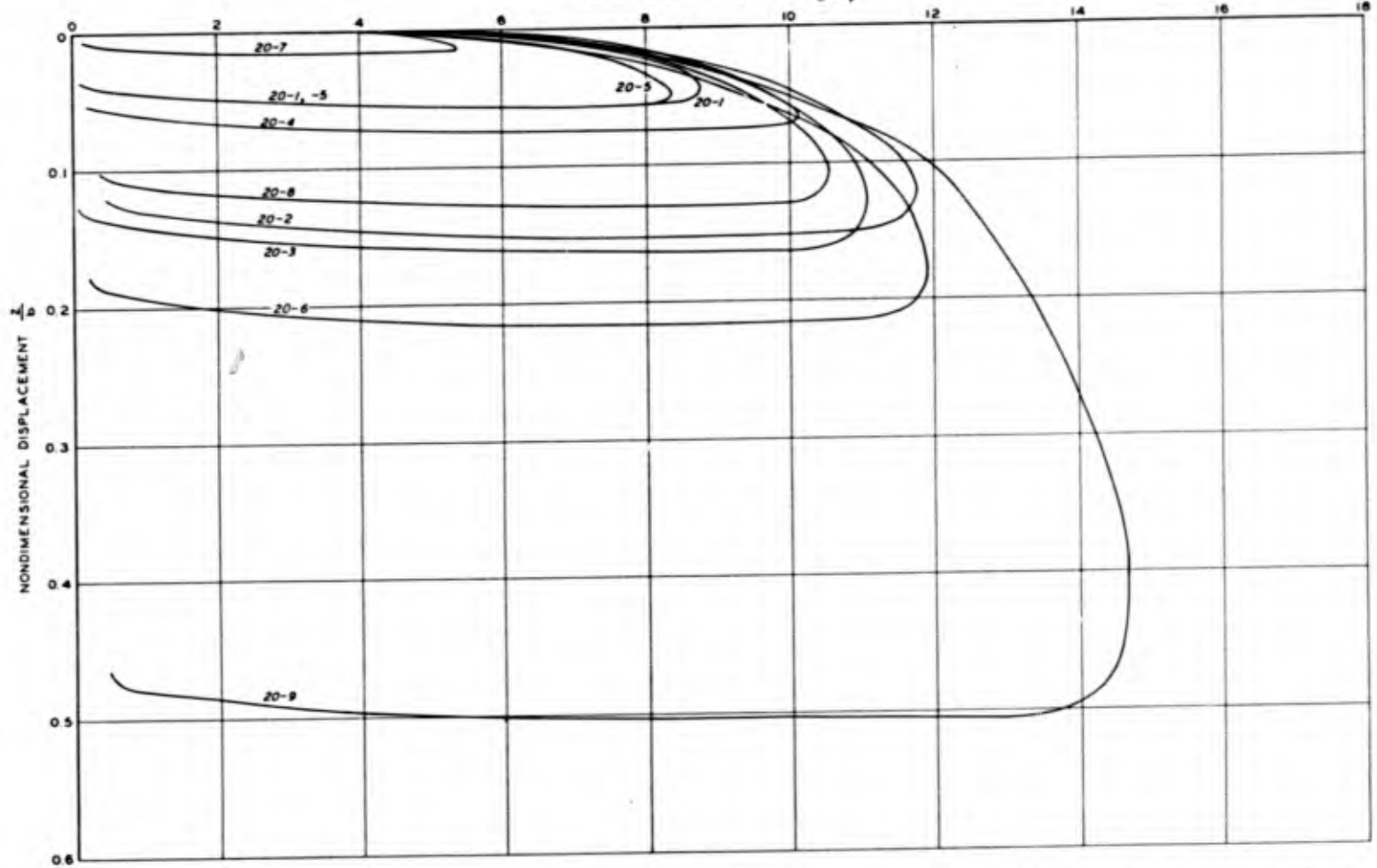

NONDIMENSIONAL FOOTING
LOAD-DISPLACEMENT CURVES

CART 20

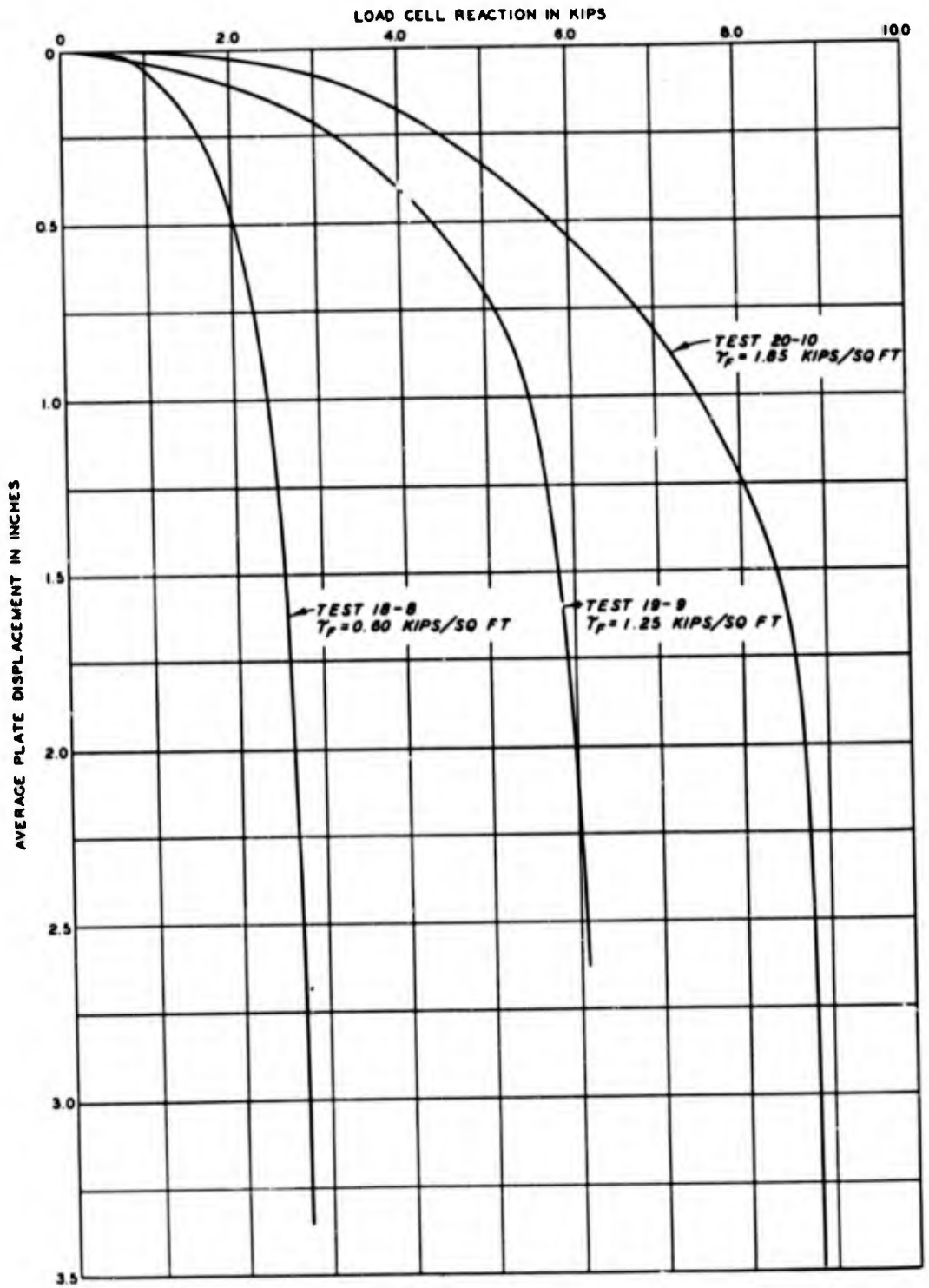

LOAD-DISPLACEMENT CURVES
STATIC TESTS ON
10-IN.-SQUARE PLATES
CARTS 18, 19, AND 20

PLATE 37

APPENDIX A: SPECIMEN PREPARATION AND TEST PROCEDURES

Test System

1. The test system used to obtain the data reported in Report 3 consisted of a 50-kip, gas-operated, dynamic loading machine,[3*] a square aluminum plate footing, a compacted specimen of a highly plastic clay contained in a track-mounted movable soil cart, and an electronic instrumentation support system. Data for this report were obtained using the same loading machine, similar footings, compacted specimens of highly plastic clay (from the same source as that used in the study reported in Report 3) contained in a 7-ft-2-in.-wide by 21.5-ft-long by 3-ft-deep soil cart, and a generally similar instrumentation system. A typical test setup is shown in fig. A1.

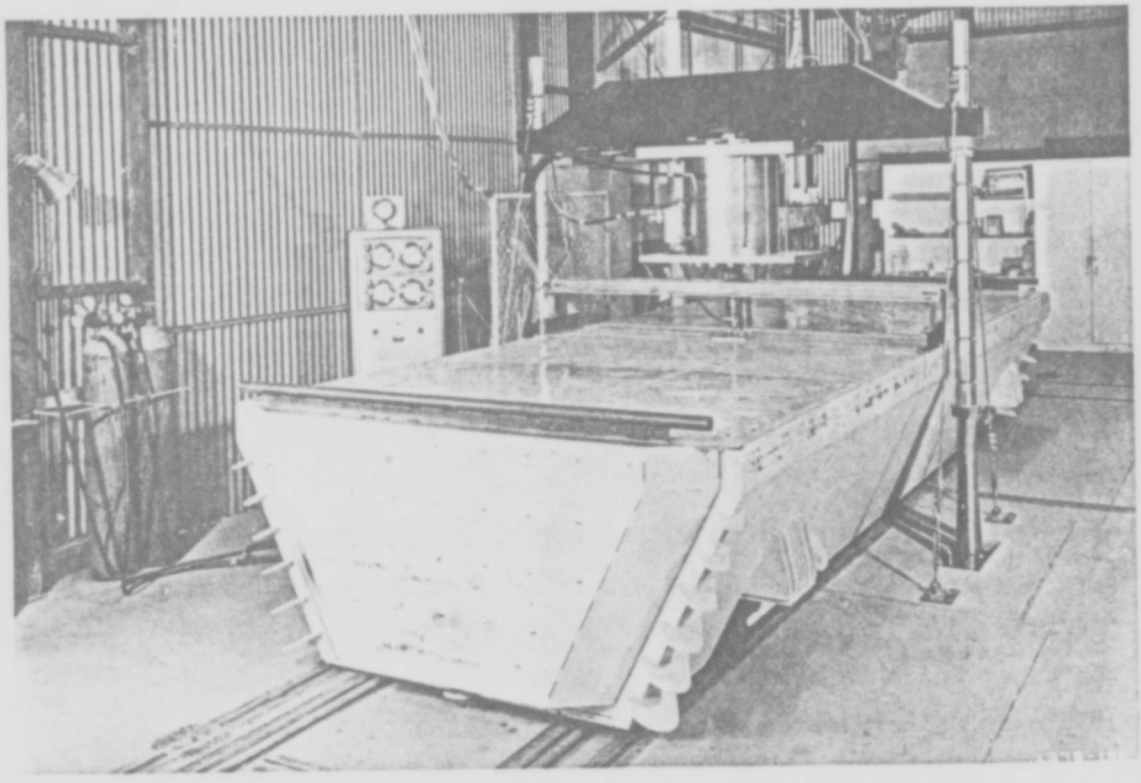

Fig. A1. Dynamic loading machine and soil-cart specimen set up for a dynamic test

---

* Raised numbers refer to similarly numbered items in Literature Cited at end of main text.

2. Figure A2a is a schematic diagram of a part of the test system. The cutaway view of a portion of the loading machine shows how the difference between the fire and cushion pressures acts to drive the load column. A detailed description of this device is presented in Report 1. Fig. A2b presents free-body diagrams of the system. As the various forces are defined in the figure itself and the behavior of each of these forces with time is very well described in Report 3, no further explanation of the loading machine operation will be offered. Fig. A2c shows idealized free-body

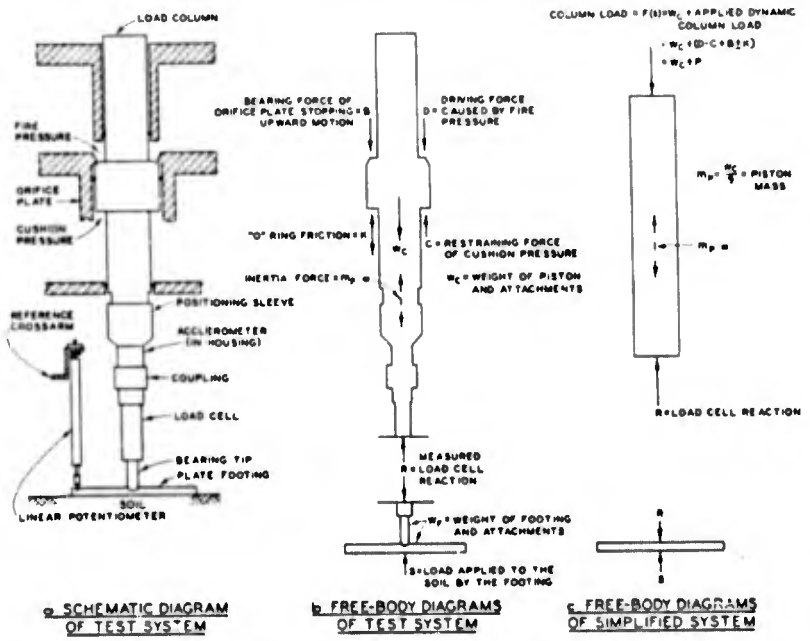

Fig. A2. Schematic and free-body diagrams of part of the test system

diagrams of the load column and the footing derived from those in fig. A2b. The similarity between the system in fig. A2c and that in fig. 1 of the main text is evident. Equation A1, relating column load, reaction, piston mass, and acceleration, results from applying D'Alembert's principle to the free-body diagram of the piston in fig. A2c.

$$F(t) - R(t) = m_p\, a(t) \qquad (A1)$$

where

$F(t)$ = column load = $P(t) + W_c$

$R(t)$ = load cell reaction or footing load

m_p = mass of piston

$a(t)$ = acceleration of the piston = $\frac{d^2z}{dt^2}$

and

$P(t)$ = applied dynamic column load

W_c = weight of the load column

3. An analysis similar to that given by equation A1 could be made for the free-body diagram of the footing. However, since the weight of the footing is very small in comparison with the magnitude of R , dead load and inertial forces due to the footing's mass are negligible and R , for practical purposes, is equal to the total force applied to the soil. The displacement response of the footing under a given dynamic loading R(t) is dependent on the stress-deformation characteristics, strength, and unit weight of the soil specimen.

Soil Properties

4. The highly plastic clay used to construct the soil specimens for this investigation was obtained from the same source as that used in the Report 3 model tests, a backswamp deposit near the Mississippi River in the vicinity of Vicksburg, Miss. It is classified as CH in the Unified Soil Classification System[12] and is locally referred to as "buckshot" clay. The material was air-dried from its natural water content of 30 to 40 percent to about 10 percent water content, crushed, and stored for use.

5. After being air-dried, the clay used in this investigation had the following average index properties:

Liquid limit	60	
Plastic limit	23	
Plasticity index	37	
Specific gravity	2.70	
Optimum water content	23.5%	(obtained by standard effort in 4-in. mold)
Maximum dry unit weight	96.2 lb per cu ft	

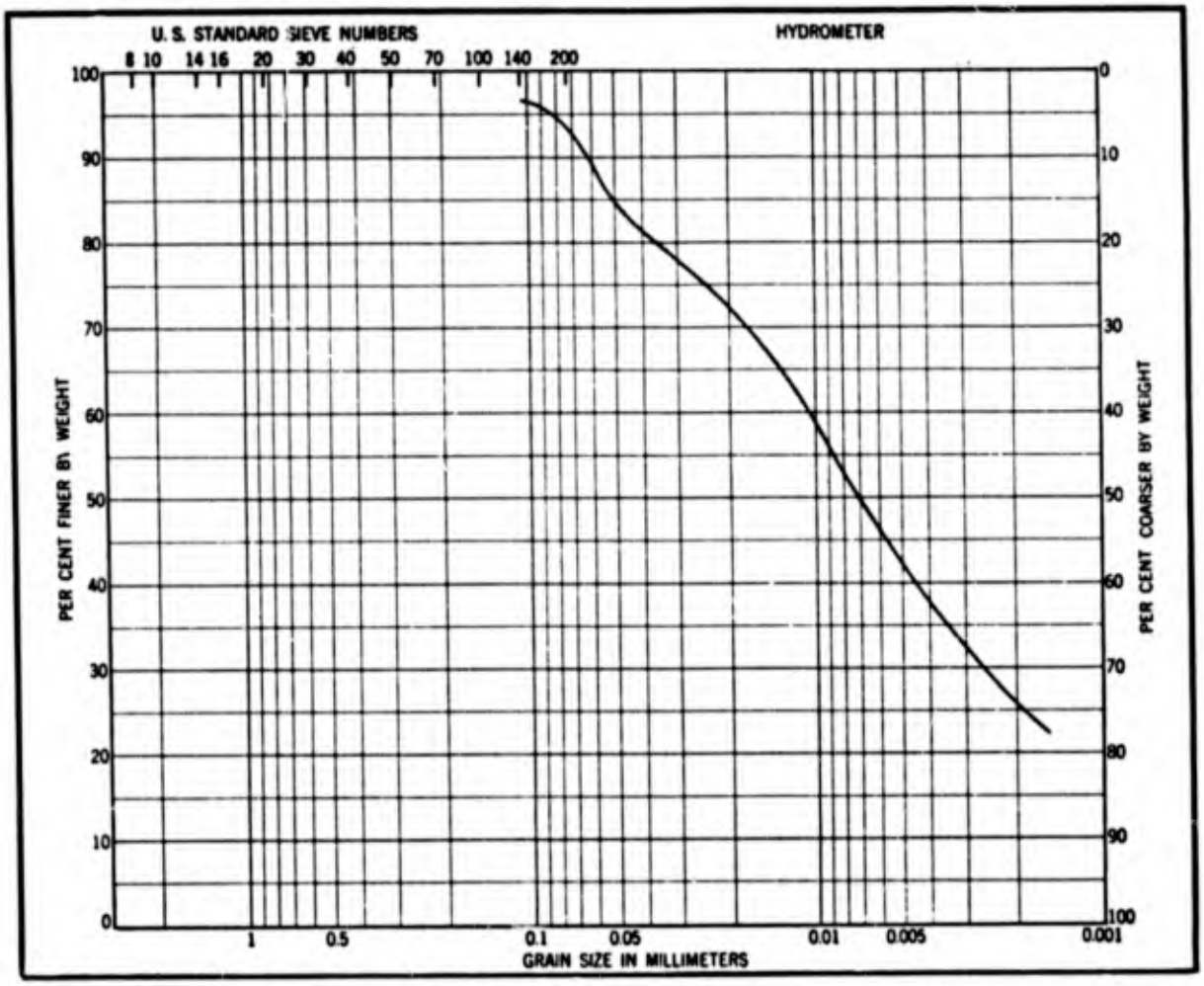

Fig. A3. Typical gradation curve, buckshot clay

A typical gradation curve for the clay is shown in fig. A3.

6. Reprinted from Report 3, fig. A4 presents the relation of water content to dry unit weight and shear strength in unconfined compression (UC) for this material when it is compacted in three lifts in a 6-in.-diameter by 4.5-in.-high mold (slightly tapered to facilitate specimen extrusion) using 55 blows of a 5.5-lb hammer falling 12 in. on each layer. For the range of water contents investigated, 26 to 35 percent, dry unit weight varied from 93.8 to 83.2 lb per cu ft and UC shear strength varied from 2.0 to 0.6 kips per sq ft.

Soil Specimen Preparation

7. Control of UC shear strength τ_f and wet unit weight γ_m of the

soil-cart specimens was necessary to design dynamic footing tests to evaluate the effect of variations in shear strength on the three nondimensional relations given in Part II of the main text of this report. In Report 3 a study of the relations of water content to dry unit weight, shear strength, and vane shear resistance was

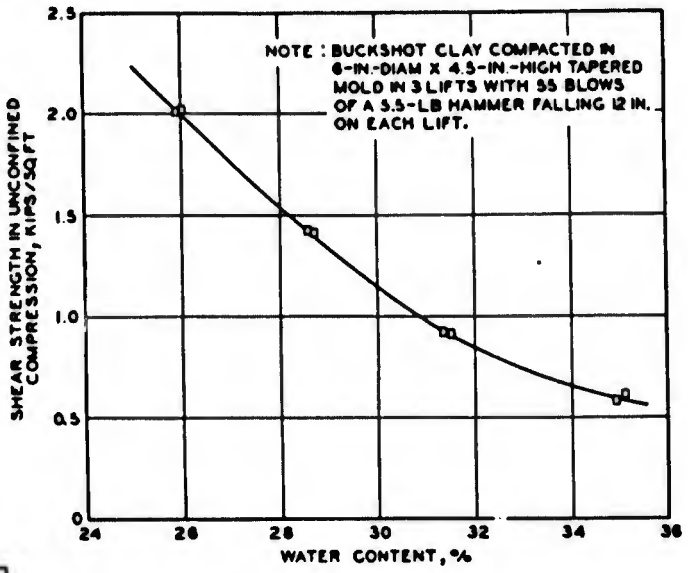

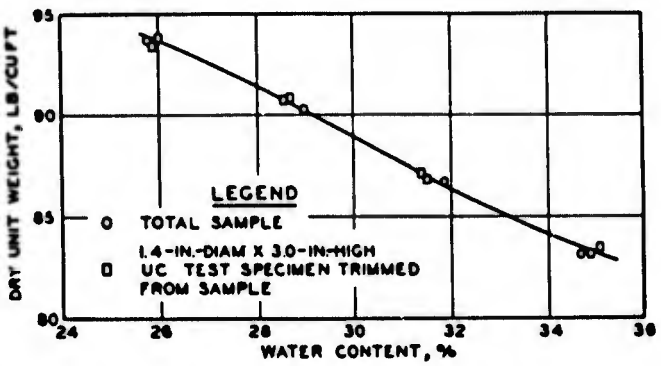

Fig. A4. Shear strength in unconfined compression and dry unit weight versus water content for compacted buckshot clay

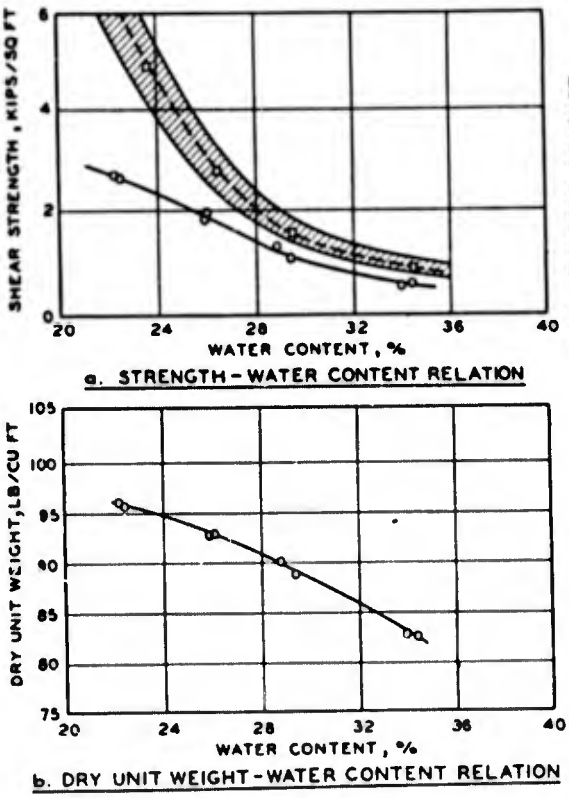

Fig. A5. Shear strength, vane shear resistance, and dry unit weight versus water content (model study compaction method)

presented for a series of specimens employing the cart-specimen compaction method used in the model study. As the same soil specimen preparation procedure was used for the footing tests described in this report, the results of the control study summarized in fig. A5 were again used for strength and unit weight control.

8. Before construction of a soil specimen in the movable soil cart shown in fig. A1, page 87, a base

layer of buckshot clay was compacted in the soil cart at approximately optimum moisture content and unit weight. This layer filled the bottom 24 in. of the 36-in.-deep cart. A polyethylene membrane was placed over the base layer to prevent loss of moisture (fig. A6d). The effect of a similar base layer on similar dynamic footing tests has been shown to be not significant.[5]

9. To obtain soil for a specimen of a desired shear strength, the air-dried buckshot clay was processed to the desired water content (determined from fig. A5a) in a pug mill mixing plant (fig. A6a) and allowed to cure for approximately two days. Four truckloads (fig. A6b) of processed soil (approx 17,000 lb) were required for the top 12-in. thickness of the specimen. The material was obtained in two batches (two truckloads each). Because of a lack of fine control over the rate at which water was added to the soil in the pug mill, it was difficult to achieve identical water contents in each of the two batches. The bottom 6 in. of the specimen was constructed in two 3-in. lifts using material from the first batch, and the top two lifts were constructed from the second batch.

10. Prior to constructing a lift, the wet unit weight was estimated from the desired water content using fig. A5b, and the amount of wet soil for a 3-in.-thick lift was determined. This amount of soil was weighed (fig. A6c), placed in the cart (fig. A6e), and spread to provide an approximately level surface (fig. A6f). The surface was lightly hand tamped (fig. A6g) and compacted with four coverages of a hand-operated mechanical backfill tamper (fig. A6h). Fig. A6, showing the soil specimen construction procedure, is reprinted from Report 3. The soil cart shown in figs. A6d through A6i is smaller than the one used in this investigation. This, however, was the only significant difference between the construction procedure and apparatus shown in Report 3 and that used in this investigation. After a specimen was prepared, its top was sealed with a polyethylene cover to minimize loss of moisture.

11. To check the unit weight of the specimen layers immediately after construction, several density tests were conducted using the Little Rock control sampler.[13] Additional control tests were conducted to check the strength of each layer using a laboratory vane shear device with a four-blade vane, 1/2 in. long and 1/2 in. in diameter, which has been previously

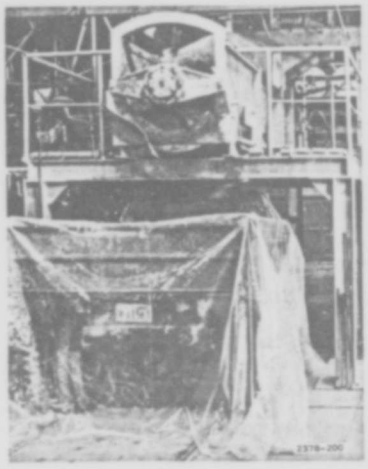

a

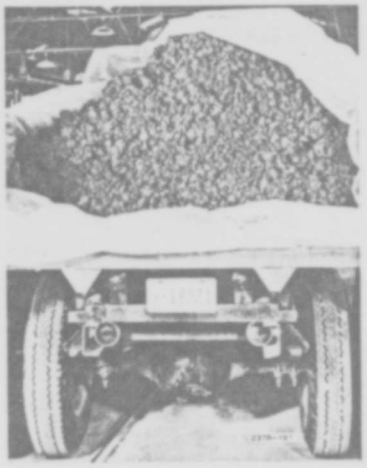

b

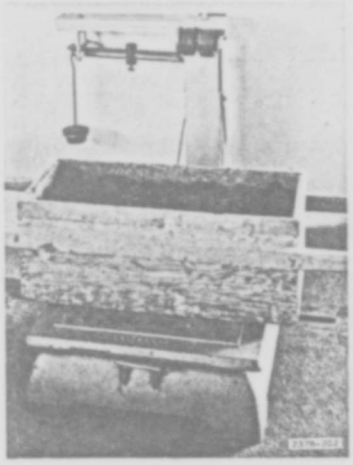

c

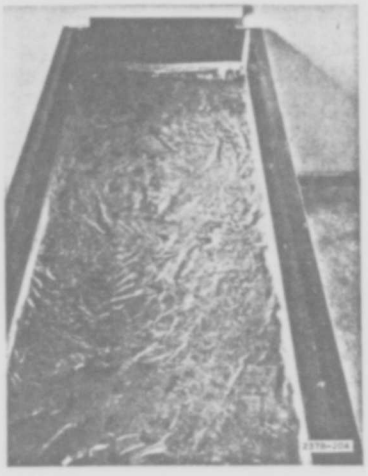

d

e

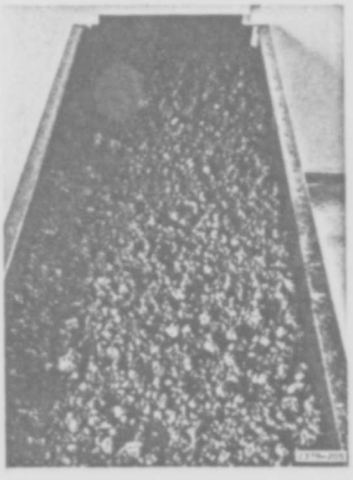

f

g

h

i

a. Fine-grained soil processing plant
b. Clay processed for specimen construction
c. Determining weight of clay for each lift
d. Membrane sealing base layer
e. Placing clay for lift
f. Spread and leveled
g. Hand tamping
h. Mechanical tamping
i. Scarifying

Fig. A6. Soil specimen construction

described in Report 3. The ratio of maximum torque measured to the first moment of the surface area generated by the vane when rotated about its vertical axis has been defined as "vane resistance" and has been correlated with UC shear strength for specimens prepared with the cart-specimen compaction technique (see fig. A5a, page 91).

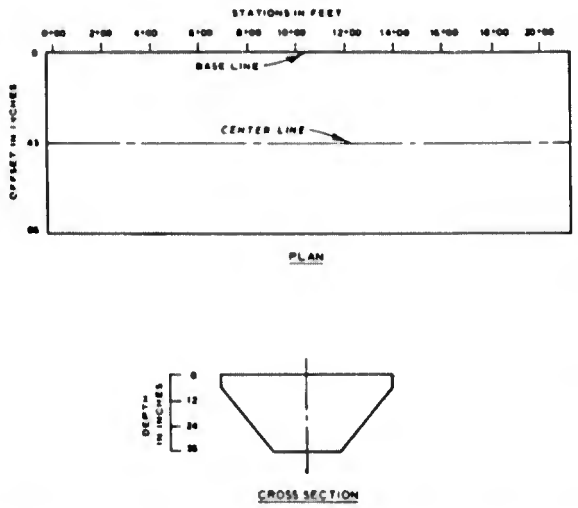

Fig. A7. Schematic diagram of large soil cart showing coordinate system for points in the soil specimen

12. To locate the position of the strength and density control tests, the coordinate system shown in fig. A7 was used. A point in the specimen is located by its distance from a reference mark 6 in. from one end of the cart (stations in feet), its offset from an arbitrarily selected longitudinal side of the cart (inches), and its depth below the final surface of the specimen (inches).

Dynamic Test Procedures

13. Before conducting dynamic footing tests on a soil specimen, it was necessary to calibrate the dynamic loading machine. The controls of the loading machine allow the operator to control the force delivered to the piston load collar (see fig. A2b, page 88). The load parameter chosen for control in this investigation, however, was not this load but that delivered to the footing, the reaction R, which is related to the controlled load by equation A1. From equation A1, it can be seen that reaction is partially dependent on footing acceleration, a function which is unknown prior to the test.

14. To overcome this difficulty, a calibration technique was employed in which the machine settings necessary to produce the desired footing load-time relation for footings 14 in. wide and smaller were determined by trial-and-error methods. For footings larger than 14 in., loading-machine settings were determined from calibration tests on

14-in. footings. A clay specimen of the same consistency as that of the soil-cart specimen to be tested was prepared in a 15- by 15-in., 21-in.-deep, steel calibration box. After a footing of the same size as that planned for the test in the soil cart was placed on the calibration specimen, the footing was dynamically loaded using the loading machine set to produce a column load equal to the maximum footing reaction desired. Although the box walls probably affected the calibration test results, the peak values of the footing reaction determined were quite similar to those for similar tests on larger specimens. A typical calibration test setup is shown in fig. A8. After the load on the footing was determined, dynamic loading machine settings were adjusted, a new specimen was prepared, and another calibration test was conducted. This procedure was repeated until the desired footing reaction was achieved.

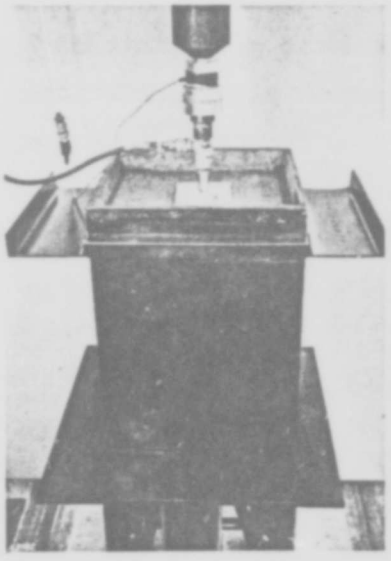

Fig. A8. Setup for typical dynamic loading machine calibration test

15. While the calibration tests were in progress, part of the polyethylene surface cover was removed, the surface of the soil-cart specimen was roughly leveled, and a series of 27 vane shear tests was performed, nine each at 1-, 3-, and 5-in. depths in the vicinity of the test location at points in a 6- by 8-in. grid centered on the test location with the 6-in. sides of the grid parallel to the long axis of the cart. After completion of the vane shear tests and the box calibration tests, the soil-cart surface was carefully trimmed at the test location. Exposure of the trimmed surface to the atmosphere was held to a minimum. The cart specimen was rolled under the dynamic loading machine, jacked up from the floor, leveled, and blocked with hardwood timbers and wedges.

Instrumentation

16. After the soil-cart specimen and plate footing were positioned underneath the loading machine, transducers, or "pickups," measuring footing reaction, footing displacement, and load-column acceleration were attached. The generated signals were amplified and recorded continuously

using a direct-writing oscillograph.

17. Acceleration of the load column was measured with a linear accelerometer[14] (Consolidated Electrodynamics Corp., Type 4-202-0001) employing a four-active-arm, unbonded, strain-gage sensor with a range of ±50g's. This unit, with overall dimensions less than 1 in., was placed in the accelerometer housing unit (see fig. A2a, page 88), which was axially connected to the load column.

18. Below the accelerometer, a four-active-arm, bonded, strain-gage load cell with a hemispherical tip in contact with the footing was used to measure the footing reaction. Four load cells with ranges of 2000, 5000, 10,000, and 100,000 lb were used. (The 100,000-lb cell was built at WES, and the others are of Baldwin-Lima-Hamilton design.) One of the load cells and the accelerometer housing are shown in fig. A8, page 95.

19. Vertical displacements of three corners of the footing were measured with linear potentiometers (Bourns Laboratories, Inc., Model 108) with a 6-in. range. A bridge circuit described in Report 3 was used with the potentiometers to permit standardization of amplifiers.

20. Amplifiers used were four-channel, 3-KC carrier amplifiers (Consolidated Electrodynamics Corp., Type 1-118). The amplifier signals were directed to light-beam galvanometers in a direct-writing oscillograph normally operating at a paper speed of 64 ips. Two oscillographs were used for this investigation. The first two soil-cart specimens were tested using a Consolidated Electrodynamics Corp., Type 5-124, oscillograph (7-in.-wide paper), and the last specimen was tested using a Midwest Instruments, Type 102-500, oscillograph (12-in.-wide paper). Each oscillograph produced 10-msec timing lines on the direct-writing paper.

21. The same procedures as are described in Report 3 were utilized in calibration of instruments, amplifiers, and galvanometers, and descriptions thereof will not be repeated here. Step calibrations, using precision resistors in the instrument circuits to cause galvanometer deflections identical with those caused by a known force, acceleration, or displacement, were placed on each oscillogram before and after each test to permit accurate scale-factor determination. It is estimated that the maximum error in the measured acceleration due to the instrumentation system is less than 2 percent of the measured value at any instant of time.

The reaction and displacement are estimated to be accurate within 1 percent of the measured values. These estimates are based on the manufacturer's instrument specifications and the methods of calibration employed.

Data-reduction procedure

22. After the instruments were installed and just prior to each test, the instruments were step-calibrated at a slow paper speed. The paper speed was then set to run at 64 ips during the test, the actuator of the dynamic loading machine was pressurized using the pressure settings determined during the calibration tests, and the shot was fired.

23. Scale factors and base lines were determined for the five data traces (three displacements, one load cell reaction, and one acceleration) on the test oscillogram. Trace departures from the base lines were measured and tabulated manually, generally using 1- or 2-msec time intervals. In addition, all peak points of the traces were carefully recorded. Displacement of the center of the footing was computed by averaging the measurements at diagonally opposite corners of the footing. The column load was computed from the reaction and acceleration using equation A1. The data (in reduced form) from a typical dynamic footing test are shown in fig. A9.

24. The column load in fig. A9 is observed to have an irregular variation in the vicinity of its peak value, which is believed to be due to the combined effects of pressure reflections and turbulence in the rapidly moving gas plus acceleration "noise" due to the relative motion of the load-column attachments caused by the threaded attachment connections. An idealized curve (shown dashed in fig. A9) has been fitted to the curve and is believed to be more representative of the column load than the computed force curve in the region of this irregular variation. The idealized curves are used for analysis purposes. Time parameters determined from the idealized curve are the rise time t_r, hold time t_h, decay time t_d, and positive-phase duration t_o, all of which are defined in fig. A9.

Static test procedures

25. The dynamic loading machine can be operated so as to apply static loads to the load column in controlled increments. In each soil-cart specimen, one static test was conducted. The test setup was similar to that for the dynamic tests, except that the accelerometer was not

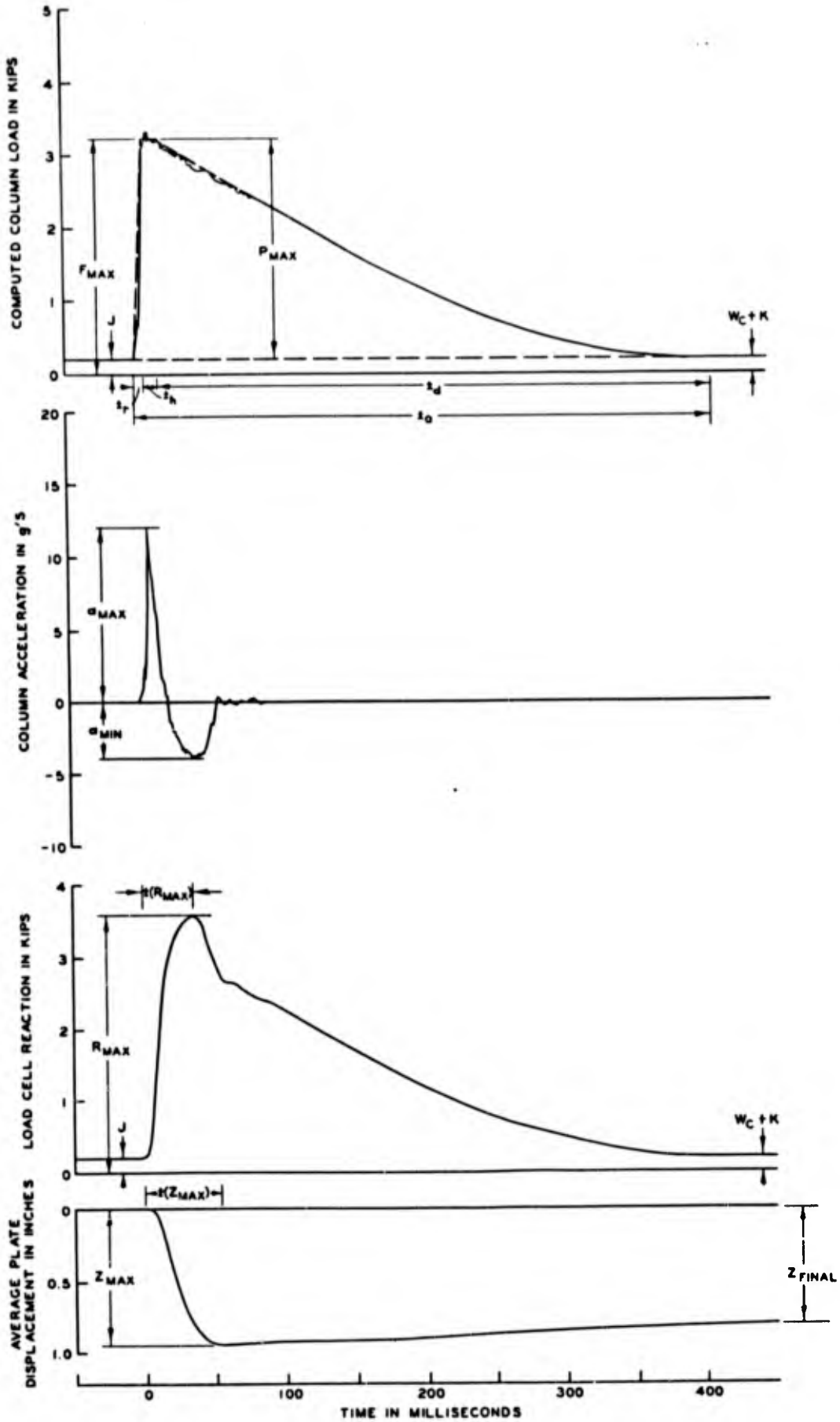

Fig. A9. Response histories for a typical dynamic test

connected, and an oscillograph paper speed of 0.25 ips was used to record the significant portions of the displacement history. An extensometer graduated to 0.001 in. was attached to measure the displacement of the load column during the static test.

26. The load, estimated to produce approximately a 3-in. displacement, was applied to the load column in from 10 to 15 increments. After application of each load increment, the extensometer was observed, and when the rate of deformation had slowed to 0.001 in. per 10 sec (1/10,000 ips) the next increment of load was applied. The loading was continued until displacements exceeded the largest displacement measured in a dynamic test on the same cart or the rate of change of load with respect to displacement approached zero. Static test duration ranged from 2.5 to 3.3 hr.

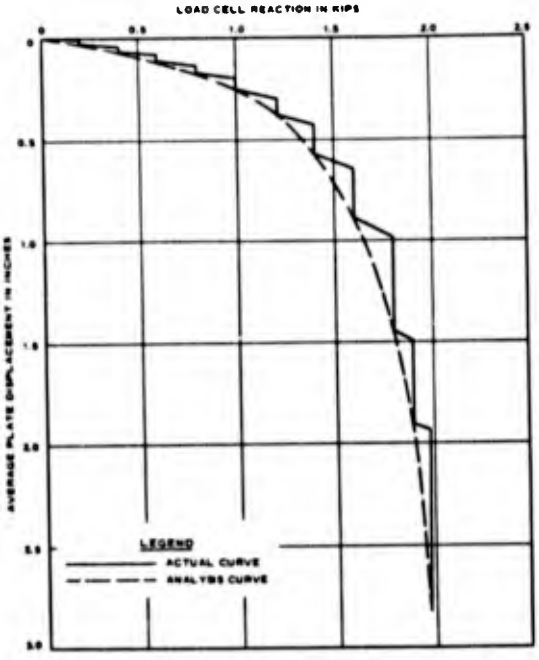

Fig. A10. Typical static test load-displacement curve

27. A typical set of static test data is shown in fig. A10. The solid lines are the plot of load cell reaction versus average plate displacement. The sloped portions of the solid curve represent the response as the load was applied, while the vertical portions represent displacement under constant load. The dashed curve through the end points of each load increment has been used for analysis purposes.

Soil Sampling and Testing

28. After completion of all dynamic and static footing tests on a soil-cart specimen (approximately two weeks after the cart specimen was built), a series of water content and wet unit weight determinations was conducted in the 0- to 3-in. depth below the specimen surface. Following this, eight undisturbed block samples (6 by 6 by 12 in. high) were trimmed from 9- by 9- by 12-in.-high soil specimens taken from the top

12 in. of the soil cart. These samples were waxed and stored in a humid room.

29. Two, strain-controlled, unconfined compression (UC) tests were conducted on 1.4-in.-diameter by 3.0-in.-high specimens from the top 4 in. of each block. Strain-controlled, unconsolidated-undrained (UU), triaxial tests (three specimens each, tested at chamber pressures of 1, 3, and 6 kips per sq ft) were conducted on 1.4-in.-diameter by 3-in.-high specimens from the top 4 in. of one block sample from each cart. The UU test specimens were taken from a block for which the UC test results were near the average for the cart.

30. Stress-controlled, consolidated-drained, direct shear tests at normal pressures of 1, 3, and 6 kips per sq ft were conducted on 2.4- by 2.4- by 0.4-in. specimens taken from the 4- to 6-in. depth of the same block sample from which the UU test specimens were taken. All strength tests utilized standard Corps of Engineers procedures.[15]

Discussion

31. The problem of the control of the test parameters has been previously discussed. The dependence of shear strength on water content was indicated in paragraph 7 of this appendix. The difficulty in obtaining identical batches of processed clay was mentioned in paragraph 9. The laborious calibration procedure necessary to achieve approximate control of the maximum footing reaction was described in paragraphs 13 and 14. To provide an evaluation of the specimen construction (carts 18-20) and test procedures used for the tests described in this report, comparisons of programed and measured test parameters are presented in the following paragraphs.

Soil specimen control

32. To achieve the desired shear strength in the cart specimens, the water content was varied and the compaction effort was held as near constant as possible. Thus, the ability to control the specimen water content determined the strength of the soil. The programed water contents of carts 18-20 were 35.0, 28.5, and 25.4 percent, respectively. The actual average water contents for approximately 16 UC test specimens taken

from the 0- to 4-in. depth of each cart specimen were 33.5, 28.3, and 25.5 percent, respectively. With the exception of the 1.5 percent deviation in cart 18, the control of water content in the top layer was good.

33. The programed shear strengths for carts 18-20 were 0.50, 1.25, and 2.00 kips per sq ft, respectively. It can be noted in the tabulation in paragraph 20 of the main text that the average shear strengths in unconfined compression for the three cart specimens were actually 0.62, 1.21, and 1.78 kips per sq ft, respectively. These values are 124, 97, and 89 percent, respectively, of the programed shear strengths for the three cart specimens. Figure All presents a comparison of UC water content-shear

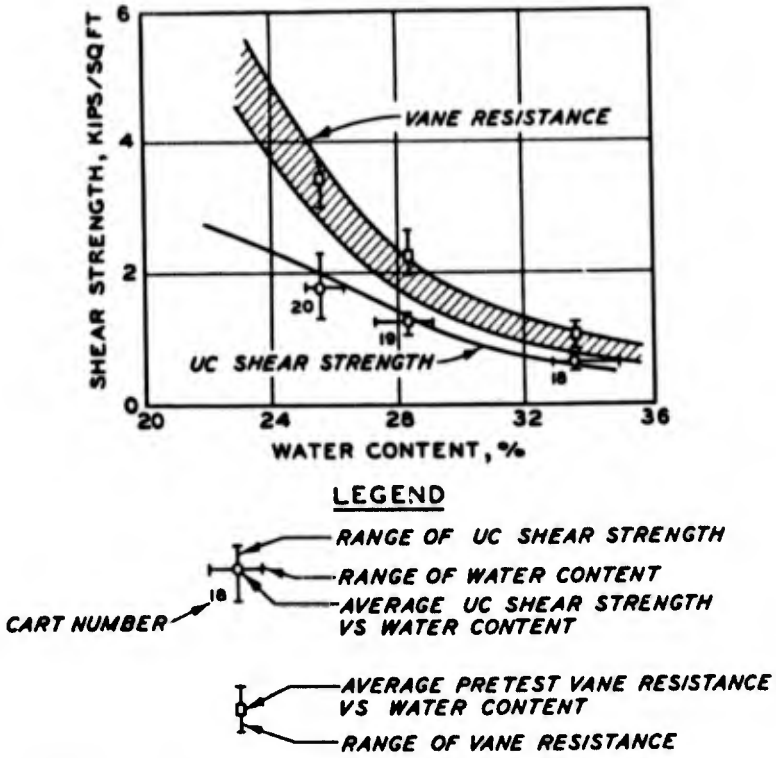

Fig. All. Comparison of soil-cart specimen UC water content-shear strength and water content-vane resistance data with control study correlation curve

strength data and pretest vane-resistance data obtained from the three cart specimens with the strength correlation curves for the model study compaction method given in Report 3. From fig. All it is observed that the average vane-resistance data lie within the correlation band while the range for carts 18 and 19 extends somewhat above it. The cause of this extended range is not definitely known. It is possible that the

speed of the hand-operated vane in carts 18 and 19 differed somewhat from that used in the original control study. It was also noted that carts 18 and 19 had slightly greater wet unit weights and degrees of saturation than those tested in the compaction-control study.

34. The UC test data for carts 18 and 19 lie nearly on the curve of water content versus UC shear strength in fig. All, page 101. The average of the UC test data for cart 20 lies somewhat below it. The average UC test water content in cart 18 was 33.5 percent, while the programed water content was 35 percent; this difference accounts for the strength being greater than that programed for cart 18. Both shear strength and water content in cart 19 were nearly equal to the programed values. The strength deviation for cart 20, whose average water content is very nearly that indicated by the correlation curve to be necessary for the programed shear strength, is believed to be due to difficulties in control of compaction effort. These difficulties become more apparent at lower water contents (close to or below optimum) where the effect of compaction on strength is significant.[16]

35. The average wet unit weights for carts 18-20, as shown in paragraph 20 of the main text, were 112.9, 116.9, and 118.2 lb per cu ft, respectively. The average wet unit weight for the Report 3 model study ranged from 113.6 to 114.7 lb per cu ft. Although the range reported for this study is somewhat larger than that given in Report 3, the wet unit weight and, therefore, the mass density are still nearly constant.

36. While considering the control of soil specimen variables, it is worthwhile to examine the uniformity of the specimen. Fig. A12 presents ranges and averages of water contents and wet unit weights obtained during construction of the top four 3-in. layers of each specimen, the programed water content of each specimen, and the anticipated wet unit weight for that water content. Within a given layer, water content range varied from 0.6 to 3.5 percent of dry weight with the average 1.6 percent. The average water contents of the various layers are with two exceptions (the 3- to 6-in. and 9- to 12-in.layers in cart 18) within 2 percent of the programed values. The average wet unit weights in carts 19 and 20 are within 2 lb per cu ft of the anticipated value and within 2 lb per cu ft of the other layers of the same specimen.

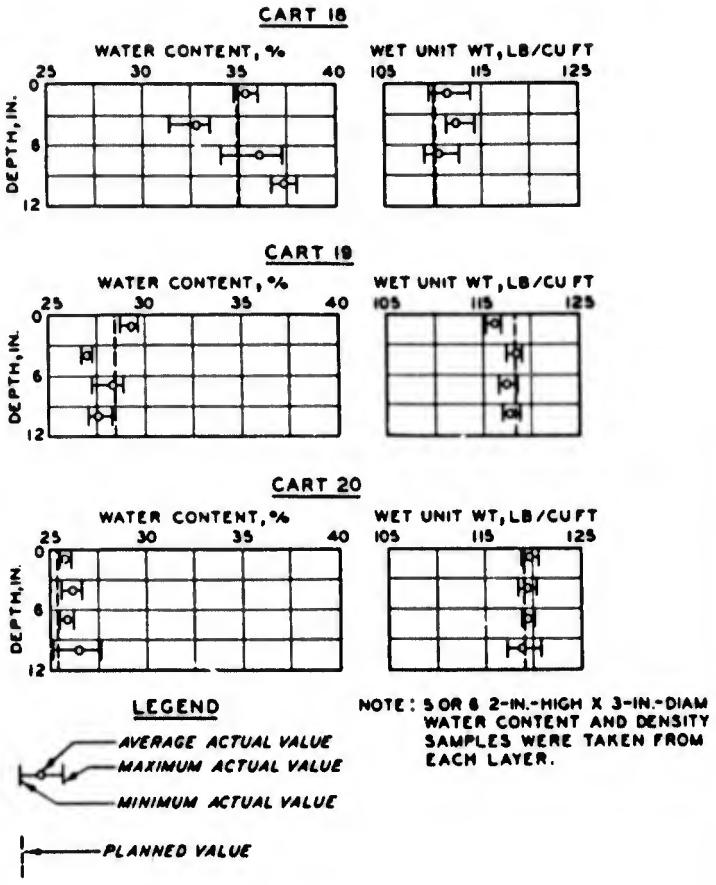

Fig. A12. Construction water content and wet unit weight profiles, soil-cart specimens

Load-pulse control

37. The following tabulation presents comparisons of the programed, measured, and computed column-load- and footing-load-pulse parameters. Of the parameters presented, computed maximum column load, rise time, hold time, and positive-phase duration pertain to the column-load pulse. The maximum footing reaction, a footing-load-pulse parameter, is also compared with its programed value in the tabulation.

	Computed Maximum Column Load P_{max}			Maximum Footing Reaction R_{max}			Rise Time t_r		Hold Time t_h		Positive-Phase Duration t_o	
Test No.	Programed* kips	As Tested kips	Deviation %	Programed kips	As Tested kips	Deviation %	Programed msec	As Tested msec	Programed msec	As Tested msec	Programed msec	As Tested msec
18-1	1.17	1.10	-6.0	1.16	1.39	+19.8	5	5	0	11	400	390
2	1.27	1.11	-12.6	1.38	1.47	+6.5		3		24		410
3	1.66	1.38	-16.8	1.78	1.91	+7.3		6		26		410
4	3.81	3.67	-3.7	3.82	4.37	+14.4		10		15		390
5	3.66	3.67	+0.3	4.00	4.43	+10.8		7		0		380
6	7.69	7.20	-6.4	7.48	8.04	+7.5		4		0		390
7	6.89	6.00	-12.9	7.11	7.35	+3.4		5		28		420

(Continued)

* Determined from calibration tests on box specimen.

Test No.	Computed Maximum Column Load P_{max} Programed kips	Computed Maximum Column Load P_{max} As Tested kips	Computed Maximum Column Load P_{max} Deviation %	Maximum Footing Reaction R_{max} Programed kips	Maximum Footing Reaction R_{max} As Tested kips	Maximum Footing Reaction R_{max} Deviation %	Rise Time t_r Programed msec	Rise Time t_r As Tested msec	Hold Time t_k Programed msec	Hold Time t_k As Tested msec	Positive-Phase Duration t_o Programed msec	Positive-Phase Duration t_o As Tested msec
19-1	1.50	1.30	-13.3	1.74	1.82	+4.6	5	10	0	30	400	430
2	3.21	3.04	-5.3	3.44	3.54	+2.9		6		10		410
3	3.86	3.73	-3.4	4.45	4.54	+2.2		4		4		420
4	9.07	8.64	-4.7	9.55	10.30	+7.9		4		34		370
5	9.06	9.13	-0.8	10.00	10.52	+5.2		5		0		390
6	18.50	17.58	-5.0	18.70	18.25	-2.4		3		0		370
7	8.81	8.73	-0.9	10.00	10.17	+1.7		5		0		340
8	9.71	9.42	-3.0	10.00	10.21	+2.1		4		0		360
20-1	2.33	2.30	-1.3	2.78	2.68	-3.6	5	6	0	0	400	410
2	5.05	5.01	-0.8	5.50	5.31	-3.5		4		0		390
3	6.68	6.59	-1.3	7.11	7.69	+8.2		3		0		360
4	15.02	13.60	-9.4	15.30	14.28	-6.7		2		0		370
5	15.02	13.25	-18.3	16.00	14.72	-8.0		2		0		400
6	9.84	9.58	-2.7	9.78	9.82	+0.4		2		0		410
7	3.89	3.78	-2.8	4.45	4.46	+0.2		6		30		420
8	4.14	4.10	-1.0	4.45	4.63	+4.0		6		0		410
9	4.40	4.06	-7.7	4.45	4.47	+0.4		6		18		380

38. The deviation of the "as tested" value of the computed maximum column load P_{max} from its programed value ranged from +0.3 to -18.3 percent. The deviation of the maximum footing reaction from its programed values ranged from +19.8 to -8.0 percent of the programed values. The deviations in footing reaction are the combined result of deviations in the column-load pulse and differences in soil consistency between the calibration box and the soil-cart specimens.

39. The column-load-pulse rise time ranged from 2 to 10 msec. Because this quantity is determined from the computed force curve, it is not precise. Hold time, the portion of the column-load pulse where the maximum dynamic column load is sustained, was programed as zero. However, hold time occurred in 11 of the 24 tests and reached a maximum value of 34 msec in test 19-4. The occurrence of hold time in nearly half of the dynamic tests despite the care taken in calibration suggested that modifications to the timing-control system were needed. The time delay relay, which controlled the hold time, was replaced with a precise numerical controller in subsequent tests. The total pulse time, or positive-phase duration, a parameter common to both the footing- and column-load pulses, ranged from 340 to 430 msec. The programed value was 400 msec.

Unclassified

Security Classification

DOCUMENT CONTROL DATA - R&D

(Security classification of title, body of abstract and indexing annotation must be entered when the overall report is classified)

1. ORIGINATING ACTIVITY *(Corporate author)*
U. S. Army Engineer Waterways Experiment Station
Vicksburg, Mississippi

2a. REPORT SECURITY CLASSIFICATION
Unclassified

2b GROUP

3. REPORT TITLE
DYNAMIC BEARING CAPACITY OF SOILS; INVESTIGATION OF A DIMENSIONLESS LOAD-DISPLACEMENT RELATION FOR FOOTINGS ON CLAY

4. DESCRIPTIVE NOTES *(Type of report and inclusive dates)*
Report 4 of a series

5. AUTHOR(S) *(Last name, first name, initial)*
Hadala, Paul F.

6. REPORT DATE	7a. TOTAL NO. OF PAGES	7b. NO. OF REFS
June 1965	104	16

8a. CONTRACT OR GRANT NO.	9a. ORIGINATOR'S REPORT NUMBER(S)
b. PROJECT NO. DASA NWER Subtask 13.010	Technical Report 3-599, Report 4
c. Chief of Engineers Project No. 1-T-0-22601-A-091-02	9b. OTHER REPORT NO(S) *(Any other numbers that may be assigned this report)*
d.	

10. AVAILABILITY/LIMITATION NOTICES
Qualified requesters may obtain copies of this report from DDC.

11. SUPPLEMENTARY NOTES	12. SPONSORING MILITARY ACTIVITY
	Defense Atomic Support Agency, and Chief of Engineers, U. S. Army

13. ABSTRACT

Three nondimensional relations developed to predict the maximum displacement and the time of its occurrence for dynamically loaded square footings on clay were presented in Dynamic Bearing Capacity of Soils, Report 3. Additional tests reported herein were conducted which verified these relations and showed them to be independent of the model scaling rules used to design the footing tests in which they were first observed.

The first relation is that of resistance parameter versus displacement parameter where the resistance parameter is the ratio of the average stress on the footing at maximum dynamic footing load to the static unconsolidated, undrained shear strength and the displacement parameter is the ratio of maximum footing displacement to footing width. The second is that of strength parameter to displacement parameter where the strength parameter is the ratio of maximum dynamic column load to the product of footing area and shear strength. The third relation is that of strength parameter to inertia parameter where the inertia parameter is the ratio of the product of maximum column load and the square of the time to maximum displacement to the product of footing width and load column mass.

In this test series it was also determined that the dynamic resistance parameter/displacement parameter relation can be approximated by converting static footing test data to the same nondimensional quantities and increasing the static resistance parameter by a factor of 1.5 to 1.9; a similar procedure could be used to approximate dynamic load-displacement curves from static plate-bearing test data.

DD FORM 1 JAN 64 1473

Unclassified

Security Classification

Unclassified
Security Classification

14. KEY WORDS	LINK A		LINK B		LINK C	
	ROLE	WT	ROLE	WT	ROLE	WT
Soils						
Soil mechanics						
Clay						
Foundations (Structures)						
Footings (Structures)						

INSTRUCTIONS

1. ORIGINATING ACTIVITY: Enter the name and address of the contractor, subcontractor, grantee, Department of Defense activity or other organization *(corporate author)* issuing the report.

2a. REPORT SECURITY CLASSIFICATION: Enter the overall security classification of the report. Indicate whether "Restricted Data" is included. Marking is to be in accordance with appropriate security regulations.

2b. GROUP: Automatic downgrading is specified in DoD Directive 5200.10 and Armed Forces Industrial Manual. Enter the group number. Also, when applicable, show that optional markings have been used for Group 3 and Group 4 as authorized.

3. REPORT TITLE: Enter the complete report title in all capital letters. Titles in all cases should be unclassified. If a meaningful title cannot be selected without classification, show title classification in all capitals in parenthesis immediately following the title.

4. DESCRIPTIVE NOTES: If appropriate, enter the type of report, e.g., interim, progress, summary, annual, or final. Give the inclusive dates when a specific reporting period is covered.

5. AUTHOR(S): Enter the name(s) of author(s) as shown on or in the report. Enter last name, first name, middle initial. If military, show rank and branch of service. The name of the principal author is an absolute minimum requirement.

6. REPORT DATE: Enter the date of the report as day, month, year; or month, year. If more than one date appears on the report, use date of publication.

7a. TOTAL NUMBER OF PAGES: The total page count should follow normal pagination procedures, i.e., enter the number of pages containing information.

7b. NUMBER OF REFERENCES: Enter the total number of references cited in the report.

8a. CONTRACT OR GRANT NUMBER: If appropriate, enter the applicable number of the contract or grant under which the report was written.

8b, 8c, & 8d. PROJECT NUMBER: Enter the appropriate military department identification, such as project number, subproject number, system numbers, task number, etc.

9a. ORIGINATOR'S REPORT NUMBER(S): Enter the official report number by which the document will be identified and controlled by the originating activity. This number must be unique to this report.

9b. OTHER REPORT NUMBER(S): If the report has been assigned any other report numbers *(either by the originator or by the sponsor)*, also enter this number(s).

10. AVAILABILITY/LIMITATION NOTICES: Enter any limitations on further dissemination of the report, other than those imposed by security classification, using standard statements such as:

(1) "Qualified requesters may obtain copies of this report from DDC."

(2) "Foreign announcement and dissemination of this report by DDC is not authorized."

(3) "U. S. Government agencies may obtain copies of this report directly from DDC. Other qualified DDC users shall request through _____."

(4) "U. S. military agencies may obtain copies of this report directly from DDC. Other qualified users shall request through _____."

(5) "All distribution of this report is controlled. Qualified DDC users shall request through _____."

If the report has been furnished to the Office of Technical Services, Department of Commerce, for sale to the public, indicate this fact and enter the price, if known.

11. SUPPLEMENTARY NOTES: Use for additional explanatory notes.

12. SPONSORING MILITARY ACTIVITY: Enter the name of the departmental project office or laboratory sponsoring *(paying for)* the research and development. Include address.

13. ABSTRACT: Enter an abstract giving a brief and factual summary of the document indicative of the report, even though it may also appear elsewhere in the body of the technical report. If additional space is required, a continuation sheet shall be attached.

It is highly desirable that the abstract of classified reports be unclassified. Each paragraph of the abstract shall end with an indication of the military security classification of the information in the paragraph, represented as *(TS)*, *(S)*, *(C)*, or *(U)*.

There is no limitation on the length of the abstract. However, the suggested length is from 150 to 225 words.

14. KEY WORDS: Key words are technically meaningful terms or short phrases that characterize a report and may be used as index entries for cataloging the report. Key words must be selected so that no security classification is required. Identifiers, such as equipment model designation, trade name, military project code name, geographic location, may be used as key words but will be followed by an indication of technical context. The assignment of links, rules, and weights is optional.

Unclassified
Security Classification